ADSORPTION OF CADMIUM AND PHENOL ON SLUDGE BASED ACTIVATED CARBON

BY

MOHAMMED DAUDA

A Thesis Presented to the
DEANSHIP OF GRADUATE STUDIES

KING FAHD UNIVERSITY OF PETROLEUM & MINERALS

DHAHRAN, SAUDI ARABIA

In Partial Fulfillment of the
Requirements for the Degree of

MASTER OF SCIENCE

In

CIVIL ENGINEERING

DECEMBER, 2016

KING FAHD UNIVERSITY OF PETROLEUM & MINERALS

DHAHRAN- 31261, SAUDI ARABIA

DEANSHIP OF GRADUATE STUDIES

This thesis, written by **MOHAMMED DAUDA** under the direction his thesis advisor and approved by his thesis committee, has been presented and accepted by the Dean of Graduate Studies, in partial fulfillment of the requirements for the degree of **MASTER OF SCIENCE IN CIVIL ENGINEERING.**

Dr. Muhammad H. Al-Malack
(Advisor)

Dr. Salah U. Al-Dulaijan
Department Chairman

Dr. Muhammad S. Vohra
(Co-Advisor)

Dr. Salam A. Zummo
Dean of Graduate Studies

Dr. Alaadin A. Bukhari
(Member)

26/12/16
Date

Dr. Basim Abussaud
(Member)

Dr. Sulayman A. Oladepo
(Member)

Dedicated to my parents and to everyone that have shown me support

ACKNOWLEDGMENTS

All praises and adoration are due to almighty Allah for his grace, and guidance in making this research work a successful one, Alhamdulillah.

First of all, I would like to extend my upmost appreciation to King Fahd University of Petroleum and Minerals, Dhahran for providing the scholarship that has enabled me to obtain my Master's degree. My sincere appreciation also goes to my thesis advisor Dr Muhammad H. Al-Malack, for his patience, guidance, and helpful criticism during the entire period of the research work. Special thanks are also due to my thesis co-advisor Dr M S. Vohra, committee members; Dr Alaadin Bukhari, Dr Basim Abussaud, Dr Sulayman Oladepo, for their valuable suggestions to this work.

I am also indebted to my parents for their endless support, love, and guidance they have shown to him throughout my life. Special appreciations are due to my siblings (Adam, Amin, Fatima, and Saratu) for their endless prayers and support. To the love of my life (Fatima), thank you very much for those "helpful" distractions and also for your endless love and care.

Next, I would like to thank the entire Nigeria community in KFUPM for their support and encouragement during the entire period of my master's program.

TABLE OF CONTENTS

LIST OF TABLES

LIST OF FIGURES

LIST OF ABBREVIATIONS

AC	: Activated Carbon
WWTP	: Wastewater Treatment Plant
SBA	: Sludge Based Adsorbent
RSM	: Response Surface Methodology
Cd^{2+}	: Cadmium ion
MB	: Methylene Blue
BET	: Brunauer Emmett Teller
SSA	: Specific Surface Area
SEM	: Scanning Electron Microscopy
XRD	: X-ray Diffraction
XRF	: X-ray Fluorescence
TGA	: Thermogravimetric Analysis
FTIR	: Fourier Transfer Infra-Red Spectroscopy
ASTM	: American Society for Testing and Materials

ABSTRACT

Full Name : Mohammed Dauda

Thesis Title : Adsorption of Cadmium and Phenol on Sludge based Activated Carbon

Major Field : Civil and Environmental Engineering

Date of Degree : December, 2016

Adsorption of cadmium (Cd^{2+}) and phenol in the both single and binary solute systems were investigated using activated carbon (AC) produced from Municipal Sewage Sludge. Several AC samples were prepared from sewage sludge using the chemical activation method with three activating agents, namely $ZnCl_2$, H_3PO_4 and KOH. After the production stage, some AC samples were selected based on their yield and methylene blue removal efficiency and characterized using, Fourier Transform Infrared spectroscopy (FTIR), Scanning Electron Microscopy (SEM), X-ray Diffraction (XRD), and Porosity and Surface area analysis. Results from the characterization studies showed that the best AC sample activated with 5M $ZnCl_2$ at a temperature of 700 ^oC for a time of 60 minutes, had a specific surface area of 319.5 m^2/g. The various adsorption experiments conducted for Cd^{2+} and phenol removal in both the single and binary solute systems, while taking into account the effect of adsorption parameters such as, pH, initial concentration, adsorbent dosage and contact time, showed that the AC offered high affinity for phenol removal than Cd^{2+} as evidenced from the adsorption capacities and removal efficiencies of each component. A removal efficiency of 28 % and 53 % were achieved for Cd^{2+} and phenol, respectively from a binary solution containing an equal concentration of 100 mg/l Cd^{2+}-phenol, at an optimum pH of 5.5, AC dosage of 0.15 g, and contact time of 480 minutes. The isotherms

modeling of the experimental data involving initial concentration variation of both component (25 to 300 mg/l), showed that Cd^{2+} and phenol adsorption were considerably fitted to both Freundlich and Langmuir isotherm models, with the Freundlich model showing the best fit based on its high R^2 and n values. Also, adsorption mechanism of both components from the binary solution was attributed to chemisorption, based on the result of equilibrium adsorption data fitting well to the pseudo-second-order kinetic model.

ملخص الرسالة

الاسم الكامل: محمد داودا

عنوان الرسالة: امتصاص الكادميوم والفينول باستخدام الكربون المنشط والمشتق من الحمأة المنشطة

التخصص: الهندسة المدنية والبيئية

تاريخ الدرجة العلمية: ديسمبر، 2016

في هذا البحث تم انتاج الكربون المحفز من المخلفات العضوية واستخدامه في معالجة المياه الملوثة بالكادميوم والفينول حيث تمت دراسة امتصاص كل عنصر على حدة وكذلك دراسة الامتصاص الثنائي للعنصرين في نفس المحلول. تم انتاج الكربون المنشط عن طريق التنشيط الكيميائي حيث استخدم هيروكسيد البوتاسيوم وكلوريد الزنك بالاضافة الى حمض الفسفوريك في عملية التنشيط. بعد مرحلة الإنتاج، تم اختيار افضل العينات العينات بناء على كمية الكربون الناتج بعد عملية الحرق بالاضافة الى نتائج ازالة ميثيليني الأزرق. تم عمل عدة اختبارات للعينات المختارة لدراسة خواصها الفيزيائية والكيميائية, من هذه الاختبارات اختبار تحديد المجموعات الوضيفية الموجودة على سطح الكربون المحفز, اختبار حالة السطح وطبيعة تكوين الفراغات البينية بالاضافة الى اختبار تحديد المساحة السطحية . من خلال النتائج تبين ان افضل الظروف لانتاج الكربون باستخدام كلوريد الزنك هي : درجة حرارة 700 درجة مئوية بتركيز 5 مول لمدة 60 دقيقة. حيث ان المساحة السطحية الناتجة هي 319.5 م^2 . تم استخدام هذه العينة في معالجة المياه الملوثة بالكادميوم والفينول حيث تمت دراسة امتصاص كل عنصر على حدة وكذلك دراسة الامتصاص الثنائي للعنصرين. تم دراسة تاثير بعض المتغيرات التشغيلية والتي لها تاثير كبير على عملية المعالجة من هذه العوامل : درجة الحموضة, وقت الاتصال بين الكربون والمحلول , كمية الكربون المستخدم و تركيز المواد الملوثة. نتائج الدراسة بينت ان الكربون الذي تم انتاجه يميل الى ازالة الفينول بدرجة اكبر من ازالة الكادميوم , حيث كانت معدل ازالة الكادميوم 28 % بينما معدل ازالة الفينول 53 % , وذلك من خلال ازالة الكادميوم والفينول من نفس المحلول والذي يحتوي على تركيز 100 مجم/ل لكل عنصر حيث كانت درجة الحموضة 5.5 والكربون المستخدم 0.15 جم والمدة الزمنية لاتصال الكربون بالمحلول 480 دقيقة. النتائج اللتي تم الحصول عليها من عملية الامتصاص تمت مطابقتها مع نموذج (لونجموير) و (فريندليك) حيث لوحظ تطابق افضل للنتائج مع نموذج (فريندليك). كما ان دراسة معدل الامتصاص للكادميوم والفينول بينيت ان عملية الامتصاص هي عملية امتصاص كيميائي

CHAPTER 1

INTRODUCTION

Utilizing organic waste materials for the production of valuable products have been a research area well explored in the past few years. Several studies carried out have been able to show the feasibility of using agriculture waste [1–5], municipal solid waste [6], and sewage sludge [7–10] in producing value-added products, such as activated carbon (AC), biochar, bio-composite material and bio-fuel. AC and biochar production from these waste material have been well documented, mainly because they have been able to serve as low-cost alternative adsorbents used for various toxic environmental pollutants removal.

The co-contamination of waterbodies with heavy metals and toxic organic compounds via wastewater effluent discharge have been a major source of environmental concern. Heavy metals are well known toxic, non-biodegradable pollutants that can be introduced into the natural environment through wastewater discharged from industrial activities such as electroplating, batteries manufacturing, pesticides production, and mining [11,12]. Cadmium is considered to be among the most toxic of these heavy metals, as its intake by humans has been linked to several deadly diseases [13]. Hence, its removal from wastewater before discharge has been an utmost priority recently [14]. Organic compounds such as phenol and its derivatives are also a major source of environmental pollutants, and their presence in the environment is normally attributed to effluent discharged by chemical industries and other allied industries[15]. They are as toxic as heavy metals and deserved to be removed from wastewater in order to prevent any of their associated problems.

Also, it is well known that two pollutants can coexist in the same environmental matrix most especially from industrial processes that utilize/generate both of them, a typical example includes plating and dying industries. It is also worth mentioning that cadmium and phenol are included in the United State Environmental Protection Agency (USEPA) priority pollutants list due to their high level of toxicity [16].

Several physical and chemical treatment methods have been reported in published literature for cadmium and phenol removal from contaminated wastewater. Some of these methods include; solvent extraction, coagulation, electrolysis, membrane separation, precipitation, reverse osmosis, and adsorption [17–19]. However, the majority of these methods have limitations that range from high operating cost, inefficiency in the removal of target pollutants, to the possibility of generating other toxic by-products. Adsorption technique using AC is widely considered among these methods due to its simplicity and high pollutant removal efficiency [14, 20-21]. Yet, its use has also been limited mainly resulting from the high production cost of AC, especially the commercial AC derived from non-renewable precursors [22]. This limitation has spurred a significant interest in recent years in investigating its production from several low-cost organic waste materials, and sewage sludge has been identified as an interesting alternative.

Sewage sludge also known as biosolids when treated is an unavoidable waste produced in significant quantity from wastewater treatment processes. There has been a reported surge in its production from wastewater treatment plant worldwide, due to the high rate of urbanization, and the increased population growth witnessed in the past years [23]. This increase has brought with it an attendant disposal problem. The conventional disposal options available that include landfill application, incineration, and composting have all

been shown to contribute to environmental pollution [23]. For example, incineration which can be very effective for its volume reduction has its own disadvantages that range from high energy cost to gaseous emission and the produced ash handling. The need for a reliable and efficient means of managing the enormous volume of sewage sludge produced by wastewater treatment plant is highly desirable. Therefore, its conversion into AC provides us not only with a valuable product which can be used for environmental decontamination, but it also provides a benign sustainable solution to sewage sludge management.

Hence, the feasibility of producing AC from a municipal sewage sludge and its use for the removal of cadmium and phenol from a synthetic wastewater was investigated in this research work. Although, numerous research work has studied the adsorption of these two pollutants from aqueous solution using AC or other forms of adsorbents according to the extensive literature review carried out. However, it was observed that majority of the published literature have only focused on the single solute adsorption of these pollutants, with few reporting their competitive or multicomponent adsorption. In addition, it was also observed that no research study has attempted to investigate the competitive adsorption of cadmium and phenol using low-cost AC such as sewage sludge AC. As such, this research work is the first of its kind that has been directed towards understanding the competitive interaction of cadmium and phenol in aqueous solution in the course of their adsorption using sewage sludge AC.

CHAPTER 2

LITERATURE REVIEW

Wastewater often collected from municipal and industrial areas, are ultimately sent to the wastewater treatment plant for treatment (WWTP). These waters can contain solid particles (suspended and floatable), colloidal particles, grits, biodegradable organic, toxic organic and inorganic compounds, and pathogens [24], that are usually removed in the various treatment processes and operations. Two outward flow streams normally result from the treatment processes and operations, which are; the clarified treated effluent and the residual solids know as sewage sludge or biosolid [7]. Sewage sludge constitutes the organic solids, inert solid and dead microorganisms removed during the wastewater treatment operations and processes. Its handling and disposal are very critical to the overall operation of the treatment process. As such, it must be effectively managed so as to prevent it from contaminating the environment.

The rapid rate of industrialization coupled with the increasing population growth, have resulted in the increase in volume of wastewater and its associated sludge produced from wastewater treatment worldwide. For example, one million tons of dried biosolid (treated sewage sludge) is reported to be produced annually in the UK [25]. Also, as of 2005, it was estimated that the sludge production from the entire European Union has increased by 50%, with sewage sludge production in France estimated to be about 950,000 tons of dried matter annually [26]. In addition, the sludge production in the entire Kingdom of Saudi Arabia is estimated to be around 451,870 tons of dry matter annually, which is expected to increase in years to come [27].

2.1 Sewage Sludge

Definition: Sewage sludge as defined by Zorpas et al [28] " is the concentrated bioactive residue of mostly organic clay-sized particles derived from wastewater treatment processes". It is an unavoidable waste from WWTP, and its source and nature usually depend on the WWTP and its method of operation [29]. The main sources of sludge in most municipal WWTPs are usually from the primary sedimentation tank and the secondary clarifier, other sources include the filtration systems, nitrification-denitrification facilities, and chemical precipitation process [30].

In the primary stage of wastewater treatment process, suspended solids and organics are usually collected via gravitational settling operations in a primary sedimentation tank. The collected particles in this stage constitute the primary sludge and is usually the bulk of the sludge produced during municipal wastewater treatment. Another notable source of sludge is the secondary sludge or biological sludge, that is produced in the secondary clarifier after the secondary treatment processes, a typical example is the activated sludge treatment process, where the sludge produced in the secondary clarifier is being recycled.

The produced sludge from the primary and secondary treatment processes are often combined, resulting in what is called the untreated sludge, this sludge is usually subjected to various treatment processes to render it safe for disposal or reuse. Different methods normally employed in sludge treatment include dewatering, anaerobic and aerobic digestion, composting, and incineration.

2.1.1 Sewage sludge management: Disposal and Utilization

Sewage sludge management encompasses all the various techniques and approach that are being employed in handling, treatment, and disposal of sewage sludge. It is regarded as one of the most daunting tasks being encountered by engineers in the field of wastewater treatment [29]. The three aged conventional practices used for sewage sludge disposal involve its use as fertilizer for agricultural purpose, landfilling for reclamation, and incineration. However, its use in the production of valuable products such as adsorbents (activated carbon and biochar), bio-fuel, and phosphorus recovery, has received significant scientific interest recently.

2.1.1.1 Agricultural application and land reclamation

The availability of nitrogen, phosphorus, potassium, and other trace elements determine the suitability of sewage sludge use as fertilizer or as a soil conditioner, as these elements are essential for plant growth. Although, sewage sludge is well known to be rich in these nutrients, most especially nitrogen and phosphorus derived from nitrification-denitrification treatment processes [31]. The presence of pathogens and other toxic compounds such as heavy metals have served as a limitation for its use as a fertilizer source.

Several stringent regulations have been put in place by various countries in recent years to limit sewage sludge use for agricultural purposes. Typical examples include the Sludge Directive 86/278/EEC from the Commission of the European Communities 1986 [25], Urban Waste Water Directive 91/271/EEC 1992 [25] and EPA biosolids laws and regulation (The Clean Water Act (CWA) of 1972) [32]. These regulations came into being

as a result of fear of accumulation of these toxic pollutants by plants from the sludge, which can easily be transferred through the food chain [24]. Nevertheless, sewage sludge use for agricultural purpose has been the most widely practiced option for its disposal [24]. Land reclamation with sewage sludge is also a viable disposal means that has been well practiced. However, sludge rheological properties, as well as its consistency, determines its suitability for use as landfills. The limitation of using sewage sludge as landfill has been the possibility of leaching toxic pollutants into ground and surface water. Also, sewage sludge low shear strength implies that lands reclaimed with it cannot be efficiently utilized for development purposes. Same as in the agricultural use, there are also legislations limiting sewage sludge use for land reclamation. Although, it is possible to dispose the sewage sludge through these highlighted options, it has to undergo various rigorous treatment processes that include stabilization, disinfection, and pollutant removal for it to meet the required legal regulations [33].

2.1.1.2 Thermal treatment

Thermal treatment remains the most sought after method for sewage sludge disposal due to its numerous advantages. Thermal incineration of sewage sludge not only provides means for its volume reduction and the destruction of toxic organics but can also provide energy recovery from it [31]. The major drawback of incineration has always been its potential as a source for NOx, CO, and particulate matter emission into the environment. Also, ashes produced from the incineration process can be hazardous, and require proper handling and safe disposal.

2.1.1.3 Precursor for producing value added products

Generally, recycling and reuse of waste materials have received significant scientific interest ever since sustainability concept was developed. This interest has also been extended to sewage sludge due to the constraints and shortcomings affecting its conventional disposal options. Several alternative disposal technologies have been developed that focuses on using the sludge as a raw material for the production of valuable end products. A typical and the most documented example is its conversion into AC. Sewage sludge is highly rich in organic matter which makes its conversion into AC easily achievable. The advantages of using sewage sludge for AC production are numerous in that, firstly, the produced sewage sludge is effectively utilized, solving the environmental problems accustomed to its other disposal options. Secondly, the AC produced from sewage sludge can be put back into the wastewater treatment process for adsorption of toxic contaminants such as dyes, sulfide, and heavy metals, and lastly, it has also been described as an effective method for carbon storage, which is of great significance in combating global warming [24].

2.2 Activated Carbon

Activated carbon is a highly porous carbonaceous adsorbent with an extended particulate surface area [24]. It has also been described by Pullket S. (18) as being made up of a defective layer of graphene, which could appear in various configurations. Moreover, Ozgur Aktas [34] described it as being composed of microcrystallites made up of fused hexagonal rings of carbon atoms which it a resemblance of graphite.

Activated carbon is the most widely used adsorbent for various environmental decontamination. It is usually characterized by its high adsorptive capacity, high

physiochemical stability, high surface reactivity and an immense specific surface area which can be as high as 2000 m^2/g depending on its preparation methods [5]. Its porous structure and particulate surface area allows it to adsorb and retain solutes and gaseous molecules.

Activated carbons are normally produced in various forms to suit a particular need or for a specific area of application. They can be broadly classified according to their physical characteristics as; powered activated carbon (PAC), granular activated carbon (GAC), activated carbon cloth (ACC), extracted activated carbon (EAC), pelleted activated carbon, fibrous activated carbon, and others. Their various forms are usually based on the starting precursor used or the modifications they are subjected to after production.

It is well known that any material with high lignocellulosic content (biomass) can be converted to activated carbon via thermal treatment and activation [35]. As such, several materials with high biomass content have been reportedly used for activated carbon production, some of which include coal, peat, coconut shell, petroleum coke, synthetic high polymer, agricultural waste, household organic waste, and sewage sludge.

2.2.1 Production of Activated Carbon

There are basically two main steps involved in activated carbon production, and they are carbonization and activation. The production process can be carried out in two steps where each step is done stepwise, or combined in a single step that involves carbonization and activation being done simultaneously.

2.2.1.1 Carbonization

Carbonization, as defined by Pullket.S [24] is the "thermal conversion of organic materials into its consolidated form of carbon, whilst eliminating non-carbon elements under an inert atmosphere". Its main purpose is for eliminating volatile matter in the precursor whilst converting it into residual char with fixed carbon content and low pore structure. The produced char is achieved through the aromatization and polymerization reactions of the carbonaceous material at high temperature [24]. Carbonization process basically involves the heating of the carbonaceous precursor at a high temperature of 400-850 ^{o}C in an inert or low oxygen atmosphere. The parameters that affect the yield and characteristic of the produced char during carbonization process include carbonization temperature, dwell time, heating rate and the nature of precursor used. Carbonization process is also commonly referred to as pyrolysis and is usually the main activity of the physical activation method.

2.2.1.2 Activation Methods

The produced char from carbonization process is usually activated either with the physical or chemical activation methods. The activation process is normally carried out to create more pore structures and extended surface area within the char/carbonaceous sample, so as to enhance its adsorptive capacity for pollutants.

Physical Activation

Physical activation is achieved through the gasification of the carbonized char with a gas (oxidant) such as steam, carbon dioxide, oxygen and air, at a high temperature (600–900^{o}C) to further aid in porosity development. Pores development in physical activation process as explained by K.Smith et al [25] is realized through the selective burn-

off of carbon atoms in the pore structure of the char by the oxidizing gas, and also resulting from the removal of pore-blocking tarry substances by the gas [25].

The characteristic of AC produced by the physical activation method usually depends on the activating gas used, as well as temperature and dwell time of the activation process. The two most commonly used activating gas as reported by G. Xu et al [36] are CO_2 and Steam. It has also been reported in published literature that at a specific temperature and dwell time, AC activated with steam do exhibit high adsorption capacity and wider pore size distribution than those activated with CO_2 activation, and this was identified to be due to the high reactivity of steam [36]. Typical reaction mechanisms that can occur during gasification with steam and CO_2 are presented as follows;

Boudouard reaction: $C + CO_2 \longrightarrow 2CO$ $\Delta H = 159$ kJ/mol

Water Gas reaction: Primary $C + H_2O \longrightarrow CO + H_2$ $\Delta H = +177$kJ/mol

Secondary $C + 2H_2O \longrightarrow CO_2 + 2H_2$ $\Delta H = 75$ kJ/mol

The above reactions are endothermic and therefore, implies that the activation process can only be started by applying high temperature [24]. A brief summary of two published literature that have employed physical activation process in AC production from sewage sludge are provided as follows;

Ros et al [37] synthesized AC from sewage sludge using the physical activation method with CO_2 as the activating gas. Initially, the sludge samples were first dried for 48 hours at 105 ^{o}C, before they were carbonized in nitrogen gas atmosphere, at a temperature of 700^{o}C for 30 minutes. Next, the activation process was conducted by placing the 4 g of the

carbonized char in a quartz cylindrical furnace with a nitrogen flowing gas, the temperature was increased gradually at a heating rate of 5 ^{o}C/min until the desired temperature of 800^{o}C was reached. At the targeted temperature the nitrogen gas flow was replaced with CO_2 and maintained for 2-4 hours. The produced AC exhibited a BET surface area of 269 m^2/g. A similar approach was also employed in a report titled D.12 by a team of researchers in London, but in this case, the activating gas used was steam [38]. A BET surface area of 215 m^2/g was reported for an activation temperature of 825 ^{o}C and dwell time of 1 hour.

Chemical Activation

Chemical activation as well reported is usually carried out via the single step approach (i.e. both carbonization and activation are done simultaneously). However, the two-step approach have also been reported, in which after carbonization, the produced char is impregnated with a chemical reagent (Oxidant) such as, KOH, $ZnCl_2$, H_3PO_4, H_2SO_4, and NaOH and thereafter subjected to another round of carbonization again. Chemical activation basically involves the impregnation or dry mixing (as applicable) of the carbonaceous precursor with a chemical reagent, with the resulting mixture being carbonized at a high temperature sufficient for pyrolytic reactions to take place [25]. The impregnation process as reported by Pullket, S. [24] normally supports the pyrolytic decomposition of organics present in the precursor, while limiting tarry residue formation in the pores and also assisting in preventing pores blockage [24].

The three most commonly used activating chemicals according to Pullket, S. are $ZnCl_2$, KOH, and H_3PO_4. They all have various reaction mechanism with the carbonaceous precursor during activation. $ZnCl_2$ is reported to act as a dehydrating agent in the early stage of carbonization i.e. at a lower temperature range, extracting moisture from the

precursor. This dehydrating effect normally results in charring and aromatization that subsequently leads to the formation of pore structures. In KOH activation, potassium present reacts with the precursor, which results in the formation of intercalation compounds (potassium compounds), that infiltrates into the carbon network causing accelerated carbon loss and pore development. As for H_3PO_4, its chemical interaction with the carbonaceous precursor usually results in porosity development by its intercalation in the internal structure of the precursor.

Chemical activation method presents significant advantages over the physical activation method, because it can be done in one step, and also at a much lower temperature which most often results in better yields [7]. According to Ahmad et al [7] in their review paper on sludge based AC, they reported that inorganic chemicals employed in chemical activation usually assist in the reduction of volatile matters released during carbonization, which in turn result in increased carbon yield. This is basically one of the main reason chemical activation method gives better yield than physical activation.

2.2.1.3 Post-Activation Treatment

This normally entails acid, alkaline or distilled water washing of the activated carbon to remove the remnant of the activating reagent, and also for freeing blocked pores. Acid washing has been shown to contribute significantly to improving the properties of produced AC [36]. Mostly, HCl is the most preferred post activation treatment agent as it can assist in the dissolution of the AC inorganic constituents [36].

2.3 Activated carbon production from sewage sludge and its application

Activated carbon derived from sewage sludge is also commonly referred to as sludge based adsorbent (SBA). Kemmer et al [39] were the first to patent the art of AC production from dried sewage sludge using chemical activation, and ever since there has been a wealth of research on this topic by several researchers. P. Hadi et al [23] and K. Smith et al [25] have both published a detailed literature review on AC production from sewage sludge, covering the production process, the AC properties, and their applications in water treatment for pollutants removal. The two reviews concluded that sewage sludge AC produced by chemical activation method do exhibit considerable high surface properties than those produced with physical activation method. Also, regarding their adsorption capability for various pollutants, it was reported to be influenced majorly by the produced AC surface area, and its surface functional groups are known to be responsible for the pollutants uptake.

High surface area AC have been reportedly produced from sewage sludge in the past few years by several researchers, while employing different activation methods [23]. Some published literature that have dealt with AC production from sewage sludge, and their various applications for pollutants removal are briefly summarized as follows;

Wang et al [40] were able to synthesize a highly porous AC from a cyclic activated sludge sample received from a secondary precipitator of the municipal wastewater treatment plant. The sludge was activated with 3M KOH at a temperature of 600 ^{o}C for 1 hour in an atmosphere of steam and was able to achieve a specific BET surface area of 382 m^2/g. Adsorption of acid brilliant scarlet (GR) dye was investigated using the produced AC, and the results showed that 99.6 % and 99.7 %, total organic carbon (TOC) and coloration were

achieved, respectively from an aqueous solution containing the dye, which indicated that the produced AC has a high adsorption capacity for the dye.

Wen et al [22] also investigated AC production from sewage sludge, which was used for gaseous formaldehyde adsorption. The AC was produced by chemical activation of the sludge with 6 M $ZnCl_2$ in an atmosphere of nitrogen gas, at a temperature of 750 ^oC and dwell time of 120 minutes, and was able to achieve a BET surface area of 509.88 m^2/g. Furthermore, the produced AC was compared with some commercial activated carbons (CAC) in the adsorption of gaseous formaldehyde. The AC was found to exhibit an excellent adsorption capacity than the CAC samples, and the author attributed this to its porous structure and appropriate surface chemistry that favors formaldehyde adsorption.

Jon Alvarez et al [8] investigated the effect of HCl and Na_2CO_3 washing of pyrolyzed sewage sludge char, on its activation with CO_2 at a temperature of 800 ^oC in a fixed bed reactor. They found that the washing step contributes immensely to the produced char gasification rate, which also further assisted in improving the produced AC properties. A BET surface area of 440 m^2/g was reported for the AC for a dwell time of 15 minutes.

2.4 Adsorption of Cadmium and Phenol using AC/ Sludge based AC

The removal of Cadmium and Phenol by adsorption using AC have been well studied by numerous authors in the past [49–52], demonstrating that AC has been identified as an important agent for their removal from aqueous solution. However, the majority of these studies have only seemed to focus on the single solute adsorption of either of these pollutants in aqueous solution, with a few reporting their combined or multicomponent adsorption. Moreover, it is well known that these two environmental pollutants do not exist

in isolation, as they both can be found as constituents in some industrial wastewater effluent, and their combined presence will either have a positive or negative impact on the removal during adsorption. Therefore, it is important to study the multicomponent adsorption of Cd^{2+} and phenol from aqueous solution, in order to better understand the competitive effect that might be exerted by each component. Some reviewed literature that have focused on single solute adsorption of cadmium or phenol using sludge derived AC or AC from other sources are briefly summarized as follows;

Yan Ma et al [45] investigated the performance of powdered activated carbon (PAC) for the removal of phenol from aqueous solution. Batch adsorption experiments were carried out to study the effect of adsorbent dose, initial solution pH, temperature, and contact time on phenol removal efficiency. Results from the study showed that phenol adsorption by the PAC was rapid, with more than 80 % removal efficiency achieved within contact time of 10 minutes.

Bousba et al [42] synthesized AC from sewage sludge employing chemical activation with H_2SO_4. The AC produced was further used to investigate phenol removal from an aqueous solution. Results from the study showed that an adsorption capacity of 26.16 mg/g was achieved for phenol at an optimum experimental condition of; initial phenol concentration 40-200mg/l, adsorbent dosage of 5 g/l, contact time of 180 minutes, and temperature of 20 ^oC. The study also concluded that phenol adsorption by the AC was highly depended on its initial concentration and its speciation which is a function of the pH (pH<pKa).

Pirzadeh and Ghoreyshi [15], also investigated phenol removal, using paper mill sludge derived AC. The produced AC was activated with $ZnCl_2$ and was able to achieve an

adsorption capacity of 15.04 mg/g for phenol. This was said to have occurred at an optimum condition of; pH 6-7, initial phenol concentration of 60 mg/l, temperature of 25 ^{o}C, adsorbent dosage of 3 g/l and at a contact time of 3 hours. Also, a removal efficiency of 79.45 % was reported for the highest phenol concentration of 60 mg/l. They also reported that temperature had a negative impact on phenol adsorption by the AC.

In another study by Hameed and Rahman [46], phenol adsorption was investigated using AC derived from rattan sawdust. Results from the study showed that an adsorption capacity of 149.25 mg/g was realized for phenol using the produced AC. They also reported that pH had a significant impact on phenol removal, as a decrease in the solution pH (below phenol pKa value of 9.9) resulted in a significant increase in the adsorption capacity.

Phenol removal from aqueous phase was also investigated by Zhu et al [47] using AC derived from solidified landfill sewage sludge by $ZnCl_2$ activation. Results from the study revealed a maximum adsorption capacity of 94.9 mg/g was achieved for phenol at a pH of 5.0, contact time of 120 minutes, and initial concentration of 100 mg/l. They concluded that phenol removal by the AC was influenced majorly by adsorbent dosage and contact time and that the pH has no influence on phenol removal.

Yu Bian et al [48] studied the aqueous phase adsorption of cadmium ion (Cd^{2+}) using an AC modified with oxygen functional groups. Results from the study revealed that a maximum removal efficiency of 88 % was achieved for Cd^{2+} over a broad range of pH value of 4.5-6.5. The effect of pH on Cd^{2+} adsorption also showed that the increase in pH above the initial value of 4.5 resulted in increased cadmium removal and its increase above 6.5 brought about little changes to the removal. The study concluded that the introduced

oxygen functional groups on the AC surface contributed significantly to Cd^{2+} adsorption, and a maximum adsorption capacity of 25.13 mg/g was reported at the optimum experiment conditions.

Ihsanullah et al [11] performed a comparative investigation of Cd^{2+} adsorption using several acid modified carbon-based adsorbents, that was inclusive of AC. Results from the adsorption experiments conducted showed that the optimum conditions were established to be as follows; pH of 7.0, adsorbent dosage of 150 mg, contact time of 2 hours and agitation speed of 150 rpm. Cadmium removal efficiency of over 90 % was achieved with the AC, and maximum adsorption capacity of 1.98 mg/g was predicted from pseudo-second order kinetic model.

Ahmed Ali [49] also performed a comparative investigation of Cd^{2+} adsorption using granular activated carbon (GAC), dead biomass and phosphate rock. Results from the study showed that the optimum conditions were found as follows; pH of 5.0, initial concentration of 100 mg/l, adsorbent dosage of 3 mg, and contact time of 270 minutes. A maximum adsorption capacity of 17.757 mg/g was realized for the GAC based on Langmuir isotherm model.

Zhai et al [50] investigated the adsorption of cadmium and nickel from aqueous phase using AC produced from sewage sludge. Results from the study showed that an adsorption capacity of 16 mg/g and 9 mg/g were achieved for the metals respectively, at an optimum pH range of 5.5-6.

The forgone reviewed literature has been able to show to some extent, that the adsorption of cadmium and phenol in the single solute system by AC derived from sludge or from other biomass material have been well researched and documented.

2.5 Competitive/Multicomponent Adsorption of Cadmium and Phenol using AC or other forms of Adsorbent

Competitive adsorption study of a binary mixture of cadmium-phenol from aqueous solution has not been well researched. As earlier noted for the two pollutants, previously reported studies seemed to focus on only their single solute adsorption, with only a few studies considering the binary mixture (multicomponent) of both the metal ion and organic compound in aqueous solution. Some previously published literature on competitive/multicomponent adsorption, covering either only phenolic compounds or heavy metals (Cadmium inclusive) or a combination of both with sludge based AC or AC from other sources are briefly discussed as follows.

Arcibar-Orozco et al [14] investigated the simultaneous removal of phenol and cadmium from an aqueous phase using an activated carbon cloth (ACC). Results from the adsorption experiments conducted showed that a decrease in Cd^{2+} adsorption capacity up to 40 % (from 0.146mmol/g – 0.088mmol/g) was realized in the presence of phenol at a pH of 7, and the author attributed this behavior to the chemistry of adsorbed phenol that creates a steric hindrance on the ACC surface for the Cd^{2+} adsorption.

Guangzhou Qu et al [13] investigated the simultaneous adsorption of cadmium and phenol from aqueous solution using pulsed corona discharge plasma combined with commercial coal derived granular activated carbon (PCDP/GAC). Results from the study showed that

a removal efficiency of 69 % and 87.3 % were achieved for $Cd^{2+}$and phenol, respectively with the combined PCDP/GAC system when used for 60 minutes.

Salim Bekkouche et al [51] investigated the competitive adsorption of phenol and some heavy metals (cadmium inclusive) onto titanium dioxide (Degussa P25). They found from the single components study that phenol and the heavy metals adsorption onto the titanium dioxide exhibited different adsorption mechanism, as derived from the Kiselev isotherm model. As for the competitive adsorption, a significant decrease in cadmium removal efficiency of up to 30 % was reported in the presence of phenol, when compared with it single solute adsorption. Likewise, a decrease in phenol removal was also reported in the presence of cadmium.

Diaz-Flores et al [52] investigated the simultaneous adsorption of cadmium and phenol using modified N-doped carbon nanotube. Based on their experiment results reported, adsorption capacities of 0.10 and 0.07 mmol/g were achieved for phenol and Cd^{2+} respectively, during their single solute adsorption. While in their competitive adsorption, an increase in cadmium adsorption was noticed at high concentrations of phenol. Similarly, phenol adsorption capacity was also affected by increased cadmium concentration.

Kavand. M et al [18] investigated the competitive adsorption of cadmium ion, lead ion and nickel ion from aqueous solution using commercial AC derived from coconut shell. Single solute and multicomponent adsorption (binary and ternary) studies were carried out. The adsorption process was optimized using RSM technique and the optimal conditions were found to be as follows; pH of 6.3, Temperature at 56.8 ^{o}C, shaking speed of 308 rpm. Also,

the preferential selectivity adsorption order for the metals were reported as, Pb^{2+}: 9.44 mg/g > Cd^{2+}: 9.37 mg/g > $Ni^{2+:}$ 4.52 mg/g.

From the few reported literature so far, it can be concluded that multicomponent adsorption of cadmium-phenol mixture using AC or other various forms of adsorbents has been studied. However, to the best available knowledge found, it evident that the use of sewage sludge based-AC for the competitive/multicomponent adsorption of cadmium and phenol from aqueous solution has not yet been investigated. Therefore, it can be concluded based on the literature review that there is a lack of information in this research area that deserves further investigation.

2.6 Experimental design based on Response Surface Methodology RSM

RSM is an experimental design method based on the collections of mathematical and statistical techniques [53]. It has been widely employed for process design, modeling, performance evaluation, and optimization of various chemical and environmental processes [54]. Its applications in process design allow for experimental configuration, assessment of the effect of one or more process variables (factors) on a single or sets of experimental outcome called response, the effect of possible interactions of the variables and their optimization to achieve the best conditions. Several RSM designs are available, and the choice of which to use usually depends on the numbers of process variables affecting the response of the system to be studied and also the economical consideration of running the experiment. Typical RSM designs available are; 3-level factorial, Box-Behnken, Central composite and Doehlert designs.

RSM designs offer numerous advantages over the conventional one factor at a time experimental design that often involves varying of one factor while keeping other constant. Some of the advantages include their ability to provides significant information regarding an experiment or process, by utilizing a few designed experimental run, and also their ability to simultaneously assess the effects of several factors and their interaction on a response, as well as the optimization of these factors.

Several studies [24,26, 55-56] have investigated the optimization of AC production from sewage sludge using RSM design, and have been able to identify and optimize the significant variables affecting the preparation process. The most significant process variables affecting the properties of produced AC such as yield and BET surface area as reported are in literature were, activating temperature, impregnation ratio (for chemical activation) or oxidizing gas flow rate (physical activation), and dwell time.

CHAPTER 3

RESEARCH OBJECTIVES

The reviewed literature have shown that there is a lack of information on combined removal of Cd^{2+} and phenol mixture from aqueous solution, using low-cost AC. Accordingly, the primary objective of this research work is directed towards the feasibility of using low-cost sewage sludge based AC for the adsorption of Cd^{2+} and phenol from a synthetic wastewater, in both the single solute and binary solute systems. In this respect, the AC will be produced from the sewage sludge sample of a municipal wastewater treatment plant (MWTP), employing statistical experimental design based on RSM. The produced AC will thereafter be used for the adsorption studies. The specific sets of objectives to be achieved are listed as follows;

- To investigate the influence of production factors on the properties of AC (yields and MB removal efficiency) produced from the sludge using RSM technique with three activating agents (H_3PO_4, KOH, $ZnCl_2$).
- To use the best AC derived from the production stage for the single solute adsorption of cadmium and phenol from a synthetic wastewater.
- To also use the best AC derived from the production stage for combined adsorption (competitive effect) of cadmium and phenol from a synthetic wastewater.
- To investigate the effect of the various adsorption parameters in both the single and binary solute adsorption experiments.

CHAPTER 4

MATERIALS AND METHODS

4.1 Materials

4.1.1 Sewage Sludge

Dewatered sewage sludge sample was collected from the belt filter press unit of AL Khobar wastewater treatment plant in the eastern province of Saudi Arabia. The collected sludge was oven dried at 105 ºC overnight and thereafter washed to remove the visible dirt on it. It was subsequently re-dried at the same temperature for 24 hours until no weight change was observed. The final sludge obtained was comminuted and sieved through a 2mm sieve size and stored in a covered plastic container ready to be used for the activated carbon production.

4.1.2 Reagents

Chemical reagents used in this study were all of analytical grade and include the following; Cadmium nitrate salt $Cd(NO_3)_2 \cdot 4H_2O$ (BDH laboratories supplies) used for preparing stock solution of cadmium (1000ppm), Phenol crystal (Sigma-Aldrich) used for preparing the stock phenol solution (1000ppm), Methylene Blue MB (Fischer), potassium hydroxide pellets KOH, (Fischer) phosphoric acid solution (Fischer) (H_3PO_4), zinc chloride $ZnCl_2$ (Fischer), nitric acid HNO_3 (Fischer), sodium hydroxide NaOH (Fischer) and pH calibration Standards (Fischer). Deionized water used was prepared using CORNING Mega Pure™ System.

4.2 Experimental Methods/Methodology

The adopted methodology for this research work comprises an initial characterization of the sewage sludge for its ash content, elemental analysis and thermogravimetric analysis. Thereafter, the activated carbon was prepared from the sludge using the three activating chemical reagents. The Box-Behnken experimental design (BBD) was considered for the production process, and three levels were chosen for each independent factor (temperature, impregnation ratio and time) affecting the production process. These factors were analyzed based on the yields and methylene blue removal efficiencies of the produced AC samples. The best AC samples obtained were characterized using, Scanning Electron Microscopy coupled with Energy Dispersive X-ray Spectroscopy (SEM/EDX), X-ray Powdered Diffraction (XRD), X-ray fluorescence (XRF), Thermogravimetric analysis (TGA), Fourier Transform Infra-Red Spectroscopy (FTIR), Elemental analysis and Porosity and Surface area analyzer for determining the BET surface areas and pore volumes.

Several adsorption experiments of cadmium and phenol removal were conducted using the best produced AC that showed high removal efficiency for methylene blue and also had the highest BET surface area and pore volume. The effect of pH, adsorbent dosage, contact time, and initial concentration were all investigated in both the single and multicomponent adsorption experiments of the two pollutants.

4.2.1 Preparation of the sewage sludge based activated carbon

4.2.1.1 Experimental Design

The experimental design method adopted in this research for preparing the AC was based on Response Surface Methodology (RSM) techniques. Box-Behnken design (BBD), a three level factorial design was chosen in designing the sets of experiments for the activation process using the three chemical reagents namely; zinc chloride ($ZnCl_2$), phosphoric acid (H_3PO_4), and potassium hydroxide (KOH).

BBD design is usually described by a multidimensional cube with selected points at the mid of each edge, with a replicated center point [57]. The number of experiment required in BBD design is given by the expression; $N = 2k\ (k - 1) + Co$; where N- is the number of experiments, k- the number of independent factors of concern, and Co- is the number of center points. In this research three independent factors namely; activating temperature, dwell time and impregnation ratio, known to influence the production process as reported in published literature were chosen and varied at three equally spaced levels. The chosen levels for each factor were coded as, low (-1), medium (0), and high (+1), as shown in Tables 4.1, 4.2, and 4.3, in correspondence to the activating agents. The effect of the chosen factors on the activation process was determined based on the yields and methylene blue removal efficiencies (responses) of the AC samples produced by the activating agents.

A total number of 13 experimental runs were created for each activating agent, with one replicated center run per block. BBD design was chosen for the activation process because it offers fewer experimental runs when compared to other RSM designs, and also because it allows for efficient estimation of first and second order coefficient of the resulting mathematical model by only considering the corner points of a three level

factorial design [53]. Mathematical models based on a polynomial equation that describes the effect of each factor on the responses were generated from the experimental designs. The mathematical response model developed is the form presented as follows;

$$y = \beta_o + \sum_{i=1}^{k} \beta_i x_i + \sum_{i=1}^{k} \beta_{ii} x^2{}_i + \sum_{i=1}^{k-1} \sum_{j=2}^{k} \beta_{ij} x_i x_j + \varepsilon \quad 4.1$$

Where, y is the predicted response, β_o constant term coefficient, β_i linear term, β_{ii} quadratic term, β_{ij} interaction term, ε error term and $x_i x_j$ coded values of the independent variables. The experimental design and the subsequent statistical analyses of the two responses obtained from each activation process were achieved aided by a statistical software called Design Expert version 9.

Table 4.1: Factor levels and codification for $ZnCl_2$ Activation

Factor	Symbol	Coded factors levels and actual values		
		-1	0	1
Temperature (°C)	A	600	700	800
Impregnation Ratio (Sludge: Reagents)	B	0.2	0.6	1
Dwell Time (min)	C	60	90	120

Table 4.2: Factor levels and codification for KOH Activation

Factor	Symbol	Coded factors levels and actual values		
		-1	0	1
Temperature (°C)	A	600	700	800
Impregnation Ratio (Sludge: Reagents)	B	0.5	1	1.5
Dwell Time (min)	C	60	90	120

Table 4.3: Factor levels and codification for H_3PO_4 Activation

Factor	Symbol	Coded factors levels and actual values		
		-1	0	1
Temperature (°C)	A	600	700	800
Reagents Conc. (%)	B	30 %	40 %	50 %
Dwell Time (min)	C	60	90	120

4.2.1.2 Experimental Procedure for the activated carbon production

In the impregnation step for both $ZnCl_2$ and H_3PO_4 activation, 10 grams of the comminuted dried sludge was mixed and stirred with 15 ml solution of the chemical reagents based on the experimental design, to achieve the desired impregnation ratio. As for the KOH impregnation, 10 grams of the sludge was dry mixed with varying weights of crushed KOH pellets according to the mix ratio of the experimental design, until a homogenous mixture was attained. The impregnation processes for $ZnCl_2$ and H_3PO_4 activation were all performed at room temperature and maintained for more than one hour to achieve full

penetration. Thereafter, the obtained slurry was oven dried at 105 ^{o}C for four hours to remove excess moisture from it.

Next, in the activation process, the impregnated samples were packed into a 30 cm long stainless steel tubes of 50mm diameter having two narrow ports of 8 mm diameter (for expelling gases). The packed tubes were positioned in a muffle furnace and heated to the desired temperatures of; 600, 700 and 800 ^{o}C as chosen in the experiment design. Heating was done slowly at 10 ^{o}C/min until the target temperatures were reached. Samples were taken out from the furnace at time intervals of; 60, 90, and 120 minutes, starting from when the targeted temperature has been reached. Then, the obtained activated carbon samples were cooled, and subjected to repeated cycle of washing with distilled water until it shows a pH value ≈ 6 -7. The final products were oven dried at 105 ^{o}C for 24 hours and were thereafter crushed and sieved to a particle size less than 0.3 mm.

Figure 4.1: Image of the produced sludge AC obtained from $ZnCl_2$ Activation

Physiochemical Characteristics of the Sewage Sludge [58]

Parameters	Raw Sludge	Dried Sludge
	Average	Average
Moisture %	97	47
Total solids %	4.0	52.8
Total Volatile Solids %	2.6	32
Oil and Grease %	5.5	0.62
pH	6.8	6.9
Total Alkalinity(mg/l)	332	251
Ammonia (mg/l)	1.4	0.37
Nitrite (mg/l)	20.1	3.4
Nitrate (mg/l)	140	35
Organic Nitrogen %	6.9	3
TKN %	8.3	3.7
Arsenic (mg/l)	24.3	11.1
Boron (mg/l)	75	39
Cadmium (mg/l)	52	28.4
Chromium (mg/l)	144	73
Copper (mg/l)	385	186
Iron (mg/l)	4817	2249
Mercury (mg/l)	10.7	3.9
Manganese (mg/l)	86	35.8
Nickel (mg/l)	106	51
Lead (mg/l)	93	47
Zinc (mg/l)	2268	664

4.2.2 Characterization of the sludge and the produced activated carbon

4.2.2.1 Thermogravimetric Analysis

Thermogravimetric analysis (TGA) measures the effect weight change of a material with respect to temperature increase in a specified environment. It primarily measures the oxidative and decomposition stability of a material with respect to temperatures changes. In this research, TGA was carried out to study the thermal response of both the sludge and some selected activated carbons produced when they are pyrolyzed in an atmosphere of argon gas. The TGA experiments were conducted using Thermal analyzer (TGA-DSC) by Mettler Toledo. An approximate weight of 20-35 mg of the samples were put in an alumina crucible and loaded onto the device. Another crucible containing Al_2O_3 used as a reference for differential scanning calorimetry (DSC) measurement was also loaded. The samples were pyrolyzed at a heating rate of 10 ^oC/min, starting from a temperature of 30 to 1000 ^oC, under an argon gas flow rate of 100 ml/min. TG and DTG (derivative thermogravimetric) curves were obtained after the analysis period.

4.2.2.2 Ash Content Analysis

Ash content of the sludge sample was determined according to the ASTM D2866-94 test method for total ash content determination. The procedure involves igniting a clean ceramic crucible in a muffle furnace at a temperature of 650 ^oC for 1 hour, for it to be cooled in a desiccator and weighed to the nearest 0.1 mg. Next, about 2 g of the dried sludge was weighed and put in the crucible and heated to a temperature of 650 ^oC until no weight change was recorded. The ash content was determined according to the relation given as follows;

$$\text{Ash content } (\%) = \frac{Ash\ weig}{oven\ dry\ weigh} * 100 \quad 4.2$$

Where Ash weight is the recorded weight of the sample left after heating, and oven dry weight is the weight of the dried sludge.

4.2.2.3 Elemental Analysis (CHNS-O)

The organic elemental composition of some of the produced AC samples and the sludge was determined using the CHNS/O Elemental Analyzer (PerkinElmer). Carbon, Hydrogen, Nitrogen and Sulfur content of the samples were derived from their combustion analysis.

4.2.2.4 Surface Morphology

Surface shapes and pore structures of some of the produced AC samples and the sludge were determined by their magnified images through Scanning Electron Microscope (SEM, JSM-6610LV) coupled with Energy Dispersive X-ray Spectrometer (EDS). The EDS was used in identifying the surface elemental compositions of each sample during SEM scan. An accelerating voltage of 20kv was employed for the SEM scan, and three scans resolutions were undertaken for each sample (10, 50 and 100 micrometers).

4.2.2.5 Powdered X-ray Diffraction (XRD) Spectroscopy

Characterization of the sludge sample and some of the selected AC samples for their mineralogical compositions was carried out using the XRD technique. The XRD analysis provides information on crystalline inorganic compounds present in a sample, through the study of its X-ray diffraction patterns. Rigaku Ultimate IV X-ray Diffractometer using copper K-α radiation was used for XRD analysis. Diffraction pattern for each sample was

obtained by a step scanning at 0.02 °/s step size with an angle ranging from 10° to 80°. Identification of the main crystalline phases was achieve using PDXL software.

4.2.2.6 X-ray Fluorescence Spectroscopy (XRF)

XRF analysis was conducted for the sludge sample and the selected AC samples using Spectro Xepos equipment(Ametex). This was done to determine and quantify the inorganic compounds present in the samples. XRF is also an elemental analysis, that is based on the emission of characteristic X-ray radiation by a material bombarded with either X-ray or gamma photons [59]. It can only quantify elements above magnesium in the period table of elements.

4.2.2.7 Fourier Transform Infra-Red Spectroscopy (FTIR)

Identification of functional groups on the surface of the selected AC samples and the sludge were achieved using the FTIR technique. The FTIR spectra of the samples were obtained using Thermo Electron Corporation Nicolet Nexus 670 FT-IR Spectrometer device, at a wavelength region of 500-4000cm^{-1}. Potassium Bromide (KBr) method was used for the analysis. Prior to analysis, samples were homogenously mixed and ground with KBr (spectroscopy grade) in a mortar, and thereafter pressed hydraulically to form pellets. The resulting pellet is then transferred to the FTIR spectroscopy device for it to be analyzed.

4.2.2.8 Porosity and Surface Area

Porosity characterization of the sludge and some of the selected AC samples was achieved using an automatic physisorption unit, Micrometric, ASAP 2020, USA. Specific surface area SSA_{BET}, pore volume, and pore size were determined through the classical BET theory and the nitrogen adsorption/desorption isotherm data at 77K.

4.2.2.9 Yield

The ratio of the mass of impregnated sludge used during the pyrolysis stage to the resulting mass of activated carbon realized after washing and drying, expressed as a percentage gives the yield of the produced activated carbon. The yields of all the prepared activated carbons were determined and used in the optimization of the production factors. The yield can also be expressed mathematically as follows;

$$Yield\ (\%) = \frac{weigh\ \ of\ activated}{weigh\ \ of\ sludge} \qquad 4.3$$

4.2.2.10 Methylene Blue Adsorption

Methylene Blue (MB) adsorption experiments were investigated for all the produced AC samples. This was done to provide an experimental response required for the optimization of the production factors. Also, the selection of best produced AC samples for characterization was done base on their methylene blue removal efficiency.

The MB adsorption experiments were performed as follows; Approximately 0.1g of various prepared activated carbons was combined with 50 ml volume of 100 or 20 mg/l MB solution in an Erlenmeyer flask. The resulting mixture was then agitated using a mechanical shaker at 200 rpm and stopped once a color change is noticed in the solution. The resulting solution is centrifuged and the supernatant is analyzed using UV spectrophotometer (Shimadzu 1650PC, Japan). MB removal efficiency was calculated using the formula provided below; where Co and Ct denote the initial and final concentration (mg/l) of MB respectively.

$$Removal\ efficiency\ (\%) = \frac{Co-Ct}{Co} * 100 \qquad 4.4$$

4.2.3 Adsorption Experiments of Cadmium and Phenol

Adsorption capability of the best AC sample in the removal of the target pollutants was investigated via the various adsorption experiments conducted. Single solute (cadmium or phenol individually) and multicomponent (binary mixture of cadmium and phenol) adsorption experiments were carried out in batches considering the various adsorption parameters that include, the effect of pH, adsorbent dosage, contact time and initial concentration. A stock solution of 1000 mg/l of Cd^{2+} was prepared from its cadmium nitrate salts ($Cd(NO_3)_2 \bullet 4H_2O$) by dissolving 2.744 g in 1liter of 0.5 M nitric acid (HNO_3) solution. Likewise, 1000 mg/l stock phenol solution was made by dissolving 1g of phenol in 1liter of deionized water. The test solutions used in the adsorption experiments were prepared by diluting the stock solution to the desired concentrations using the mass balance relationship. Batch adsorption experiments conducted, were achieved by adding a different amount of the produced AC to 50 ml solutions containing a different concentration of cadmium, phenol and cadmium-phenol mixture in 125 ml Erlenmeyer flask. The resulting mixtures were agitated with a mechanical shaker at different times. Details of each experiment are discussed as follows;

4.2.3.1 Effect of Initial pH

The pH adsorption study of cadmium and phenol, in both single and binary solute systems, were investigated using 100 mg/l concentration of the pollutants at different pH values starting from 3 to 7. Procedure for adsorption experiments involves, adding 0.15 g of the produced AC with 50 ml solutions of 100 mg/l Cd^{2+}, 100 mg/l phenol and 100 mg/l Cd^{2+}-phenol. The solution pH was adjusted to the desired value using 0.1N NaOH and 0.1N

HNO_3.The mixtures were continuously mixed for 2 hours at room temperature using a mechanical shaker at 200 rpm.

4.2.3.2 Effect of contact time (kinetic experiment)

Procedure for the kinetic experiments in both the single and multicomponent adsorption of cadmium and phenol were achieved as follows; 0.15 g of the AC sample were added to 50 ml solutions of 100 mg/l, Cd^{2+}, phenol and a binary mixture of Cd^{2+}-phenol in 125 ml Erlenmeyer flask. The pH was adjusted to the optimum value realized from the pH-adsorption study. The prepared samples were agitated with a mechanical shaker at 200 rpm and were withdrawn at different time intervals in the order 1,5, 10, 15, 30, 60, 120, 240, 480, 720, and 1440 minutes.

4.2.3.3 Effect of adsorbent dosage

Procedure for adsorbent dosage variation experiments were also carried out using 50 ml solutions of 100 mg/l of Cd^{2+}, phenol and a binary mixture of Cd^{2+}-phenol in 125 ml Erlenmeyer flask. Different AC dosage in the range of 25 to 300 mg was investigated for the single solute system and 25 to 500 mg for the binary solute system. The optimum contact time and pH values realized from the kinetic experiment and pH-adsorption study respectively were used for the experiments.

4.2.3.4 Effect of Initial Concentration

The effect of concentration variation in both the single and binary solute systems were also investigated. The optimum pH and contact time realized from the kinetic experiment and pH-adsorption study were employed. Procedure for the adsorption experiments involve adding 0.15g of AC to 50 ml solutions of a different concentration of Cd^{2+}, phenol and the

binary mixture of Cd^{2+}-phenol. Details of the pollutants concentrations used, and other experimental parameters investigated in this research are provided in Tables 4.4 and 4.5 as follows;

Table 4.4: Adsorption experiment parameters investigated

Single Solute and Binary Solute Adsorption Parameters				
Compound	Concentration (mg/l)	Adsorbent Dosage (mg per 50 ml)	pH	Time (minutes)
Cd^{2+}	(25, 50,100,200,300)	25 50 100 200 300.	3 4 5 6 7	0 5 10 15 30 60 120 240 480 720 1440
Phenol	(50,100,150,200,250)			
Cd^{2+} -Phenol	Same concentration as in the single phase.			

Table 4.5: Initial concentrations variation for the multicomponent adsorption experiments

Cd^{2+} / Phenol	25	50	100	200	300
25	(25, 25)	(25, 50)	(25, 100)	(25, 200)	(25, 300)
50	(50, 25)	(50, 50)	(50, 100)	(50, 200)	(50, 300)
100	(100, 25)	(100, 50)	(100, 100)	(100, 200)	(100, 300)
200	(100, 25)	(100, 50)	(100, 100)	(100, 200)	(100, 300)
300	(300, 25)	(300, 50)	(300, 100)	(300, 200)	(300, 300)

4.2.3.5 Analytical techniques for the water samples

Each experimental sample was prepared in duplicate, with an included blank sample in each experimental run which has no added AC. pH measurements were conducted using the standard pH electrode-meter (Accumet XL15 pH meter). The samples were filtered off the AC using a filter paper (Whatman Grade no 41) and analyzed for their pollutants concentration. Cadmium analysis was done using Atomic Absorption Spectroscopy AAS (PerkinElmer, 700), by direct air-acetylene flame method. For each set of experiments, a non-linear calibration curve was created using the standard cadmium ion solution (1 g/l, Sigma-Aldrich). As for phenol, its analysis was conducted using UV-vis Spectrophotometer system (Shimadzu, Japan). Separate calibration curves were created for each set of experiments using the prepared blank samples of each experimental run. For each of the analysis, the sample was put into a cuvette, and the absorption value recorded

at a wavelength of 264 nm. The corresponding concentration was automatically calculated based on the calibration curve by the Spectrophotometer.

The following expressions provided were used in computing the removal efficiencies of each pollutant, and also their adsorption capacities by the AC sample.

$$q_e(mg/g) = (Co - Ct) * \frac{V}{m} \quad 4.5$$

$$Removal\ efficiency = \frac{Co-}{Co} * 100 \quad 4.6$$

q_e- is equilibrium adsorption capacity, which represents the pollutants in mg adsorb per gram of AC at equilibrium. C_o and C_t represent the initial and final concentration of the pollutants respectively. V- is the solution volume, and m (gram) - is the mass of the activated carbon used.

CHAPTER 5

RESULTS AND DISCUSSION

5.1 Preparation of Activated Carbon

5.1.1 Experimental Design layout and results

Sewage sludge was utilized as a precursor for AC production using the chemical activation method with three activating agents, namely $ZnCl_2$, KOH and H_3PO_4. Box-Behnken design (BBD), which is a special type of RSM techniques that consider three factors with three equally spaced levels, was chosen for the experimental design and response analysis. Factors of concern considered in the experimental design were, activating temperature, impregnation ratio and dwell time. Three equally spaced levels were chosen for each factor and coded as, low (-1), medium (0), and high (+1), as shown in Tables 4.1, 4.2, and 4.3. A total number of 13 randomized experimental runs were created for each activating agent with the aid of statistical software, Design Expert V.9. The responses values used for the analyses were based on methylene blue removal efficiencies and yields of the produced AC samples. The complete experimental design layout together with the obtained responses for each activation process are presented in Tables 5.1, 5.2, and 5.3. It should be noted that the factors were designated as A, B, and C, which represent temperature, impregnation ratio and dwell time, respectively.

Table 5.1: Experiment design and response results for $ZnCl_2$ activation

		Factor 1	Factor 2	Factor 3	Response 1	Response 2
Std	Run	A: Temp	B: Impreg R	C: Time	Yield	MB Removal
		(°C)	(Sludge: $ZnCl_2$)	(min)	(%)	(%)
6	1	800	1:0.6	60	56.5	96.3
10	2	700	1:1	60	58.4	97.9
5	3	600	1:0.6	60	55.4	91.825
11	4	700	1:0.2	120	48.2	20.3
3	5	600	1:1	90	59.6	97.8
12	6	700	1:1	120	64.7	96.225
9	7	700	1:0.2	60	54	28.075
1	8	600	1:0.2	90	49	21.2
4	9	800	1:1	90	53.9	96.6875
8	10	800	1:0.6	120	48	58
2	11	800	1:0.2	90	51.9	56.45
13	12	700	1:0.6	90	54.8	58.55
7	13	600	0.6	120	56	91.65

Table 5.2: Experiment design and response results for KOH activation

		Factor 1	Factor 2	Factor 3	Response 1	Response 2
Std	Run	A: Temp	B: Impreg R	C: Time	Yield	MB removal
		(°C)	(Sludge: KOH)	(min)	(%)	(%)
8	1	800	1:1	120	19.6	83.15
12	2	700	1:1.5	120	18.4	96.775
7	3	600	1:1	120	19.5	86.15
13	4	700	1:1	90	24.7	94.7
3	5	600	1:1.5	90	32.3	92.625
2	6	800	1:0.5	90	21.6	92.1
6	7	800	1:1	60	24.7	97.1
11	8	700	1:0.5	120	20.9	94.7
5	9	600	1:1	60	28.6	91.75
9	10	700	1:0.5	60	25.3	92.9
1	11	600	1:0.5	90	44.3	92.15
4	12	800	1:1.5	90	15.4	80.05
10	13	700	1:1.5	60	19.1	93.5

Table 5.3: Experiment design and response results for H_3PO_4 activation

		Factor 1	Factor 2	Factor 3	Response 1	Response 2
Std	Run	A: Temp	B: Conc.	C: Time	Yield	MB Removal
		(°C)	(% wt.)	(min)	(%)	(%)
10	1	700	50	60	57.1	92.65
13	2	700	40	90	54.2	80.125
1	3	600	30	90	65	75.875
2	4	800	30	90	56.2	14.75
5	5	600	40	60	59.4	91.55
11	6	700	30	120	66.8	69.675
6	7	800	40	60	52.4	15.45
8	8	800	40	120	49.8	16.85
12	9	700	50	120	51.6	92.3
3	10	600	50	90	58.2	94.4
4	11	800	50	90	45.3	45.6
9	12	700	30	60	67.6	79.475
7	13	600	40	120	59.3	97.05

5.1.2 Statistical Analysis and Model Fitting

Data analyses were automatically carried out with the Design Expert V.9.0 software. The software employs the least square regression method in fitting the experimental data to the selected polynomial function. Response transformation was done as needed on some of the responses in order to satisfy the normal distribution criteria. Different model types suggested by the software for both responses (yield and methylene blue removal efficiency) were refined by adjusting some of their terms, this was done to ensure that the model terms were not aliased. The derived empirical model for each activating agent with respect to the coded factors are presented as follows;

Models equation in terms of Coded Values

$ZnCl_2$ Activation

$$
\begin{aligned}
1/(\text{Yield}) = {} & +0.018 \\
& +6.562\text{E-}004 * A \\
& -1.672\text{E-}003 * B \\
& +1.403\text{E-}004 * C \\
& +7.287\text{E-}004 * AB \\
& +8.319\text{E-}004 * AC \\
& -9.739\text{E-}004 * BC \\
& +6.074\text{E-}004 * A^2 \\
& -1.833\text{E-}004 * C^2 \\
& +5.854\text{E-}004 * A^2B \\
& +5.949\text{E-}004 * A^2C \\
& -4.977\text{E-}004 * AB^2
\end{aligned}
$$

$$
\begin{aligned}
1/(\%\text{MB Removal}) = {} & +0.017 \\
& +1.456\text{E-}003 * A \\
& -0.016 * B \\
& +2.587\text{E-}003 * C \\
& +7.393\text{E-}003 * AB \\
& +1.709\text{E-}003 * AC \\
& -3.366\text{E-}003 * BC \\
& -4.927\text{E-}003 * A^2 \\
& +9.088\text{E-}003 * B^2 \\
& +4.989\text{E-}003 * A^2B \\
& -8.790\text{E-}003 * AB^2
\end{aligned}
$$

KOH Activation

$$\text{Sqrt (Yield)} = +4.99 - 0.092A - 0.24B - 0.25C + 0.062AB + 0.23A^2 - 0.43C^2 - 0.32A^2B - 0.85AB^2$$

$$\text{Sqrt (MB removal)} = +9.72 + 0.028A + 0.034B + 0.065C - 0.17AB - 0.11AC + 0.019BC - 0.27A^2 - 0.19A^2B - 0.32A^2C - 0.20AB^2$$

H_3PO_4 Activation

$$\text{Yield (\%)} = +59.46 - 4.13A - 6.42B - 1.13C - 1.03AB - 3.76A^2 + 2.00A^2B - 1.30AB^2$$

$$\text{MB \%R} = +82.84 - 39.08A + 10.65B - 2.54C + 3.08AB - 26.40A^2 + 4.26A^2C + 11.59AB^2$$

Table 5.4 shows a comparison between the observed experimental responses for each activating agent with the predicted responses based on the derived empirical models. As can be seen from the table, the predicted yields and methylene blue removal efficiencies for each activation process were in good agreement with the observed experimental responses. Correlation coefficient values (R^2) of the models, as shown in Table 5.5 were all close to unity (1), which support the similarity observed between the experimental and predicted data, and also affirming the reliability of the models.

As shown in Table 5.5, R^2, adjusted R^2, and the predicted R^2 computed for the $ZnCl_2$ activation process models were; Yield: 0.9996, 0.9952 and 0.8648, respectively, and MB removal efficiency: 0.9976, 0.9854 and 0.9042, respectively. As part of the conditions for model adequacy, Adjusted R^2 and predicted R^2 need to be in agreement, and this can only occur whenever their difference is less than or equal to 0.2. The observed difference for the yield model was 0.1304 and that of MB removal model was 0.0812. The adequate precision value of a model measures the signal-to-noise ratio, and a value greater than 4 is desirable for a model for it to adequately predict the experimental data within the design space. Adequate precision values of 50.60 and 24.258 achieved for the two models, showed that they are both of adequate signals. The average absolute deviation value (AAD) indicates the predictive capability of the developed models, and that highly reliable models usually present low AAD value. AAD values of 0.1388 and 4.8195 % were realized for the two models, respectively.

The two models developed for the KOH activation process presented an, R^2, adjusted R^2, and the predicted R^2 values for the Yield model as; 0.9701,0.9104 and 0.8119, respectively; and MB removal model; 0.9993,0.9956 and 0.9511, respectively. Adjusted R^2 and the predicted R^2 of the two models were found to be in good agreement as their difference in both cases were less than 0.2. Adequate precision values of 15.325 and 53.619 obtained for the two models show that they are both of adequate signal and can be used for predicting the experimental data. Likewise, the AAD values of 3.239 and 0.1374 % realized for both models also support their predictive capability for the experimental data.

As for the H_3PO_4 activation process the R^2, adjusted R^2, and the predicted R^2 values realized for the two models were; Yield: 0.9153,0.7966 and 0.6478, respectively; MB

removal: 0.9943,0.9862 and 0.9546, respectively. The difference between the Adjusted R^2 and the predicted R^2 for the two models were found to be less than 0.2 which shows that they are in good agreement. Adequate precision values of 9.417 and 27.814 realized for two models, also show that they are of adequate signal. Additionally, their AAD values of 2.1785 and 3.4637 %, respectively also support their predictive capability for the experiment data.

Table 5.4: Responses predictions for each of the activation process based on developed models

$ZnCl_2$ Activation				KOH Activation				H_3PO_4 Activation			
Yields (%)		MB Removal (%)		Yields (%)		MB Removal (%)		Yields (%)		MB Removal (%)	
Actual	Predicted	Actual	Predicted	Actual	Predicted	Actual	Predicted	Actual	Predicted	Actual	Predicted
56.5	57.10	96.3	108.31	19.6	19.78	83.15	79.98	57.1	54.17	92.65	96.03
58.4	58.90	97.9	92.02	18.4	16.56	96.78	96.79	54.2	59.46	80.13	82.84
55.4	55.97	91.83	102.68	19.5	21.46	86.15	89.25	65	64.52	75.88	76.72
48.2	48.54	20.3	20.82	24.7	24.90	94.70	94.48	56.2	55.72	14.75	15.58
59.6	60.12	97.8	97.36	32.3	30.69	92.63	89.61	59.4	60.96	91.55	94.16
64.7	65.31	96.23	107.42	21.6	22.81	92.10	89.00	66.8	64.75	69.68	69.65
54	54.42	28.08	27.67	24.7	24.48	97.10	100.26	52.4	52.7	15.45	16
49	49.35	21.2	21.24	20.9	20.70	94.70	94.71	49.8	50.44	16.85	19.44
53.9	54.32	96.69	99.71	28.6	26.34	91.75	88.30	51.6	51.91	92.30	90.95
48	48.43	58	56.10	25.3	25.50	92.90	92.93	58.2	57.74	94.40	91.86
51.9	52.29	56.45	57.92	44.3	46.02	92.15	95.61	45.3	44.82	45.60	43.04
54.8	55.56	58.55	58.82	15.4	14.29	80.05	83.21	67.6	67.01	79.48	74.73
56	56.59	91.65	86.99	19.1	20.88	93.50	93.51	59.3	58.7	97.05	97.6

Table 5.5: Important characteristics of the models

Activation	Response	Response Transformation	Adeq. Precision	R^2	Adj.R^2	Pred.R^2	AAD%
$ZnCl_2$ Activation	Yield %	Inverse	50.60	0.9996	0.9952	0.8648	0.1388
	MB R %	Inverse	24.258	0.9976	0.9854	0.9042	4.8195
KOH Activation	Yield %	Square Root	15.325	0.9701	0.9104	0.8119	3.239
	MB R %	Square Root	53.619	0.9993	0.9956	0.9511	0.1374
H_3PO_4 Activation	Yield %	None	9.417	0.9153	0.7966	0.6478	2.1785
	MB R %	None	27.814	0.9943	0.9862	0.9546	3.4637

Results of analysis of variance (ANOVA) performed at 5 % (0.05) level of significance on the models are presented in Table 5.6. The table shows the significance level of each model and its term based on the probability value (p-value) and the F-statistic value. A p-value > F > 0.050 indicate that the model or the term is statistically significant in predicting the experimental response, and if it is otherwise, it denotes the term or the model is insignificant.

Focusing on the $ZnCl_2$ activation process, the yield model presented a p-value of 0.0517 which is greater than 0.05 and therefore, implies that model is not significant. The significant model terms were found to be B, AB, AC, BC, as their p-value were all less than 0.05. As for the MB removal model, the model itself and the following terms, AB, AC, A^2, A^2B, A^2C, AB^2 were all statistically significant. Based on this outcome, it was concluded that for the two models developed, both

temperature (A), and dwell time (C) had no significant effect on the yield of the AC samples produced by $ZnCl_2$ activation, but impregnation ratio (B), and various cross product contribution (Interaction term) of each factor all showed a significant effect on the yield. As for MB removal model, all the single model terms i.e. temperature (A), impregnation ratio (B) and dwell time (C) showed a significant effect on the methylene blue removal efficiency of the produced AC samples, and some of the interaction terms were found to be insignificant.

Next, with regards to KOH activation process, the p-value of the yield model was found to be 0.0084 which is less than 0.05, and implies that the model is significant. Majority of yield model terms are all insignificant except for, C, C^2, AB^2 that showed P-value greater than 0.05. This outcome basically implies that dwell time and the cross-product interaction of temperature and impregnation ratio have a significant effect on the yield of AC samples produced by KOH activation. As for the MB removal model, the model itself was found to be significant as it presented a low p-value of 0.0036. The significant model terms for MB removal were C, AB, AC, A^2, A2B, A^2C, AB^2.

Similarly, for H_3PO_4 activation process, both the yield and MB removal models were all statistically significant due to their low p-value (yield:0.0194 and MB R:<0.0001). The significant model terms for the yield model were, A (temperature) and B (H_3PO_4 concentration), which denote they both have a great influence on the reported yields of the AC samples. As for of MB removal model, the significant model terms were, A, B, A^2, AB^2. This also implies that temperature, H_3PO_4 concentration, and their higher order term shown, contribute immensely to the outcome of methylene removal efficiency of the AC samples.

Table 5.6: Analysis of variance (ANOVA) at 5 % ($P < 0.05$) level of significance for each model developed

Activation	Response	Model	A	B	C	AB	AC	BC	A^2	B^2	C^2	A^2B	A^2C	AB^2
$ZnCl_2$ Activation	Yield %	0.0517	0.0531	0.0209	0.2374	0.0479	0.0419	0.0358	0.0685		0.2188	0.0839	0.0826	0.0985
	MB R %	0.0121	0.2366	0.0029	0.0523	0.0136	0.1888	0.0609	0.0419	0.0129		0.0559		0.0191
KOH Activation	Yield %	0.0084	0.4403	0.0929	0.0293	0.5920			0.1412		0.0287	0.2812		0.0050
	MB R %	0.0036	0.0897	0.0629	0.0186	0.0029	0.0067	0.1736	0.0014			0.0045	0.0016	0.0041
H_3PO_4 Activation	Yield %	0.0194	0.0404	0.0079	0.3378	0.5252			0.0795			0.3895		0.5672
	MB R%	<0.0001	<0.0001	0.0005	0.2348	0.1620			<0.0001				0.1697	0.0073

5.1.3 Response surface plots

The 3-D response surface and contour plots of the measured yield and methylene blue removal efficiency for each activation process were developed. This was done to be able to visualize and discern the effects of each factor (temperature, impregnation ratio, and dwell time) on the two observed experimental responses (yield and MB removal). Two factors 3-D response plots for each activation process are displayed in Figures 5.1 to 5.6. It should be noted that some of the plots only displayed the two interaction factors that were significant to the response, based on the developed models. The obtained plots were generated automatically with design expert software.

5.1.3.1 Effect of production factors on the yields of produced AC samples

Figures 5.1, 5.2 and 5.3, present the 3-D response surface and contour plots, showing the effects of temperature, impregnation ratio, dwell time and their interactions on the yields of AC samples produced by the three activating agents. As can be observed from Figure 5.1 which is for the $ZnCl_2$ activation process, impregnation ratio seems to have a more pronounced effect on the yields of the AC samples than temperature and dwell time. As depicted in Figure 5.1 a, an increase in impregnation ratio from 0.2 to 1 shows a favorable rise in the yield up to the maximum value of 64.5 %. This implies that the concentration of $ZnCl_2$ employed, during the activation process has a greater influence on the outcome of the yields obtained than other factors. This result was in line with what was also reported by S. Ucar et al [4] in their research work on AC production from pomegranate seed, in which they also observed that the concentration of $ZnCl_2$ affects the final yield of the produced AC sample. Also, the interaction effects of the temperature-impregnation ratio (Fig.5.1 a) and temperature-time (Fig.5.1 b) were both found to have an antagonistic effect

on the obtained yields, while the interaction of temperature-impregnation ratio (Fig.5.1c) shows a favorable effect for the conditions studied.

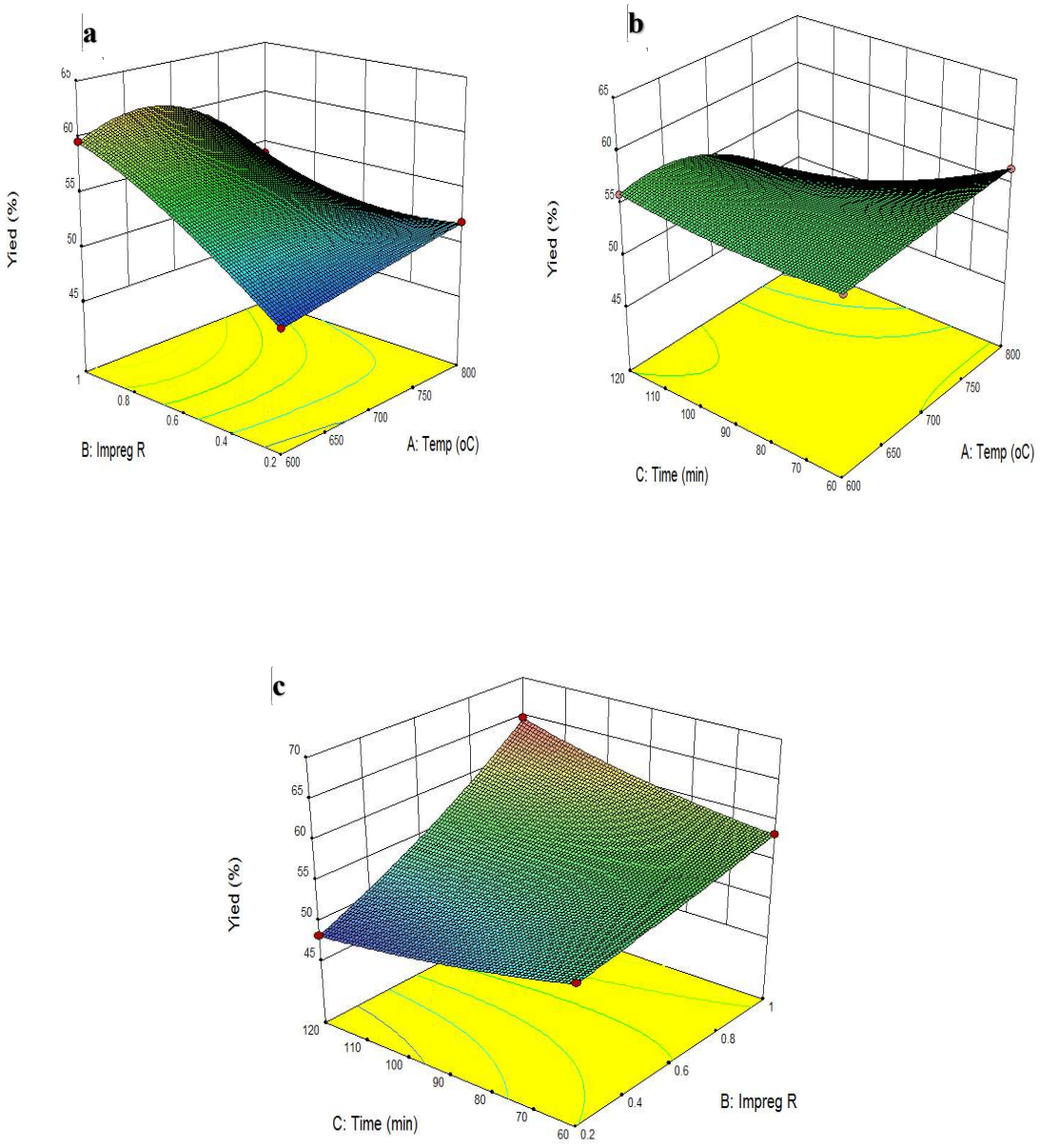

Figure 5.1: 3-D response surface plot showing the combined effect of the factors on the yields of AC samples produced by $ZnCl_2$ activation

Figure 5.2 shown is for KOH activation process, and it can be observed from the figure that the interaction of temperature with impregnation ratio have a negative impact on the yields of AC samples produced by KOH activation. As depicted, at the lowest level of both temperature and impregnation ratio, a high yield of 44 % can be observed, but as you move up to high levels for both factors a sharp drop in the response curve can be observed. This outcome was found to be in agreement with the statistical analysis result presented for KOH activation shown earlier. The influence of these factors on the yield can be attributed to the increase rate of gasification reactions (devolatilization) that occur at higher temperatures during carbonization, and also to the reaction mechanism of KOH with the carbonaceous precursor, that leads to high carbon loss during pores development [60]. Some authors have reported in their research work that in the course of pore development in KOH activation, intercalation compounds (K_2O and others) formed at high temperature do penetrate the carbon network, and in the process resulting in high carbon loss during volatilization [35,69]. The range of yields recorded for KOH activation were quite low for the chosen experimental conditions, which was around 15-45 %. However, this was found to be in agreement with previously reported studies on AC production with KOH activation [69–71].

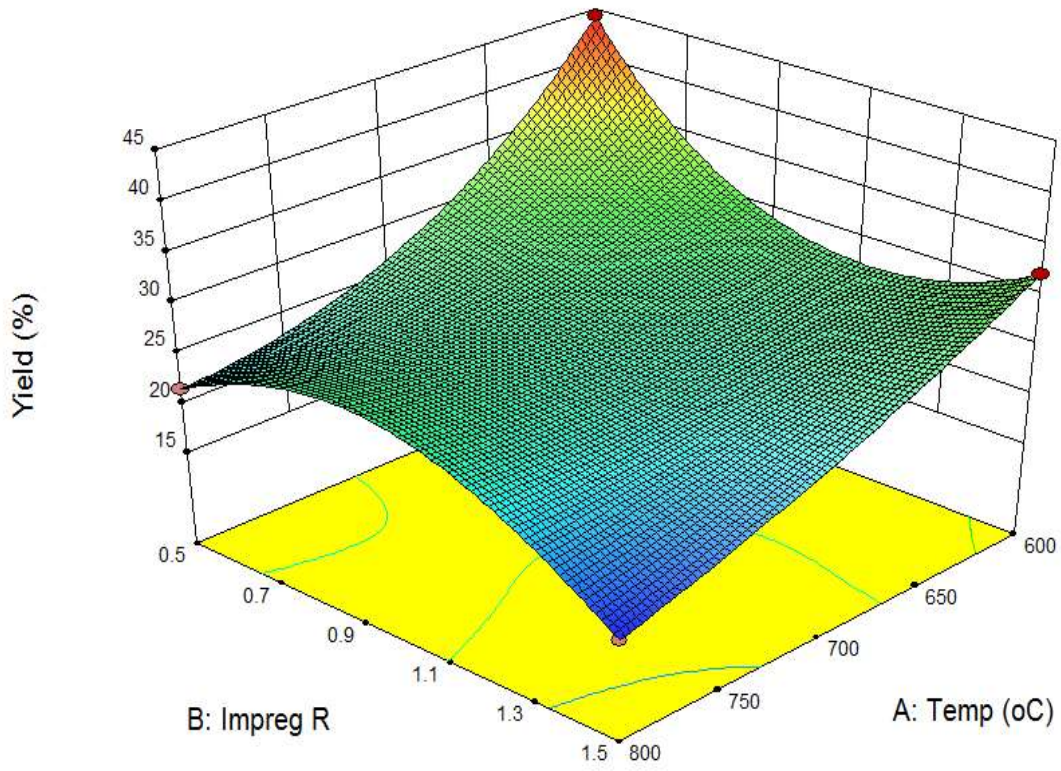

Figure 5.2: 3-D response surface plot showing the combined effect of the factors on the yields of activated carbons produced by KOH activation

The effect of the activation conditions on the yields of AC samples produced by H_3PO_4 activation are shown in Figure 5.3. It can be observed from the figure that the interaction of temperature and H_3PO_4 concentration have a negative impact on the yields of the produced AC samples. The increase in H_3PO_4 concentration from 30 to 40 % brought about a slight decrease in the yield as shown, this same trend pattern was also observed for temperature increase.

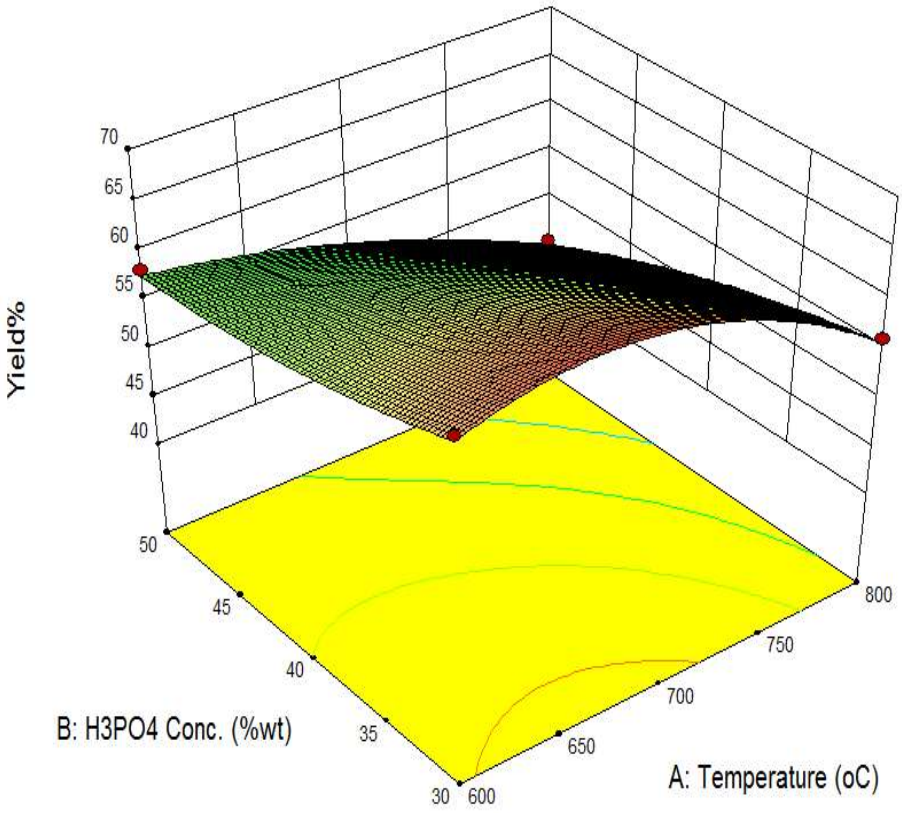

Figure 5.3: 3-D response surface plot showing the combined effect of the factors on the yields of activated carbons produced by H_3PO_4 activation

5.1.3.2 Effect of production factors on MB removal efficiency for the produced AC samples

Figures 5.4, 5.5 and 5.6 present the 3-D response surface and contour plots, showing the effect of temperature, impregnation ratio, dwell time and their interactions on methylene blue removal efficiency of the AC samples produced by the three activating agents. Figure 5.4, which is for the $ZnCl_2$ activation process shows that impregnation ratio has the most significant impact on the outcome of methylene blue removal efficiency than other factors. Figure 5.4 c shows a decrease in MB removal efficiency from 97 to 20 % as the impregnation ratio decreases from 1 to 0.2. This outcome can be better explained by noting that at higher impregnation ratios, the possibility of developing more pores according to

reaction mechanism of $ZnCl_2$ with the precursor, is more likely to occur than at lower ratios during the activation process. Zhang et al [64], have described in their research work on AC production from sewage sludge, that high $ZnCl_2$ concentration during activation process leads to its deposition on the external structure of the carbon particles, which consequently results in the decomposition of organic matter in its close vicinity, and further aiding in creating more porous structures [64]. As such, the high MB removal efficiency recorded for the high impregnation ratios AC sample is justifiable.

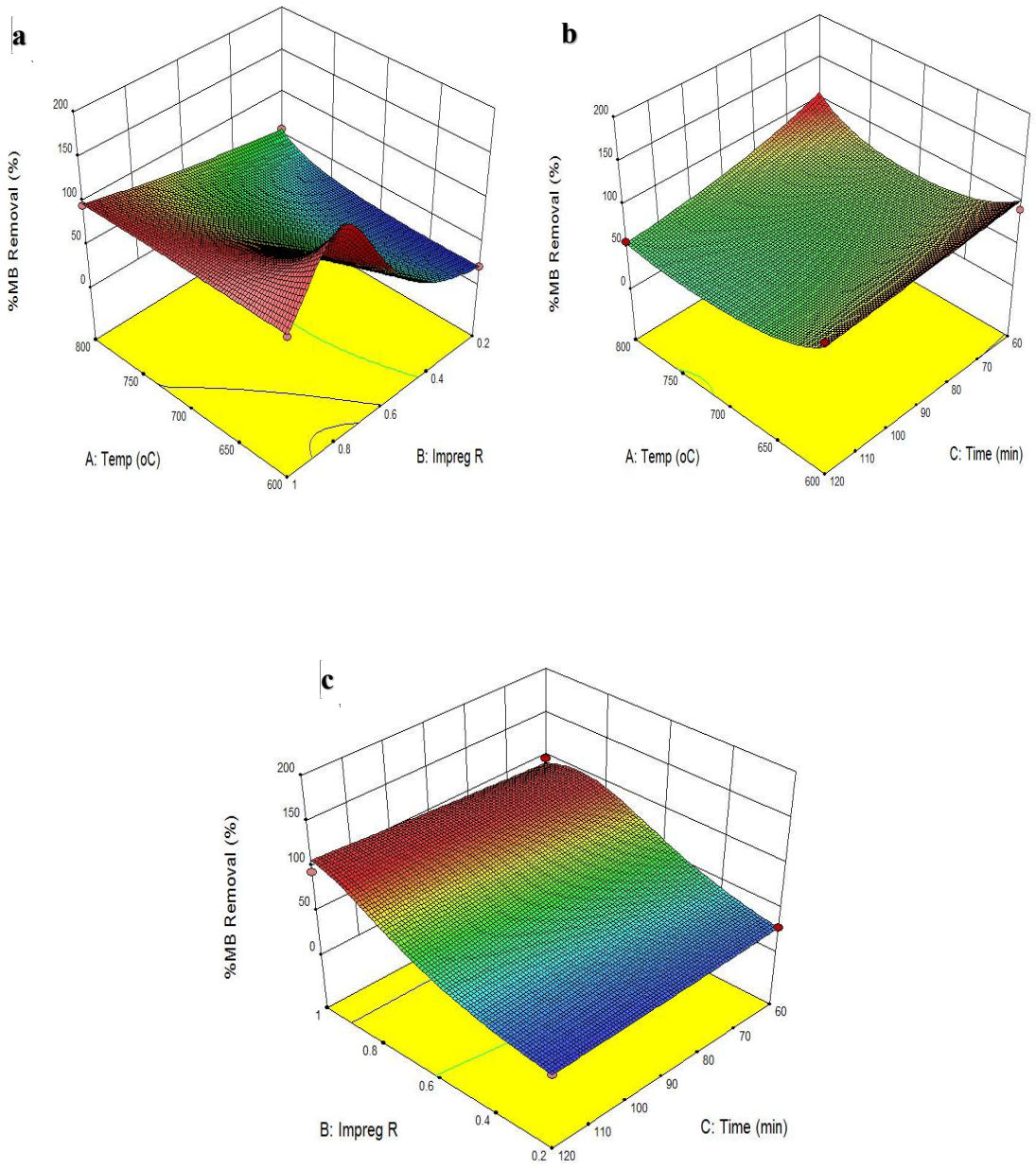

Figure 5.4: 3-D response surface plot showing the combined effect of the factors on MB removal efficiency of AC samples produced by $ZnCl_2$ activation

Figure 5.5 shown, presents the effect of the production factors on MB removal efficiencies of the AC samples produced by KOH activation. As can be observed from the figure, temperature appeared to be the dominant factor affecting the MB removal efficiencies. In both Figures 5.5 a and b, a high MB removal efficiency can be observed at high temperature values, with a corresponding low removal efficiency at low temperature. This outcome might have resulted from the effect of high temperature on the activation process that leads to increased rate of reaction of the sludge with the reagent, and in the process resulting in more pore structures formation. Several researchers have also reported the implication of high activation temperature on the adsorption properties of produced AC samples. For example, Djati et al [65] observed in research work on MB adsorption using biochar (non-activated) derived from sewage sludge, that sludge samples heated at high temperatures showed a high removal efficiency for MB. A maximum removal efficiency of 95 % was reported for a sludge sample heated at 700 ^{o}C for 2 hours.

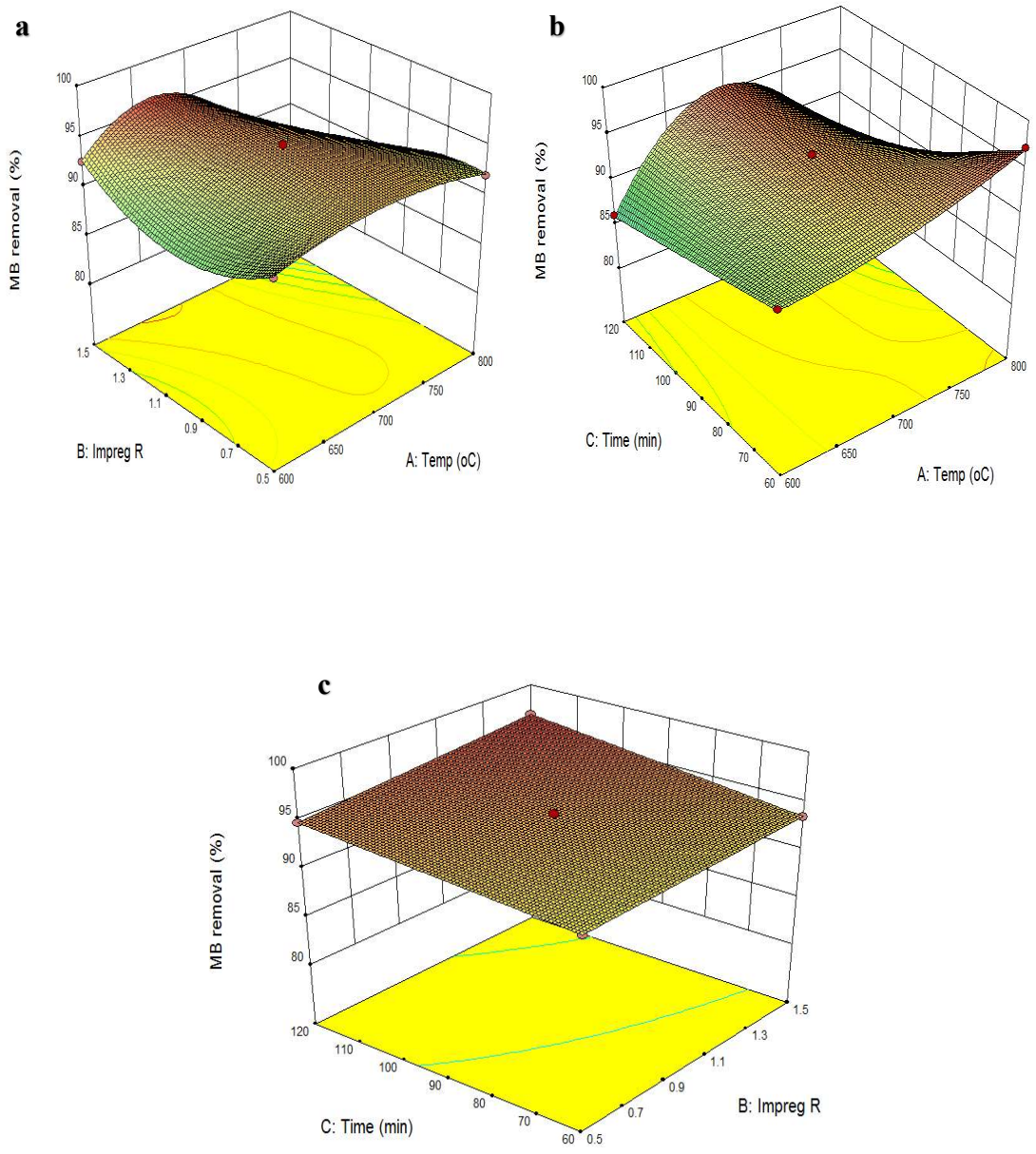

Figure 5.5: 3-D response surface plot showing the combined effect of the factors on the MB removal efficiency of AC samples produced by KOH activation

The effects of the production factors on MB removal efficiency for the AC samples produced by H_3PO_4 activation are presented in Figure 5.6. As can be observed from the figure, the influence of temperature on MB removal efficiency for all the samples is quite significant when compared to other factors. Figures 5.6 a, and b, show that an increase in temperature from 600 to 800 ^oC resulted in a decrease in MB removal efficiency to its lowest value of 15 %. This outcome was also attributed to the effect of high temperature as described for KOH activation earlier.

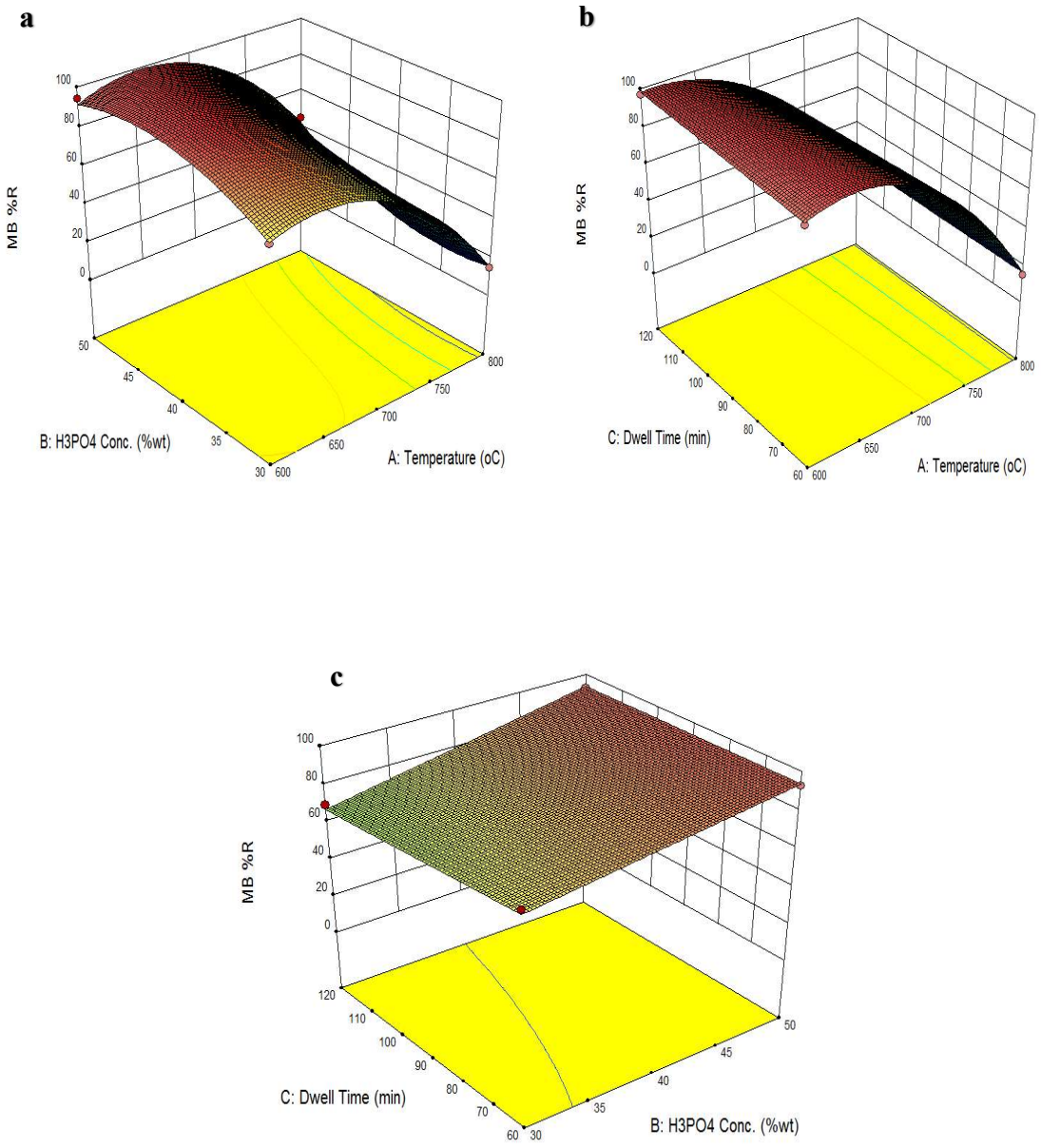

Figure 5.6: 3-D response surface plot showing the combined effect of the factors on MB removal efficiency of AC samples produced by H_3PO_4 activation

5.2 Characterization of the sludge and the AC samples

Some AC samples were selected from each of the activation processes, based on their high yields and high percent MB removal efficiency. These AC samples were further subjected to another round of MB adsorption experiment with a high concentration of MB (100 mg/l) for further screening. At the end, three AC samples were found to have outperformed the others in the adsorption of MB and were chosen for the characterization studies.

Two AC samples were chosen from $ZnCl_2$ activation process, and one from KOH activation process. The AC samples from the $ZnCl_2$ process were designated as AC1-$ZnCl_2$ and AC2-$ZnCl_2$. Where, AC1-$ZnCl_2$ was activated at a temperature of 700 ^oC, impregnation ratio of 1:1 (10 g sludge with 15 ml of 5 M $ZnCl_2$ solution), and dwell time of 120 minutes, AC2-$ZnCl_2$ was activated at the same conditions of impregnation ratio and temperature as AC1-$ZnCl_2$ but its dwell time was at 60 minutes. The selected AC sample from KOH activation process was designated as AC3-KOH and was activated at a conditions of temperature of 700 ^oC, impregnation ratio of 1:1.5, and dwell time of 60 minutes. Different characterization studies presented as follows were conducted for these AC samples and the sludge, to determine their surface properties, pores structures, and elemental compositions.

5.2.1 Elemental Analysis

Results of the elemental analysis presented in Table 5.7 shows the elemental composition of the AC samples and sludge. When comparing the carbon content of the sludge with those of the AC samples, a remarkable decrease can be observed which most likely might have resulted from initial volatilization of organics at a lower temperature of pyrolysis stage, and the carbon burn-off at higher temperature [24]. The low nitrogen content in the

AC samples (<3%) could indicate that majority of the functional groups are oxygen based [14]. The increase in the carbon-hydrogen (C/H) ratio of the AC samples in comparison to that of the sludge signifies an increase in the aromatization of the carbon structure resulting from the activation processes. The increase in the C/H ratio is of this order, AC1-$ZnCl_2$ < AC2-$ZnCl_2$ < AC3-KOH.

Table 5.7: Elemental composition of the sludge and the AC samples

Parameters	AC1-$ZnCl_2$	AC2-$ZnCl_2$	AC3-KOH	Sludge
C (%)	22.14	22.91	14.36	38.24
H (%)	1.05	1.35	1.11	5.17
N (%)	2.02	2.27	1.33	5.80
S (%)	1.24	1.19	0.12	1.33
Others (%)	73.55	72.28	83.08	49.46
C/H	21.09	16.97	12.94	7.40

5.2.2 Thermogravimetric Analysis (TGA)

The combined thermogravimetric (TG) and derivative thermogravimetric (DTG) curves of the d AC samples and the sludge are presented in Figure 5.7. Figures 5.7 a, and b, show those of $ZnCl_2$ AC samples and from these figures, it can be observed that both samples exhibited three stages of weight loss in response to temperature increase. The first stage occurring in the temperature range of 30-100 ^oC account for about 7 % losses and was attributed to the release of moisture from the AC samples. A negligible loss of approximately 4 % can be noticed in the temperature range of 100 -725 ^oC, with a more pronounced loss of approximately 22 % in the range of 725-1000 ^oC, both of which were

ascribed to the decomposition and volatilization of fused $ZnCl_2$ or ZnO and other inorganic constituents in the carbon structure resulting from the activation process [66].

The TG curve for the KOH AC sample is shown in Figure 5.7 c, and it can be observed that two stages of weight loss are apparent. In the temperature range of 30-150 ^oC an abrupt weight loss of approximately 9 % depicted, can be attributed to moisture loss resulting from vaporization, while the steady decline in weight from 150 to 1000 ^oC with a total loss of approximately 20 % was ascribed to the decomposition and volatilization of metallic oxides and some functional groups present in the carbon structure resulting from the activation process.

Figure 5.7 d, shows the TG curve of the sludge sample, and it can be observed from the curve that an appreciable weight loss of approximately 48 % appeared to have occurred at the temperature range of 200 - 600 ^oC. This outcome can be attributed to the pyrolytic reaction occurring within this temperature range, that results in the decomposition of organic constituents present in the sludge, followed by the release of volatile compounds [24]. The decomposition of aliphatic compounds and organic acids into gaseous byproduct have been reported by Pullket. et al [24] to occur at this temperature range. Organic compounds such as paper and cellulose present in the sludge might have been the source of this sharp weight decline [24]. At the temperature range of 600 -1000 ^oC, a much lower steady weight loss of approximately 14 % was observed, signifying that the sludge is thermally stable at this temperature range. In total, a weight loss of approximately 66 % is observed from the TG analysis of the sludge.

The DTG curves show the decomposition peaks for each of the AC samples and sludge, they identify the temperature region at which weight loss is most apparent in the samples. The DTG curves of the AC samples bear similar peak type, with sharp peaks occurring close to the temperature region of 100 ^{o}C in all samples (inclusive of the sewage sludge). A second shorter broad peak can be found around 750-800 ^{o}C for the $ZnCl_2$ AC samples, while in KOH AC sample a short sharp peak can be seen at the same temperature range. The sludge produced a considerable sharp peak at the temperature range of 750-800 ^{o}C, which was attributed to weight change resulting from inorganic constituents decomposition [24].

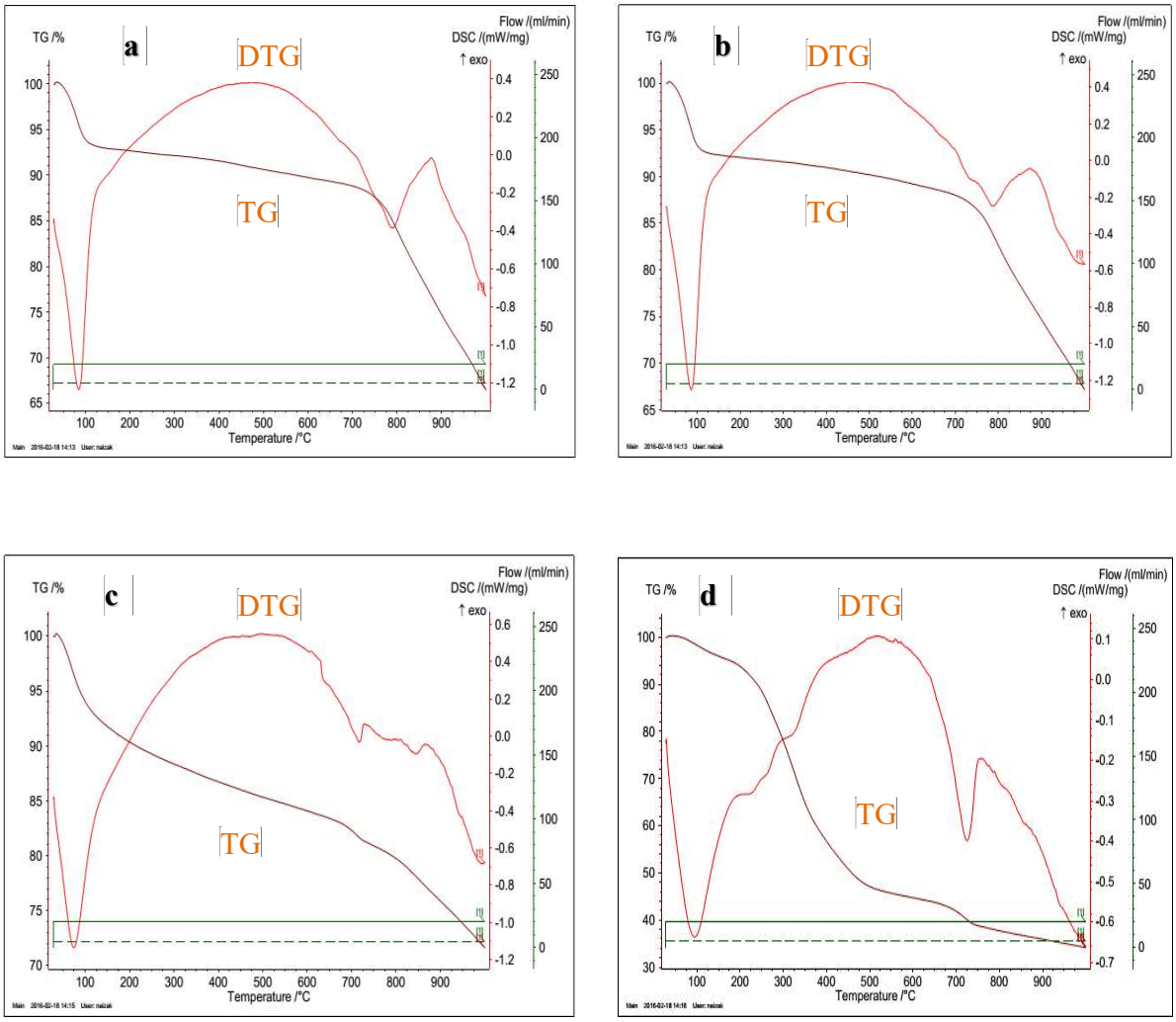

Figure 5.7: TG and DTG curves of the AC samples and the sludge

5.2.3 Porosity and Surface Area Analysis

Table 5.8 shows the surface properties of the AC samples and that of sludge, as determined from the Nitrogen adsorption-desorption isotherm at 77 K, using the Accelerated Surface Area and Porosimetry System (ASAP) 2020 (Micromeritics) instrument. The specific surface area (SSA) was determined using BET method, and micropore area and volume obtained via t-plot method.

The specific surface area (SSA_{BET}) of the sewage sludge was low (0.664 m^2/g), when compared to reported values in the literature of approximately 3 m^2/g [7,10], and this was attributed primarily to the characteristics of the sludge used. An improvement in the surface properties of the sludge after the chemical activation process as shown by the SSA_{BET} of the AC samples, directly indicate the removal of organics and inorganics present in the sludge which resulted in the improved surface properties [10]. The SSA_{BET} of the three AC samples were low and marginally close, being around 314 to 348 m^2/g, thus, suggesting that the activating reagents ($ZnCl_2$ and KOH) employed do not contribute significantly to pore development. These values were lower than those reported in the literature for sewage sludge AC. For example, the highest SSA_{BET} reported for sewage sludge activation by KOH (KOH: Sludge ratio 1:1) was 1882 m^2/g achieved by Lillo-Rodenas et al [63] in their two stage activation method, where the sludge was firstly carbonized i.e. charred, before impregnation and activation. Also, Guoren Xu et al [36] review on sludge-based adsorbents reported that the highest SSA_{BET} achieved from $ZnCl_2$ activation of sewage sludge was 757 m^2/g. The low SSA_{BET} values achieved in this current research work is most likely due to AC samples non-microporous nature. The pore sizes of the AC samples were found to be in the range of 3-7 nm, and based on this, it can be concluded that the activation

processes created a mesoporous AC, where mesopores diameter are between 2 and 50 nm. Similar results were also observed by Anirudh Gupta et al [10] in their AC production from sewage sludge using KOH and $ZnCl_2$ as the activating agent. Although, their reported SSA_{BET} (495–515 m^2/g) was higher than those achieved in this study, the difference could be attributed to the production method employed, where the pyrolysis was not done in inert environment but in low oxygen environment, also the disparity might be due to the low organic contents of sludge used in this study as shown in the elemental analysis.

Table 5.8: Specific surface area properties of the sludge and the AC samples

Sample	Activation Conditions (temp./time/Conc)	SSA_{BET} Total (m^2/g)	Micro pore Area (m^2/g)	External Area (m^2/g)	V_{Total} (cm^3/g)	V_{micro} (cm^3/g)	D_p (A^o)
AC1-$ZnCl_2$	700°C/120min/5M	314.4	101.06	213.35	0.246	0.176	31.31
AC2-$ZnCl_2$	700°C/60min/5M	319.5	102.45	217.04	0.249	0.0056	31.28
AC3-KOH	700°C/120min/1:1.5	347.7	67.79	279.96	0.640	0.0364	69.51
Dried Sludge	N/A	0.664	N/A	N/A	0.0127	0.0016	763.82

5.2.4 Surface Morphology

The surface morphology of the sludge and AC samples was investigated using the SEM technique as presented in Figure 5.8. It can be observed from the figure that image (a) which is for sludge without activation shows a compact sample with no sign of visible pores. This image thus supports the low S_{BET} (0.664 m^2/g) realized for the sludge. However, upon the sludge activation with $ZnCl_2$ and KOH, an improvement was noticed, as shown in the SEM image of (b), (c) and (d) which are for AC1-$ZnCl_2$, AC2-$ZnCl_2$, and AC3-KOH respectively. When comparing the images of the $ZnCl_2$ AC samples with that of KOH, few cavities and pore structures can be clearly seen in AC1-$ZnCl_2$ and AC2- $ZnCl_2$, with no sign of pores in AC3-KOH. This outcome could explain better why the $ZnCl_2$ AC samples have more micropore surface area than that of the KOH, Although KOH AC sample presented the highest total surface area as realized from the BET analysis results.

The formation of these cavities and pores in the $ZnCl_2$ AC samples might have resulted from the decomposition of $ZnCl_2$ during the carbonization process leaving behind those pores and cavities [2]. Additionally, the washing step might have assisted in making the pores visible via the removal of trapped $ZnCl_2$ and ZnO [25]. As for AC3-KOH, the effect of its activation process have resulted in increasing its surface roughness, as evidenced from its SEM image, as well as its high external surface area. Similar findings were also reported by Glaydson et al [67] in their research work on AC production from sewage sludge [67].

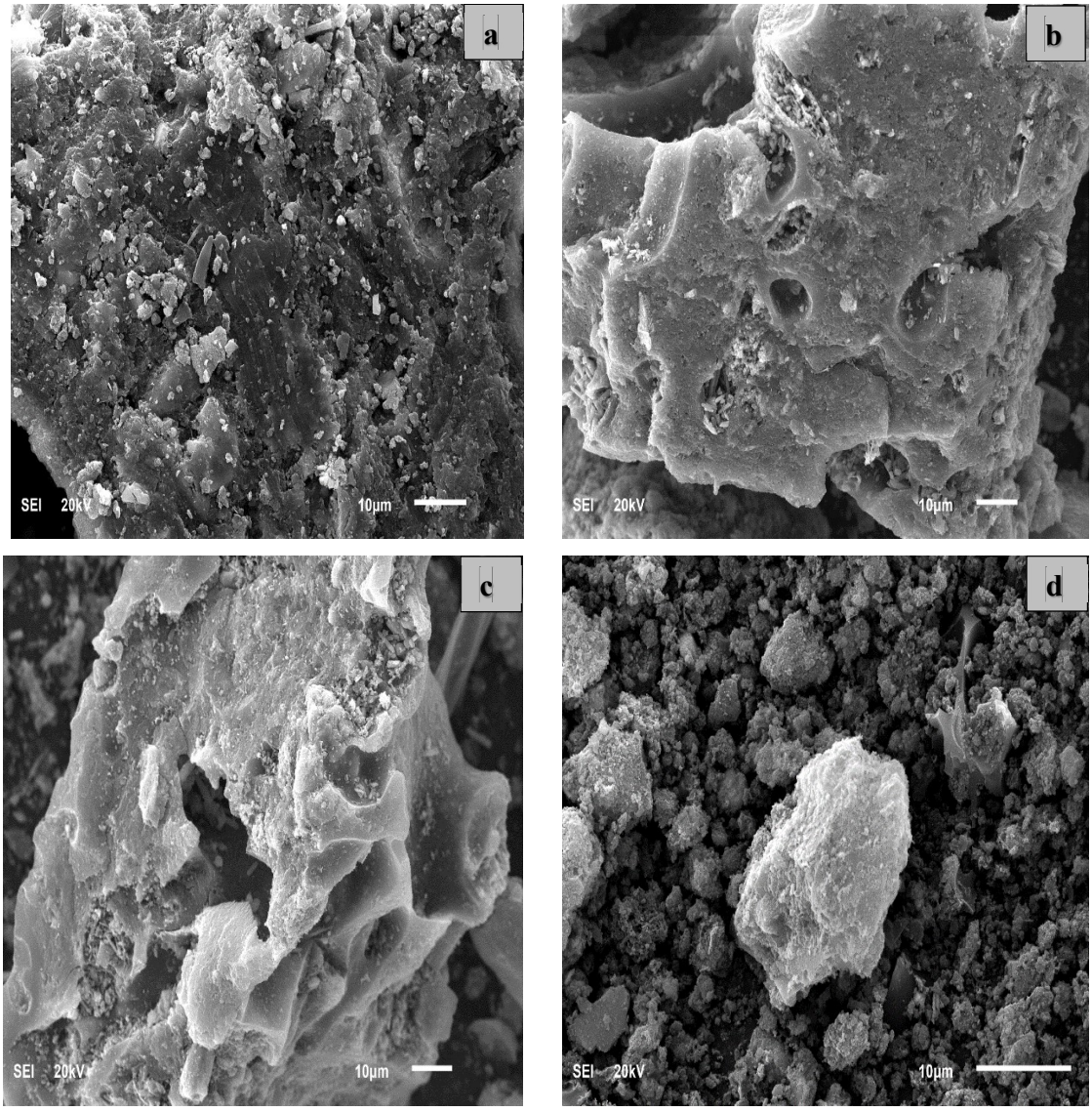

Figure 5.8: SEM image of (a) Sewage Sludge (b) AC1-ZnCl2 (c) AC2-ZnCl2 (d) AC3-KOH

5.2.5 X-ray Diffraction Spectroscopy

The XRD patterns of the sludge and those of the AC samples are depicted in Figure 5.9 as shown. The appearance of several sharp peaks in all the samples confirms the presence of crystalline minerals in all the AC samples and in the sludge. The sludge XRD pattern shows several sharp peaks identified to have been due to the presence of calcite, dolomite, carbon, and quartz. Zinc silicate mineral (Willemite) was observed to be prominent in the $ZnCl_2$ AC samples (AC1-$ZnCl_2$ and AC2-$ZnCl_2$), and this most likely might have resulted from the reaction of quartz (SiO_2) present in the sludge with the $ZnCl_2$. AC1-$ZnCl_2$ and AC2-$ZnCl_2$ share similar XRD pattern, except for the graphite (carbon) peak which appeared lower in AC1-$ZnCl_2$, that was attributed to the high carbonization time employed, which was 120 minutes as opposed to 60 minutes used for AC2-$ZnCl_2$. Also, the presence of Hematite (Fe_2O_3) in both AC1-$ZnCl_2$ and AC2-$ZnCl_2$ might have resulted from the iron tubes used during the carbonization process.

The diffraction pattern of AC3-KOH shows the presence of calcite, graphite, and quartz. Calcite peak in AC3-KOH appears to have decreased when compared to that of sewage sludge. This as reported by Ahmad et al [7] in their review paper on sludge based adsorbent, might have been due to the decomposition of calcite ($CaCO_3$) into calcium oxide (CaO) at high temperature. Results of the XRF analysis also confirm the presence of a relatively high percentage of calcium oxide in AC3-KOH.

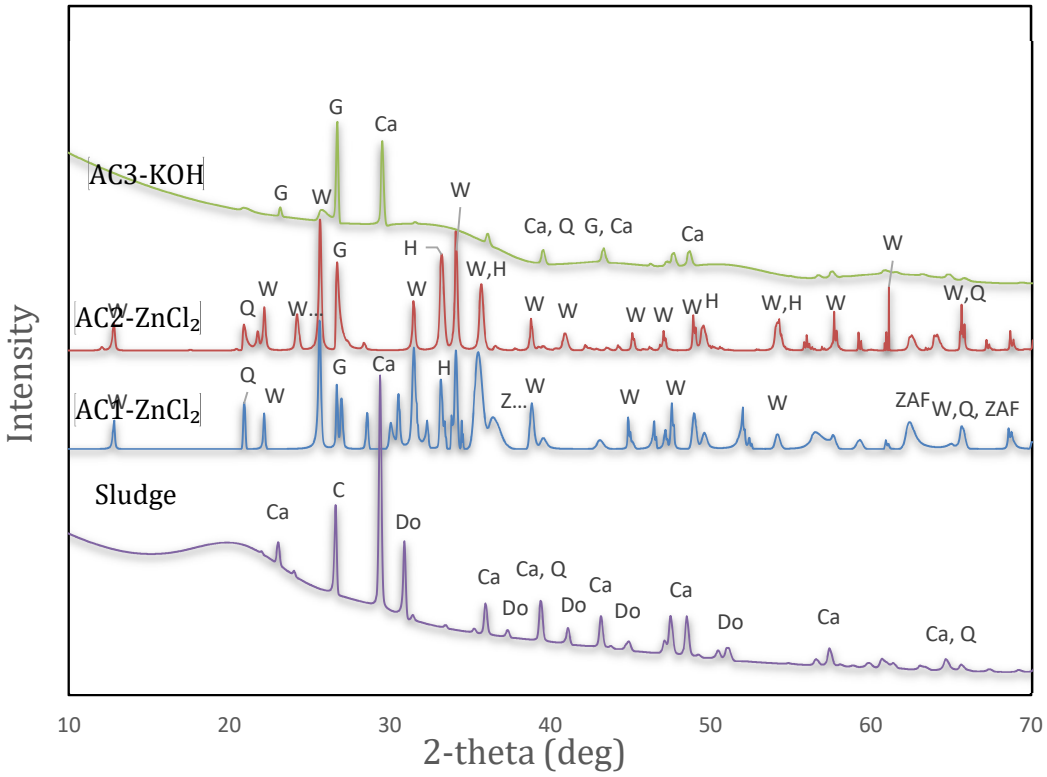

Figure 5.9: XRD pattern of the dried sludge and the AC samples

Abbreviations		
W	Willemite	Zn_2SiO_4
Ca	Calcite	$CaCO_3$
C	Carbon	C
G	Graphite	C
Do	Dolomite	$CaMg(CO_3)_2$
Q	Quartz	SiO_2
H	Hematite	Fe_2O_3
ZAF	Zinc Aluminum Iron Oxide	$Al_2FeO_2O_4ZnO_8$

5.2.6 X-ray Fluorescence Analysis

Table 5.9 provided shows the XRF results of the sludge and the AC samples. The Table depicts the percent concentration of oxides of elements present in the samples. Major oxides identified in the sludge were calcium oxide, Iron(III) oxide, and Silica, which are 36 %, 13%, and 8%, respectively. A similar proportion of these oxides but with a slight increase can also be seen in the AC3-KOH. The cause of this increase is likely due to the concentration of inorganic constituents of the sludge during the carbonization process, where organics are volatilized. Similar observation was reported by Ros et al [37] in their research work, where they observed that concentration of inorganic minerals in the sewage sludge char (pyrolzed sludge) tend to double after thermal treatment. As expected, the concentration of potassium oxide (K_2O) in AC3-KOH was more when compared to those of the sludge and other AC samples. Also, the percent concentration of Zinc Oxide (ZnO) in AC1-$ZnCl_2$ and AC2-$ZnCl_2$ was also found to be higher, and this must have resulted from their activation with $ZnCl_2$.

Table 5.9: XRF analysis results showing the elemental compositions of the AC samples and the sludge

Concentration (%)	Symbols	AC1-$ZnCl_2$	AC2-$ZnCl_2$	AC3-KOH	Sludge
Aluminum	Al_2O_3	2.208	2.354	4.710	3.606
Silicon	SiO_2	4.672	4.651	12.41	8.387
Phosphorus	P_2O_5	5.090	5.089	10.07	7.819
Sulfur	S	1.552	1.651	0.4405	5.098
Chlorine	Cl	2.845	3.035	0.2411	0.815
Potassium	K_2O	0.04734	0.04302	1.668	1.106
Calcium	CaO	9.479	10.85	39.29	35.78
Chromium	Cr_2O_3	3.13	3.146	0.7051	0.1529
Iron	Fe_2O_3	39.32	34.93	15.46	12.60
Zinc	ZnO	24.76	27.89	3.605	2.721

5.2.7 Fourier Transform Infrared Analysis (FTIR)

FTIR spectra of the sludge and those of the AC samples are presented in the Figure 5.10. As can be observed from the figure, the broad bands appearing in the range of 3700-3200 cm^{-1} for all the samples can be attributed to the presence of free O-H functional group or N-H amides group. The N-H amides group is mostly likely to be present in sludge, as it could result from the presence of protein structure [24]. The appearance of strong intensity band at this range for AC3-KOH could signify the presence of significant O-H functional group, which might have been due to its activation with KOH.

The band at 2924.6 and 2851.3 for the sludge spectra was ascribed to C-H stretching of aliphatic hydrocarbon structure, which can be associated with the glicydic part of lipids [23, 36]. These two bands were absent in the AC samples and could have been due to lipid removal during the pyrolysis stage.

The strong bands at 1666.1 and 1636.8 for the sludge and AC3-KOH, respectively, were assigned to C=O (Carbonyl group) stretching in primary amide, which also supports the presence of lipids in the sludge [7]. Moreover, the band at 1540.9 for the sludge was attributed to N-H stretching in primary amides, confirming the presence of protein structure in the sludge [9]. In addition, the band at 1412.7 for the sludge and 1388.3 for AC3-KOH were assigned to the presence of organic sulfate. Similar band was also reported by Ros et al [33] in their research on AC production from sewage sludge.

AC1-$ZnCl_2$ and AC2-$ZnCl_2$ both have a weak band at 1100.7 and 1043.5 respectively, that was attributed to carboxyl group (C-O stretching) presence. Similarly, the band at 1591.8 for both samples were associated with C-C stretching of aromatic group.

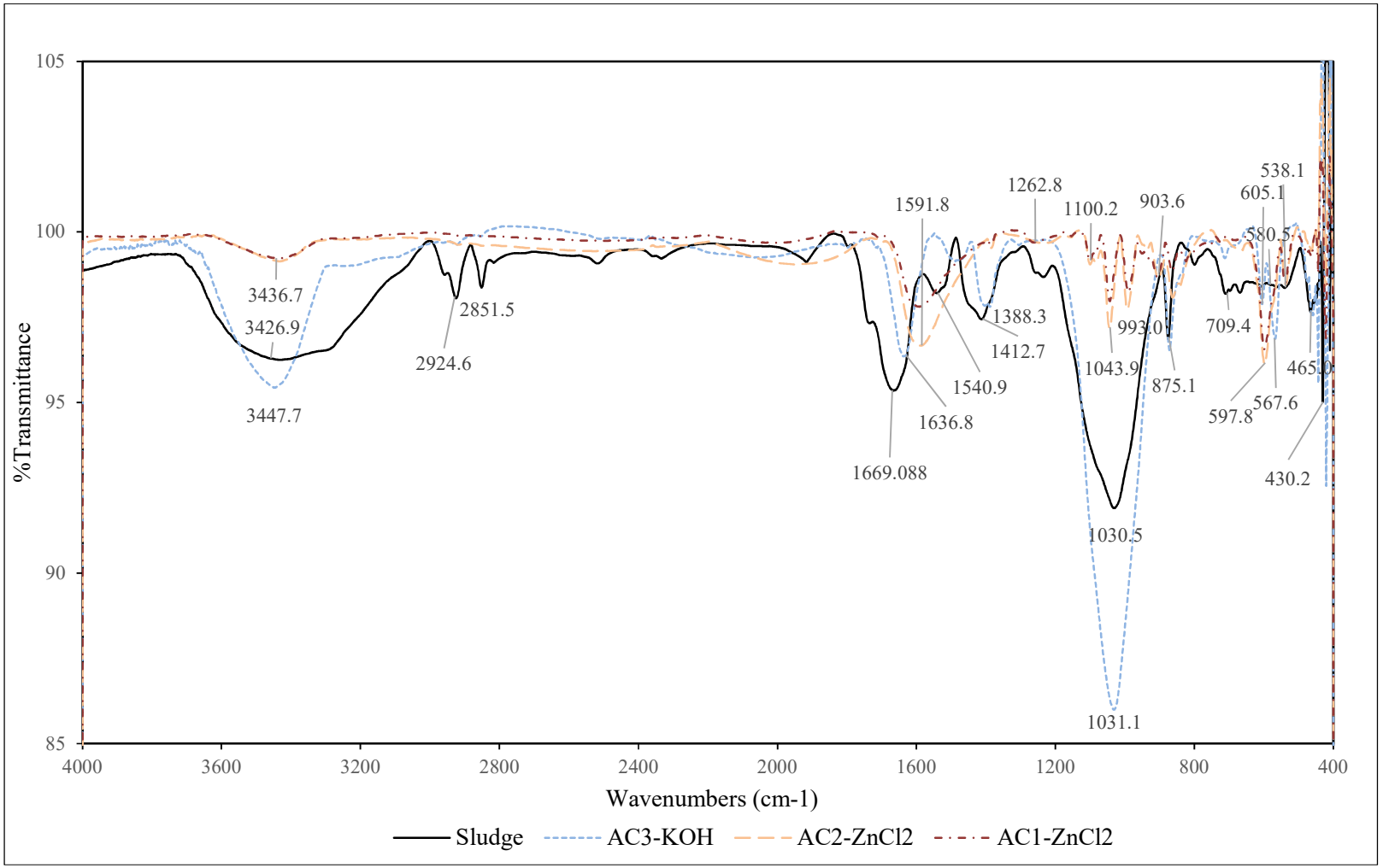

Figure 5.10: FTIR spectra of the sludge and the AC samples

The presence of inorganic compounds in the sludge is noticeable in the strong bands appearing at 1030.5 and other weak bands at 463.0, 443.6 and 432.3. Which were all assigned to silica ion Si-O-Si bending, resulting from the presence of quartz or feldspar [24]. These same sets of bands were also found in AC3-KOH, but with a stronger band at 1031.1, signifying the presence of significant amount of silica. The XRF analysis also confirms the presence of a relatively high percentage of silica in AC3-KOH.

The silica ion band were also found in AC1-$ZnCl_2$ and AC2-$ZnCl_2$ at bands 463.0, 443.6,432.3 and 461.0, 443.4, 420.4, respectively. Still, on the inorganic constituents, sharp bands at 871.1, 871.3, 862.2 and 864.1for the sludge, AC1-$ZnCl_2$, AC2-$ZnCl_2$ and AC3-KOH, respectively were assigned to calcite presence [23,36]. This also supports the XRD and XRF results that indicated the presence of calcite in all the samples. Another notable inorganic compound identified in all the samples was phosphate, which appeared in form of PO_4^{3-} bending, and was noticeable in the band region of 500-600 cm^{-1}.

When comparing the spectra of the sludge with those of the AC samples, it can be deduced that the conversion of the sludge to AC through the chemical impregnation process and carbonization, brought about an improvement in the surface properties, where new functional groups were noticeable in the AC samples. In summary, the functional groups identified in the AC samples were O-H, C-C, C-O, and C=O, and the presence of these groups on AC surface have been reported to be highly effective for heavy metals and toxic organics uptake[15,48]. Tables 5.10-5.13 give a summarized information of the functional groups identified in all the samples.

Table 5.10: FTIR functional groups identification for the sewage sludge

Band and Peak Position (wavelength cm^{-1})	Functional Groups/Compounds	References with the same band
3700-3200 peak~3426.9	O-H group of Alcohols, -NH2 and N-H Amine groups	[7], [9], [24], [68]
2924.6 and 2851.3	C-H Stretching in Aliphatic Carbon	[7], [24]
1784-1635 peak~1666.1	C=C stretch Aromatic Carbon or C=O carbonyl group	[7], [24]
1540.9	N-H stretching in Amides	[7], [24]
1412.7	S-O stretching in Sulfate ester Organic Sulphate	[37]
1200-900 peak~1030.5	Si-O-Si bending in Silica Quartz or feldspar	[24]
875.1, 709.4	Calcite band	[24], [37]
580.5, 538.1	Phosphate (PO_4^{3-}) bending	[18]
465.0, 430.2	Si-O-Si bending in Silica quartz and feldspars	[18]

Table 5.11: FTIR functional groups identification for AC1-$ZnCl_2$-700 ^oC-120 minutes

Band and Peak Position (wavelength cm^{-1})	Functional Groups Groups/Compounds	References with the same band
3600-3300 peak~3436.7	O-H group of Alcohols Hydroxyl group or N-H group of Amides	[10]
1700-1400 peak~1591.8	C-C stretching in Aromatic	
1100.7	C-O Stretching in Alcohols Carboxylic group	[24]
1043.5	C-O Stretch in Alcohols Carboxylic group	[10], [68]
989.4, 907.1	=CH deformation in Alkene	
864.1, 823.6	Calcite band	[37]
597.8, 537.7	Phosphate (PO_4^{3-}) bending	[24]
463.7, 443.6, and 421.4	Si-O Bending Silica Quartz or feldspar	[24]

Table 5.12: FTIR functional groups identification for AC2-$ZnCl_2$-700 ^oC-60 minutes

Band Position (wavelength cm^{-1})	Functional Groups Groups/Compounds	References with the same band
3700-3400 peak~3434.6	O-H group of Alcohols Hydroxyl group or N-H group of Amides	[6]
1700-1400 peak~1591.8	C-C stretch in Aromatic	
1100.2	C-O Stretch in Alcohols Carboxylic group	[6,75]
1043.9	C-O Stretch in Alcohols Carboxylic group	(6,75)
993.0, 903.6	= CH deformation in Alkene	[33]
862.2	Calcite band	(33)
597.8, 536.6	Phosphate (PO_4^{3-}) bending	[18]
463.0, 443.6 and 432.3	Si-O Bending Silica Quartz or feldspar	[18]

Table 5.13: FTIR functional groups identification for AC3-KOH-700 ºC-60 minutes

Band Position (wavelength cm^{-1})	Functional Groups	References
3700-3300 peak~3447.7	O-H group of Alcohols Hydroxyl Group or N-H group of Amides	[18,19]
1636.8	C=O Stretching in Amides or carbonyl group	[18]
1388.3	SO_2 anti sym. stretch in sulfonyl chlorides	[33]
1031.1	Si-O-Si bending in Silica Quartz or feldspar	[18]
871.6	Calcite band	[33]
605.1, 567.6	Phosphate (PO_4^{3-}) bending	[18]
461.0, 443.4 and 420.4	Si-O Bending Silica Quartz or feldspar	[18]

5.3 Adsorption Experiments

Porosity and surface area characteristics of an AC such as its surface functional groups, pores structures, and elemental compositions, are major influencing factors that determine its adsorptive capability for pollutants. These factors, with a preliminary adsorption experiment conducted for Cd^{2+} and phenol removal, were employed as criteria for selecting the best AC sample for the adsorption experiments. AC2-$ZnCl_2$ was selected among the characterized AC samples, due to its better surface properties and high adsorption capacity for the pollutants. In this regards, the optimum activation conditions for the $ZnCl_2$ AC samples were noted as that for AC2-$ZnCl_2$, which were; temperature of 700 ^oC, impregnation ratio of 1:1, and dwell time of 60 minutes. Single solute and multicomponent adsorption experiments of Cd^{2+} and phenol were carried out from a synthetic wastewater employing the AC2-$ZnCl_2$ AC sample.

5.3.1 Single Solute adsorption of Cd^{2+} and Phenol onto the prepared AC

Single solute batch adsorption experiments of Cd^{2+} and phenol were carried out from an aqueous solution using the produced AC, and the various adsorption parameters that include pH, initial concentration, adsorbent dosage and contact time were all investigated.

5.3.1.1 Effect of initial pH on adsorption of Cd^{2+} and Phenol

The influence of pH on adsorption process is an important parameter, as it determines the ionization of the adsorbate in the aqueous phase as well as the surface charge of the adsorbent being employed. The interaction of the adsorbate with the adsorbent, which ultimately determines the adsorption efficiency is pH dependent. Hence, the effect of initial pH on the single solute adsorption of Cd^{2+} and phenol was investigated at different pH

values varied from 3 to 7 (3, 4, 5, 6, and 7). Results of batch adsorption experiments conducted employing 50 ml solution of 100 mg/l of Cd^{2+} and phenol, with AC dose of 0.15 g, and contact time of 2 hours, are presented in Figures 5.11 and 5.12. Also included in these figures, are the effect of pH adjustment on the concentration of blank samples of Cd^{2+} and phenol. From the figures, it can be observed that the increase in pH for both Cd^{2+} and phenol resulted in increased removal efficiency. Cadmium adsorption in Figure 5.11 shows an initial removal efficiency of 16 % at pH 3, with an enhanced removal of up to 40 % at pH 7. This observed removal efficiency can be primarily attributed to the existence of an electrostatic force of attraction between the AC surface and Cd^{2+} ions in solution. Results of the FTIR analysis conducted has confirmed the presence of oxygen-based functional groups such as O-H and C-O on the AC surface (see section 5.2.7). So, it can be deduced that Cd^{2+} removal from the solution by the AC must have been due to its electrostatic interaction with these negatively charged functional groups. Furthermore, the low Cd^{2+} removal efficiency noticed at lower pH value could be related to Cd^{2+} and hydrogen ion (H^{+}) competing for adsorption sites on the AC surface, and as it can be noticed, as pH was increased removal efficiency increases, resulting from H^{+} ions decrease and in the process freeing more space for Cd^{2+} ions to bind onto the AC surface. Results of pH variation on Cd^{2+} concentration (blank samples) also depicted in Figure 5.11 shows a significant Cd^{2+} removal at a pH range of 6-7, that can be attributed to the effect of combined adsorption and precipitation occurring within these pH range. Similar observation was also reported by Al-Malack and Basaleh [6] for Cd^{2+} adsorption onto AC derived from municipal organic solid waste.

Based on this outcome, an optimum pH value of 5.5 was selected and use for all other experiments to ensure that Cd^{2+} removal is mainly due to adsorption and not with combined precipitation. Phenol adsorption as depicted in Figure 5.12, can be seen to experience a slight increase in removal efficiency from 47 to 50 % as pH increases from 3 to 5, and thereafter it became constant with no change in removal efficiency noticed for both pH 6 and 7 (50%). Similar adsorption behavior was also been reported by Pirzadeh and Ghoreyshi [15] in their research work on phenol removal using paper mill sludge AC. It can be observed from the result of pH variation on phenol concentration of blank samples also shown in Figure 5.12, that the chosen pH values had no effect on phenol concentration. This is possibly due to phenol high pKa value of 9.95, which implies that it will appear in undissociated form in the chosen pH range. As such, it could be ruled out that phenol adsorption by the AC is not based on electrostatic force of attraction. Several research works have attributed phenol adsorption on AC has been due to its chemical interaction with the AC surface functional groups (O-H and C=O) via electron-donor acceptor reaction mechanism [10,54]. Where, the AC functional groups act as an electron donor, and phenol being the electron acceptor. It is possible that this reaction mechanism might have accounted for phenol removal. Due to the high removal efficiency noticed at a pH range of 5-7, a pH value of 5.5 was also selected as optimum for phenol and used for other adsorption experiments.

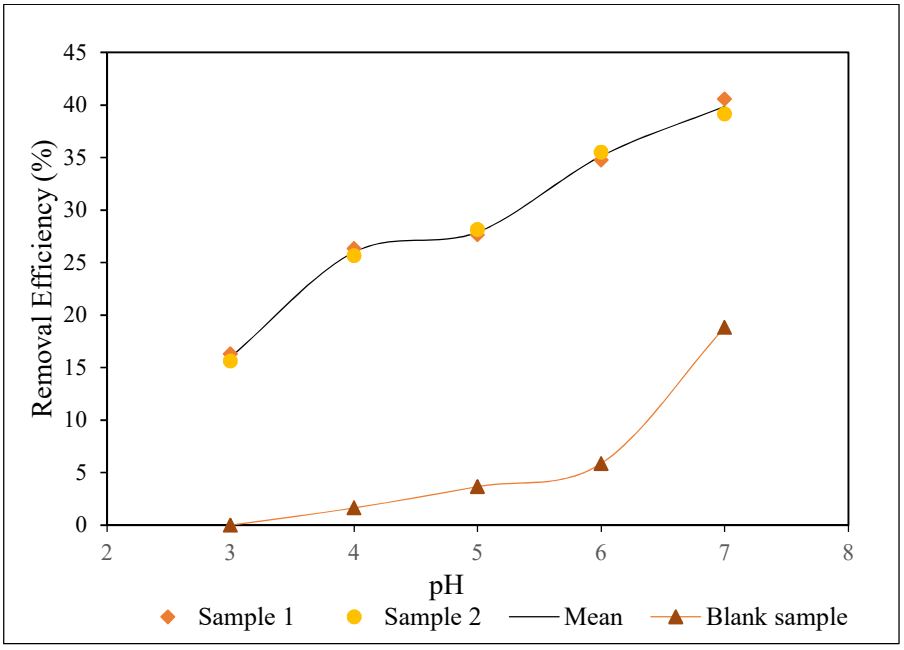

Figure 5.11: Effect of initial pH on single solute adsorption of Cd^{2+} (Blank sample indicate removal due to precipitation alone)

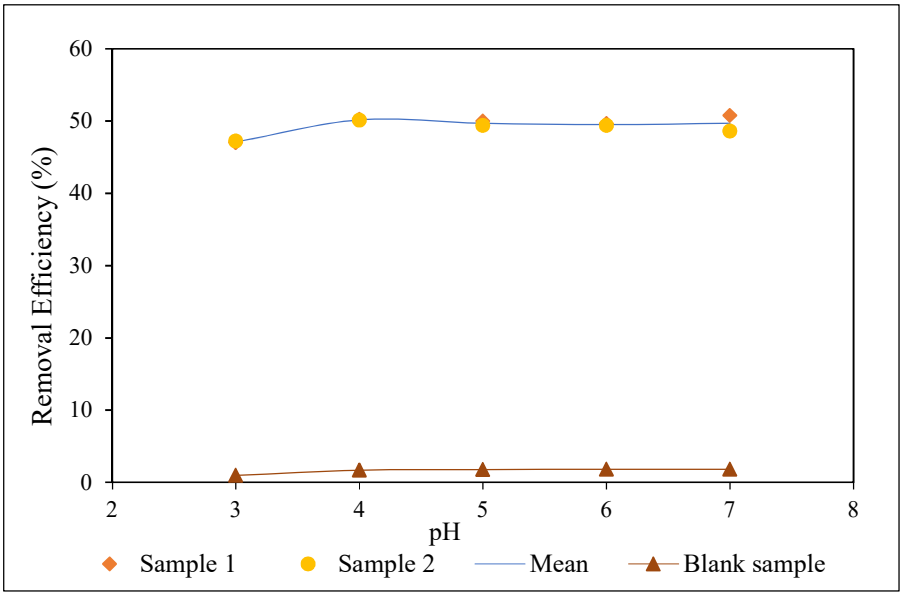

Figure 5.12: Effect of initial pH on single solute adsorption of phenol (Blank sample indicate removal without AC)

5.3.1.2 Effect of Contact Time

The effect of contact time variation on Cd^{2+} and phenol removal in the single solute system were also investigated using the produced AC. Batch adsorption experiments were carried out with 50 ml solutions of 100 mg/l of Cd^{2+} and phenol, with AC dosage of 0.15 g, pH of 5.5 (optimum) and at different contact times varying from 1 to 1440 minutes. Results presented in Figure 5.13 for both pollutants shows that Cd^{2+} adsorption was rapid at the initial stage with a significant removal of 27 % achieved within the first 60 minutes of contact time. A slight increase in removal efficiency of up to 28 % was noticed after 120 minutes, with this same removal efficiency also recorded at prolonged time period, signifying that equilibrium condition was established after 120 minutes of contact time. Considering this obtained result, an equilibrium time of 180 minutes was chosen for all other Cd^{2+} adsorption experiments to ensure that equilibrium condition is well established. As for phenol, a similar fast adsorption rate was also noticed at the initial stage, before it became gradual and thereafter constant at the equilibrium time. The equilibrium condition was found to be established after 720 minutes of contact time with a constant removal efficiency of 56 % recorded in those periods.

The fast removal rate noticed for both pollutants at the initial stage can be ascribed to the availability of numerous active vacant sites on the AC surface, and also it could possibly due to the effect of the high concentration gradient between the bulk solution and the AC surface at the initial stage. However, the gradual increase noticed in the later stage might have been due to the surface hindrance created by the repulsive force between the adsorbed solute on the AC surface, with the remaining solutes in the bulk solution.

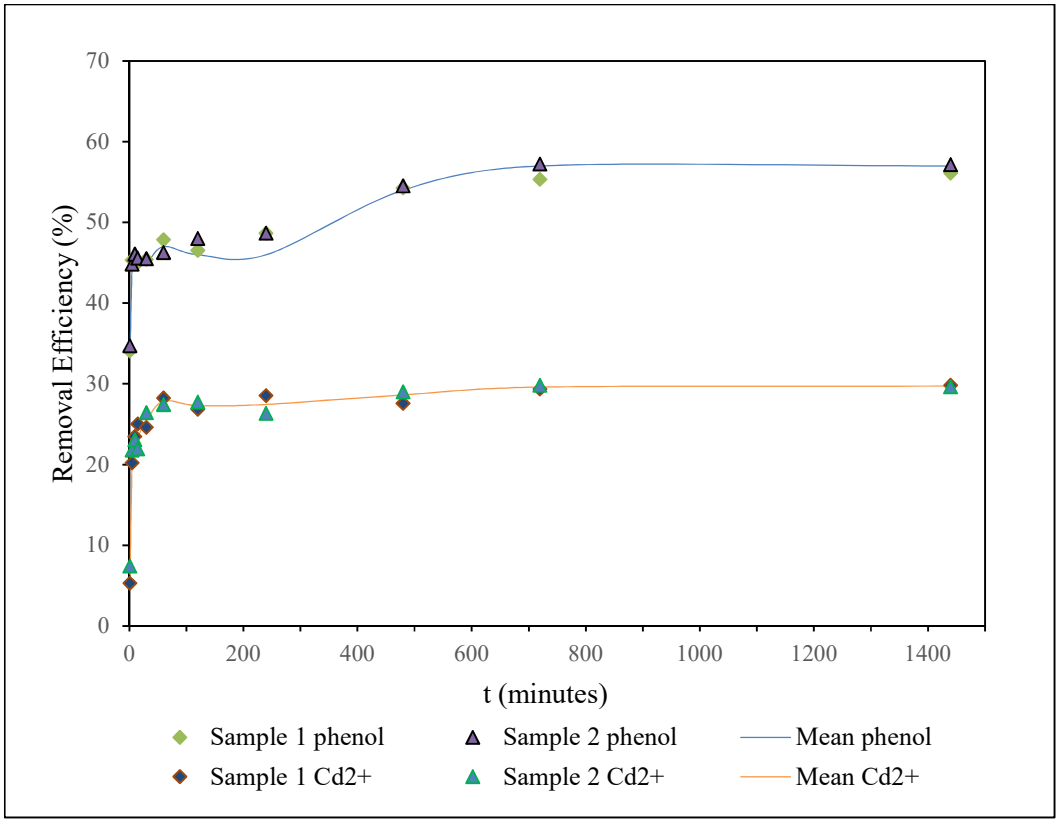

Figure 5.13: Effect of contact time on single solute adsorption of Cd^{2+} and Phenol

5.3.1.3 Effect of Adsorbent Dosage

The effect of AC dosage on the removal efficiency and adsorption capacity of both Cd^{2+} and phenol in the single solute systems were also investigated. Equilibrium batch adsorption experiments were performed by adding different amounts of AC (25, 50, 100, 200, 300, 400 and 500 mg) to 50 ml volume of 100 mg/l of Cd^{2+} and phenol solutions, at pH of 5.5 and at a contact time of 180 and 720 minutes for Cd^{2+} and phenol, respectively. Results presented in Figures 5.14 and 5.15 depict the removal efficiencies and adsorption capacities of each pollutant at different AC dosages. As expected, there was an increase in removal efficiency of both Cd^{2+} and phenol as AC dosage was increased. A significant rise in removal efficiency from 3 to 59 % and from 7 to 78 % can be observed for Cd^{2+} and

phenol, respectively as AC dosage was increased from 25 to 300 mg. This observed increase can be attributed to the fact that with more AC in solution, there will be an increase in total surface area and surface functional groups available for the pollutants uptake. Contrary to the removal efficiency, adsorption capacity for each pollutant was found to decrease with the increase in AC dosage. A decrease in Cd^{2+} adsorption capacity from 16.90 to 8.07 mg/g and that of phenol from 20.04 to 12.05 mg/g was observed. This observed decrease in adsorption capacity was attributed to the effect of unsaturation of adsorption sites that could occur at higher AC dosages for a fixed concentration of pollutants, as compared to complete or nearly complete saturation that could occur at lower dosages for the same concentration. This effect was explained by Gutiérrez-Segura et al [12] to have resulted from Cd^{2+} dilution at the solid phase at higher AC to solution ratios. Similar findings were also reported by Gutiérrez-Segura et al [12] and Weiqin Zhu et al [47] for Cd^{2+} and phenol adsorption on AC derived from sewage sludge, respectively.

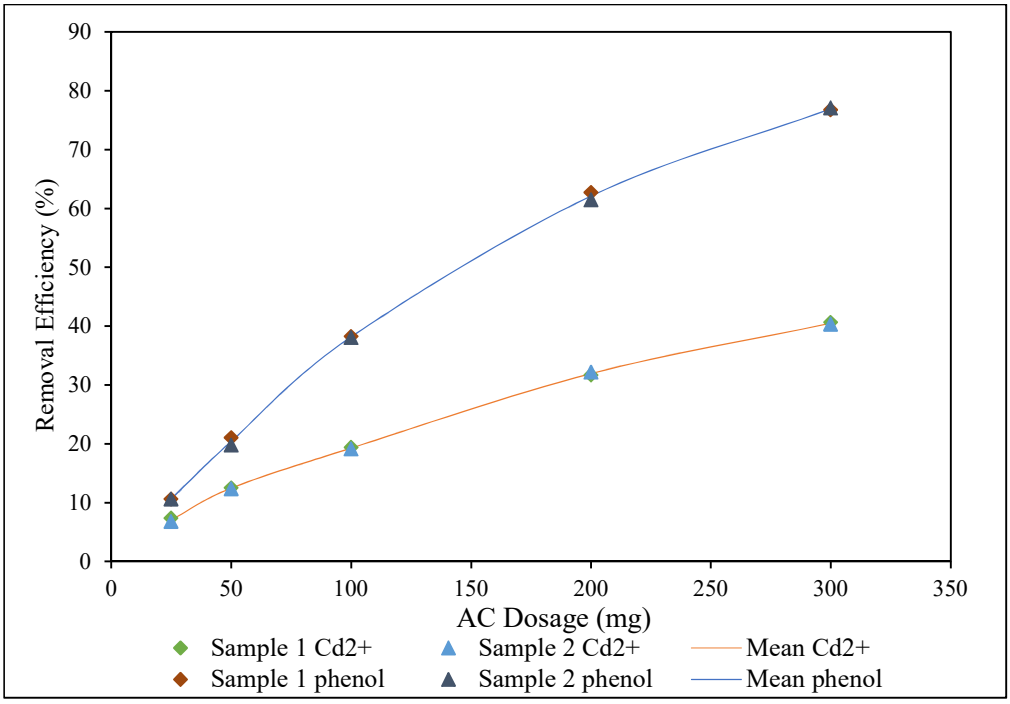

Figure 5.14: Effect of AC dosage on the removal efficiency of Cd^{2+} and Phenol

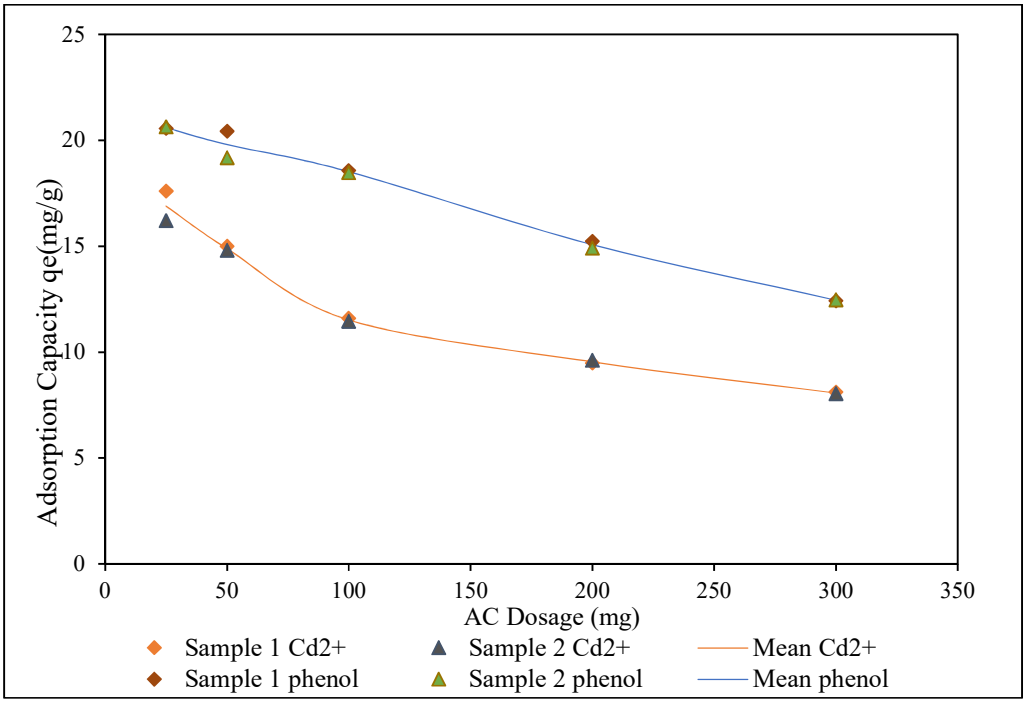

Figure 5.15: Effect of AC dosage on adsorption capacity of Cd^{2+} and phenol

5.3.1.4 Effect of initial concentration variation

To investigate the effect of initial concentration on the removal efficiency and adsorption capacity of both Cd^{2+} and phenol in the single solute system, batch adsorption experiments were carried out with series of different concentrations of the pollutants starting from 25 to 300 mg/l, with AC dosage of 0.15 g, pH of 5.5 and contact times of 180 and 720 minutes for Cd and phenol. Results in Figure 5.16 depicts the removal efficiency and adsorption capacity of both Cd^{2+} and phenol, with respect to initial concentration variation. In Figure 5.16 a, a decrease in Cd^{2+} removal efficiency from 57 to 18 %, and that of phenol from 59 to 28 % were observed as the initial concentration was increased from 25 to 300 mg/l. The observed behavior of each pollutant can be explained based on the AC surface energy sites. As described by Hassoon Ali [49], for a fixed amount of AC, and at low initial concentration of pollutants, adsorption normally occurs at high energy sites of the AC, but as concentration is increased, the pollutant-adsorbent ratio is increased, which result in higher energy sites being saturated and adsorption shifting to lower energy sites, and resulting in decreased removal efficiency as noticed in this work [49].

On the other hand, it can be seen that the adsorption capacity of both Cd^{2+} and phenol increases with increase in initial concentration as depicted in Figure 5.16 b. Cd^{2+} adsorption capacity increased from 6.38 to 18.70 mg/g, and that of phenol from 4.95 to 29.52 mg/g as initial concentration was increased from 25 to 300 mg/l. Possible explanation for this phenomenon might have resulted from the increased interaction of the pollutants at a higher concentration with the AC surface mainly because of the high concentration gradient between the solid phase of the AC and the bulk liquid phase of the pollutants.

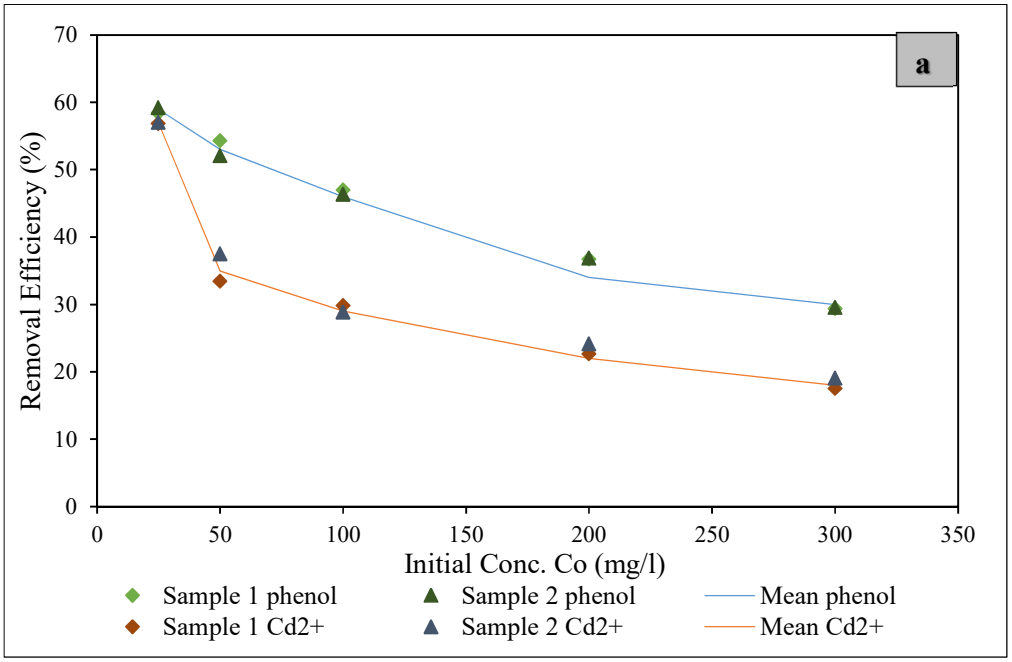

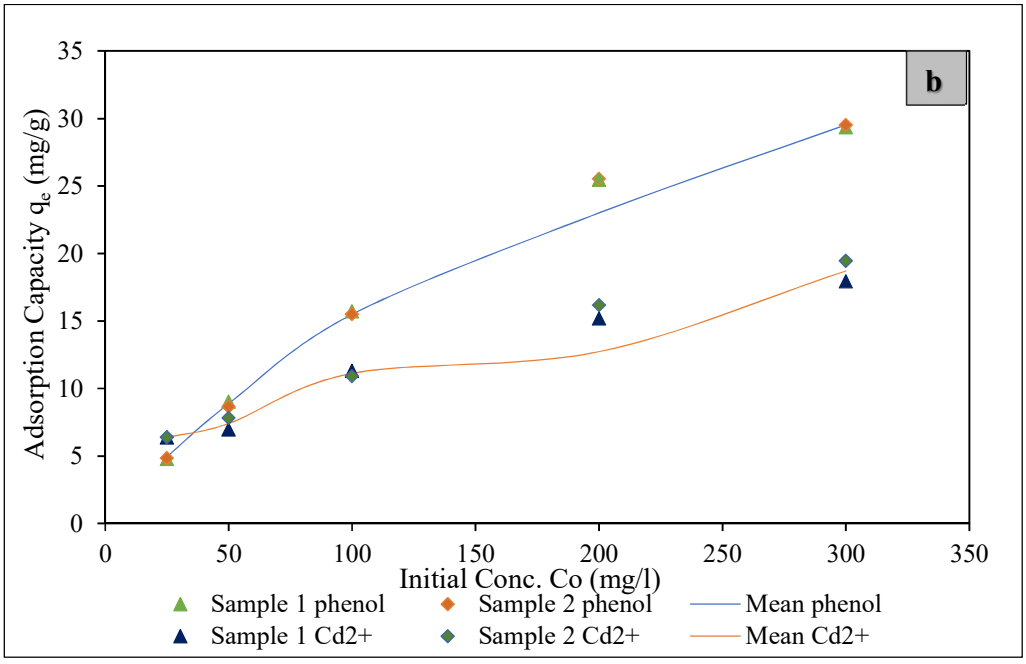

Figure 5.16: Effect of initial concentration on (a) removal efficiency and (b) adsorption capacity of Cd^{2+} and phenol

5.3.2 Equilibrium adsorption isotherms for adsorption of Cd^{2+} and phenol onto the AC

The obtained adsorption isotherm data based on initial concentration variation for both Cd^{2+} and phenol were modeled using the two conventional isotherm models; namely Langmuir and Freundlich isotherm models as presented in Equations 5.1 and 5.2, respectively. The model's parameters in Table 5.14 were calculated based on the slope and intercept of the linear plot of the model terms displayed in Figure 5.17.

Linear Freundlich Isotherm

$$\log q_e = \log K + \frac{1}{n}\log C_e \tag{5.1}$$

Linear Langmuir Isotherm

$$\frac{1}{q_e} = \frac{1}{q_m K_{ads}}\left(\frac{1}{C_e}\right) + \frac{1}{q_m} \tag{5.2}$$

Where, Ce is the equilibrium aqueous concentration of adsorbate (mass/volume), q_e is the adsorption capacity (mass adsorbate /mass adsorbent), K and n are the Freundlich constants related to the sorption capacity and sorption affinity of the adsorbent and q_m maximum adsorption capacity for adsorbates.

Cd^{2+} adsorption by the produced AC fitted well to the Freundlich isotherm with a correlation coefficient (R^2) of 0.9231, which was higher than the low value of 0.7877 realized from the Langmuir isotherm. Based on the good fit of the Freundlich isotherm it was deduced that Cd^{2+} adsorption occurs in multilayer over the heterogeneous surface of the AC, and sites having a higher affinity for Cd^{2+} were occupied first [69]. The high n-value (adsorption intensity) of 2.76 >1 obtained for the Freundlich model also confirmed

the heterogeneous nature of the AC surface and the favorable nature of the adsorption process under the conditions studied [70].

As for phenol adsorption onto the AC, both the two isotherm models offer good fitting to the obtained experimental data, with Langmuir isotherm showing the best fit based on its higher R^2 value of 0.9960. Considering this outcome, it can be concluded that phenol adsorption occurs in monolayer over the entire active surface sites of the AC. Maximum adsorption capacity (q_m) of 33.11 mg/g was calculated for phenol based on the Langmuir isotherm model. Also, the Freundlich isotherm model n value of 1.72 realized also support the favorable nature of phenol adsorption onto the AC.

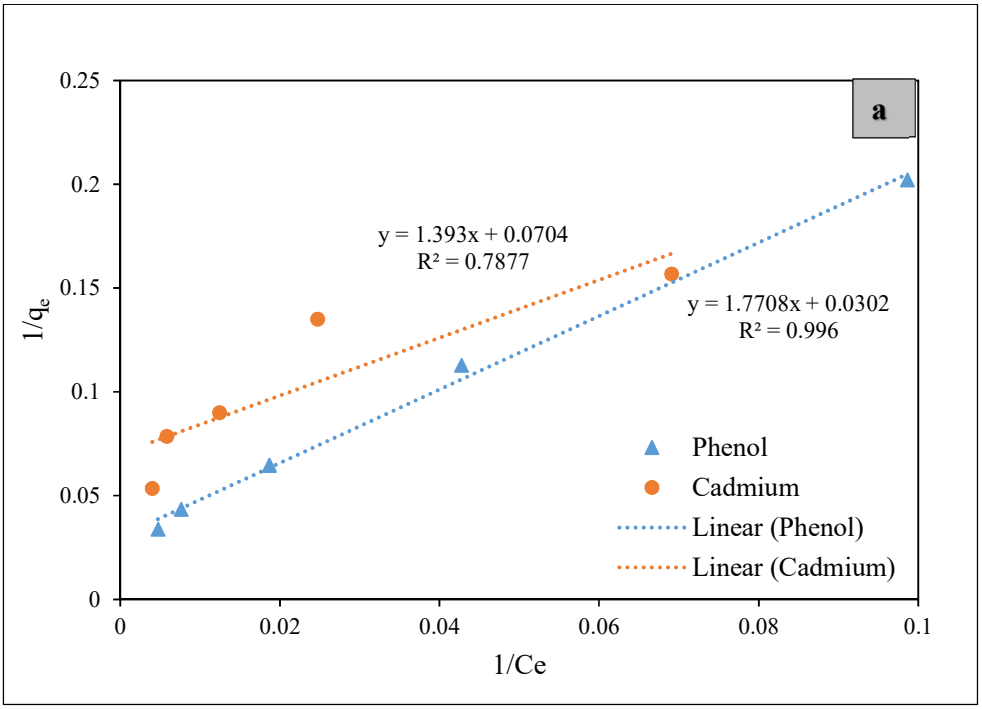

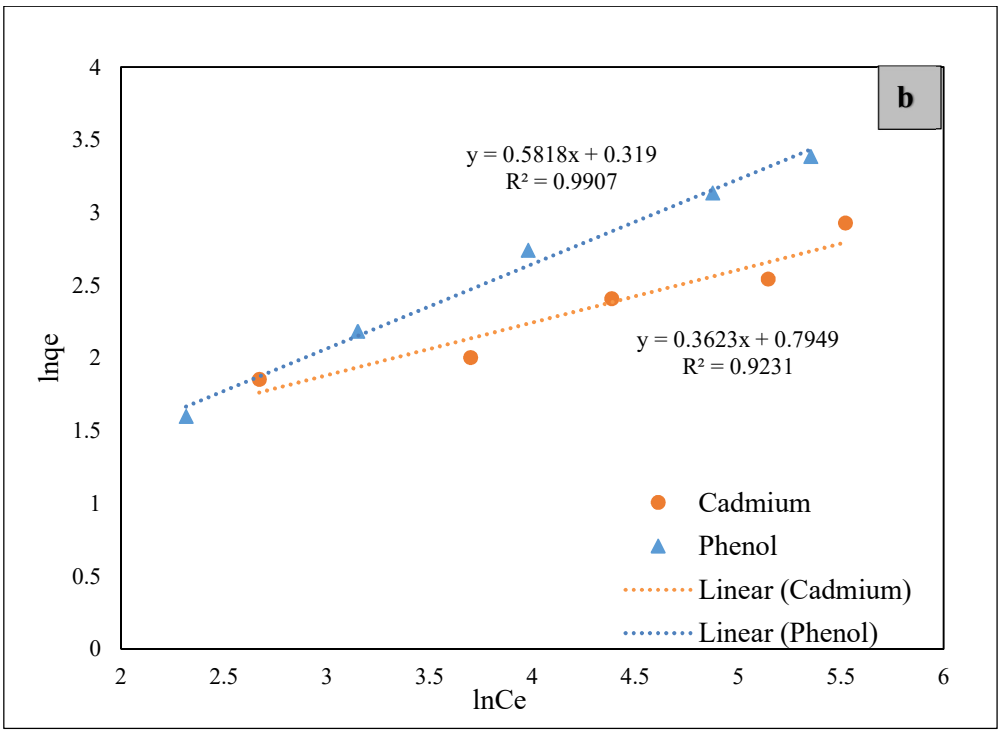

Figure 5.17: Isotherms plot for Cd^{2+} and phenol adsorption onto the AC: (a) Langmuir isotherm (b) Freundlich isotherm

Table 5.14: Freundlich and Langmuir parameters of Cd^{2+} and phenol single solute adsorption onto the AC

Components	Freundlich Parameters			Langmuir Parameters		
	n	k_F mg g-1$(Lmg^{-1})^{1/n}$	R^2	q_m (mg/g)	K_L (L/mg)	R^2
Cd^{2+}	2.76	2.21	0.9231	14.20	0.051	0.7877
Phenol	1.72	1.38	0.9907	33.11	0.017	0.9960

5.3.3 Adsorption Kinetics for single solute adsorption of Cd^{2+} and phenol

Adsorption kinetics describe the rate at which adsorption process approaches equilibrium condition. It provides useful insight in determining the main mechanism involved in adsorption process which could be physisorption or chemisorption. Also, the kinetic parameters normally obtained from the study provides valuable information that is useful for adsorption process design and modeling [15]. Hence, the mechanisms of Cd^{2+} and phenol adsorption onto the produced AC were investigated by fitting the obtained experimental data to both pseudo-first order and pseudo-second order kinetics models as presented in Equation 5.2 and 5.3 as follows.

Linear pseudo-first order model

$$\ln(q_e - q_t) = \ln q_e - k_1 t \tag{5.3}$$

Linear pseudo-second order model

$$\frac{t}{q_t} = \frac{1}{k_2 q_e^2} + \frac{1}{q_e} \tag{5.4}$$

Where, (q_e) is the theoretical equilibrium adsorption capacity (mg/g) derived from the model's plot. (q_t) represent the adsorption capacity (mg/g) at any of the chosen time (t) derived from the experimental data. k_1 represent the pseudo-first order rate constant (min^{-1}) which was calculated from the intercept of a plot of $\ln(q_e-q_t)$ against t (time). k_2 on other hand represent the pseudo-second order rate constant (g/mg min) and it values were derived from the slope and intercept of $\frac{t}{q_t}$ against $\frac{1}{q_e}$.

Figure 5.18 shows the pseudo-first and second order kinetic plots for both Cd^{2+} and phenol adsorption onto the AC. Table 5.15 provides the kinetic parameters computed from each plot. Results of Cd^{2+} adsorption revealed that it was well fitted to pseudo-second order model compared to the pseudo-first order model (R^2: 0.8564) with an R^2 value of 0.9996. This implies that the obtained Cd^{2+} experimental data can be adequately described by the second order model. Additionally, the computed Cd^{2+} adsorption capacity (theoretical q_e) of 9.49 mg/g from the pseudo-second order model was in agreement with the obtained experimental adsorption capacity of 9.48 mg/g (experimental q_e).

In the case of phenol adsorption, it was observed that it fitted well to both the pseudo-first order and second order model with R^2 values of 0.9659 and 0.9987, respectively. However, theoretical q_e of 5.61 mg/g computed from pseudo-first order plot deviate greatly from the experimental q_e of 19.40 mg/g. Thus, implying that pseudo-first order model failed in describing the experimental data. The pseudo-second order model presented a theoretical q_e of 19.34 mg/g that agreed well with the experimental q_e of 19.40 mg/g.

Therefore, based on the outcomes realized for both Cd^{2+} and phenol, it was concluded that their single solute adsorption by the AC can be described by the pseudo-second order model, with adsorption mechanism resulting from chemisorption that involves electron sharing or ion exchange between Cd^{2+}/phenol with AC surface functional groups [69]. It also worth mentioning that similar observation was also reported by Yan Ma et al [45] and Yu Bian et al [48] on adsorption kinetics study of phenol and Cd^{2+}, respectively using AC.

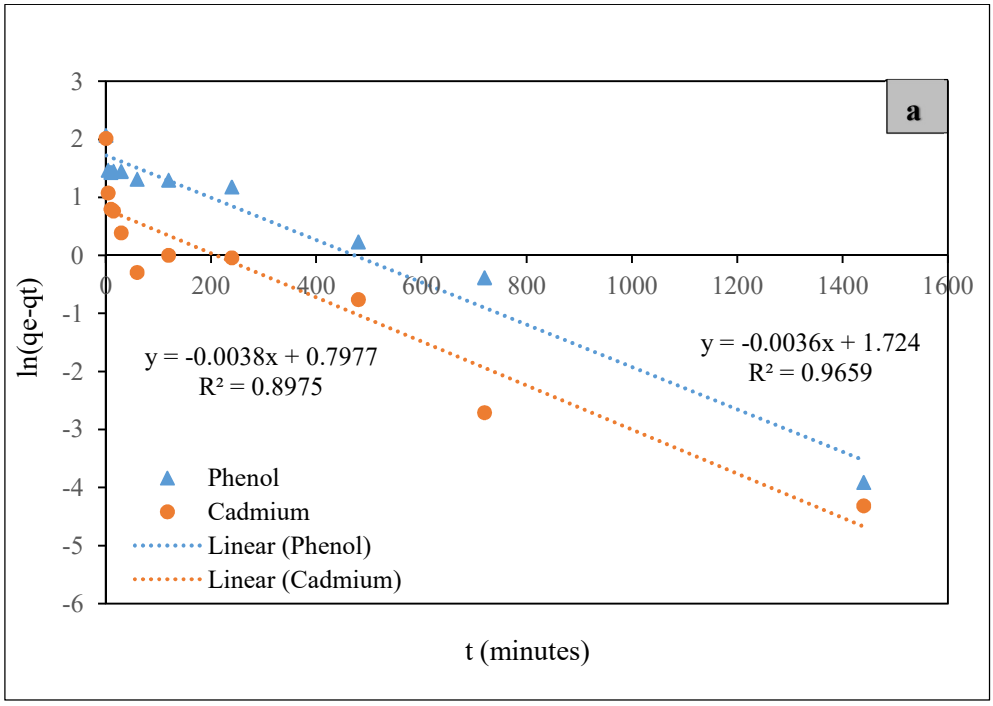

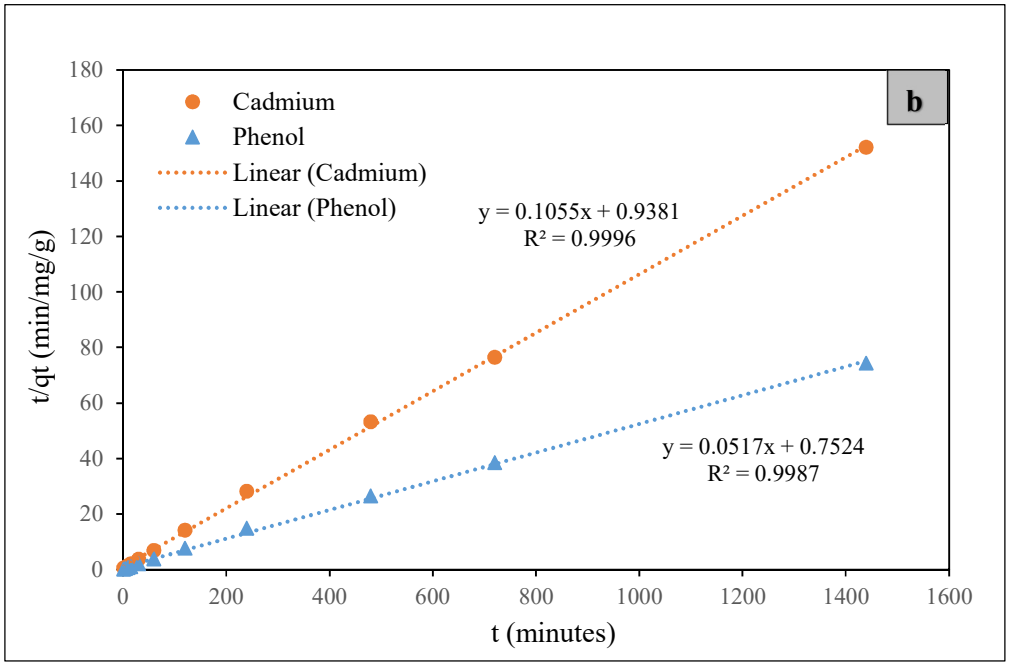

Figure 5.18: (a) Pseudo-first order and (b) Pseudo- second order kinetic plots for Cd^{2+} and phenol adsorption onto the AC

Table 5.15: Kinetic parameters for single solute adsorption of Cd^{2+} and phenol onto the produced AC

Component	pseudo-first order model				pseudo-second order model			
	k_1 (min^{-1})	q_e (mg/g)	R^2	Exp. q_e (mg/g)	k_2 (L/gmin)	q_e (mg/g)	R^2	Exp. q_e (mg/g)
Cd(II)	0.0041	2.22	0.8564	9.48	0.012	9.49	0.9996	9.48
Phenol	0.0036	5.61	0.9659	19.40	0.004	19.34	0.9987	19.40

5.3.4 Multicomponent adsorption of Cd^{2+} and Phenol onto the prepared AC

Multicomponent adsorption involving Cd^{2+} and phenol in binary solution (Cd^{2+}-phenol) was also investigated using the produced AC. Similar to the single solute experiments, adsorption parameters that include pH, adsorbent dosage, contact time, and initial concentration were all investigated and their respective results compared.

5.3.4.1 Effect of pH

The effect of pH on multicomponent adsorption of $Cd^{2+}$and phenol using the produced AC was investigated at pH values starting from 3 to 7, similar to those employed in their single solute adsorption experiments. Batch adsorption experiments were conducted using 50 ml volume of 100 mg/l binary solution of Cd^{2+}-phenol (ratio 1:1), with AC dosage of 0.15 g, and at a contact time of 480 minutes. Results presented in Figure 5.19 show the removal efficiency of each component at different pH values. It was observed that phenol adsorption from the binary solution was not affected by the chosen pH values, as a relatively constant removal efficiency of 48 % was noticed throughout. This behavior was in agreement with the slight increase in removal efficiency (from 47 to 50 %) observed in its single solute adsorption for the same set of pH variation.

As for Cd^{2+} adsorption, a slight increase in removal efficiency was observed as the pH was increased from 3 to 5, and thereafter it became constant with no changes in removal efficiency at both pH 6 and 7. A maximum removal efficiency of 28 % was recorded at pH 5 and above, similar to what was obtained in the single solute Cd^{2+} adsorption study. Based on this observed phenomenon, it was concluded that phenol presence in the binary solution has a negligible effect on Cd^{2+} adsorption by AC. Considering the high removal efficiency

realized for Cd^{2+} at pH value above 5, a pH value of 5.5 was selected as optimum and used for all other subsequent experiments, and besides similar pH value have also been reported by some researchers [10,56-57].

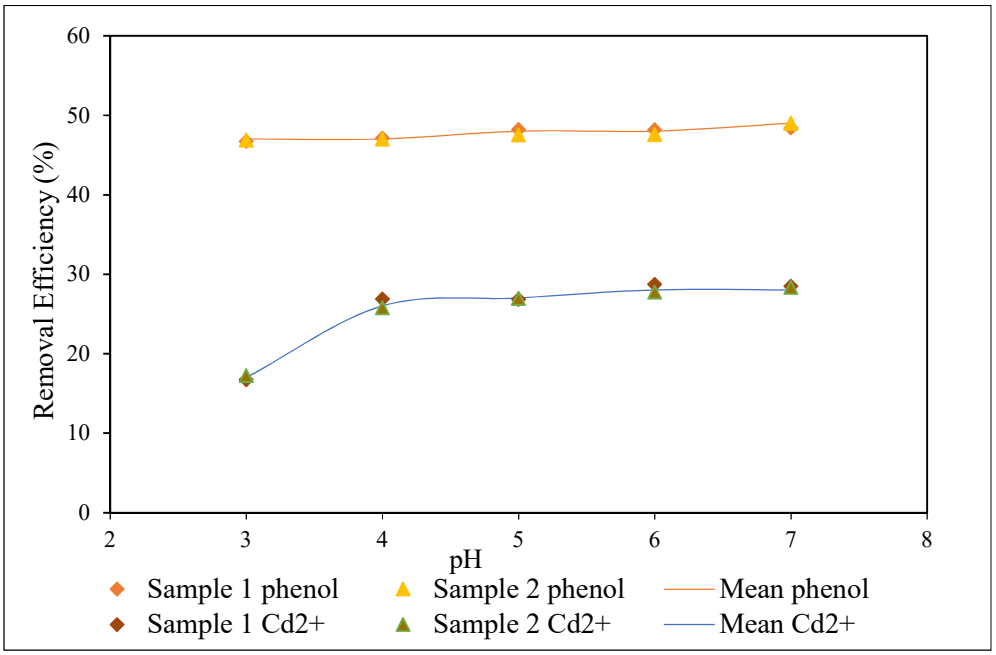

Figure 5.19: Effect of pH on the multicomponent adsorption of Cd^{2+} and phenol

5.3.4.2 Effect of contact time

The variation of contact time on multicomponent adsorption of Cd^{2+} and phenol from binary solution was also investigated. Batch adsorption experiments were carried out using 50 ml solution of 100 mg/l binary solution of Cd^{2+}-phenol ratio 1:1, with AC dosage of 0.15 g, pH of 5.5 (optimum) and at different contact time varying from 1 to 1440 minutes. Results presented in Figure 5.20 for both components show that the equilibrium condition for Cd^{2+} was attained after 120 minutes of contact time with maximum removal efficiency of 28 % realized, which was similar to what was attained in its single solute adsorption. Therefore, it can be explained that at the employed initial concentration for both

components in the binary solution, phenol presence in the binary solution does not in any way impact Cd^{2+} adsorption by the AC. This results, further support the similar behavior observed in the pH adsorption study.

Phenol adsorption, on the other hand, presented a much higher equilibrium time of 480 minutes, than Cd^{2+} in the multicomponent adsorption. However, this was less than the 720 minutes realized in its single solute experiment and must have been due to Cd^{2+} presence in the solution which resulted in quicker saturation of adsorption sites. Based on the obtained results, all other subsequent adsorption experiments were carried out using a contact time of 480 minutes (8 hours) in other to ensure that equilibrium condition is well established for both components. In addition, similar phenol adsorption equilibrium time of 9 hours have been reported by Gupta A. and Balomajumder C, [71], in their research work on simultaneous removal of phenol and chromium using iron impregnated rice husk.

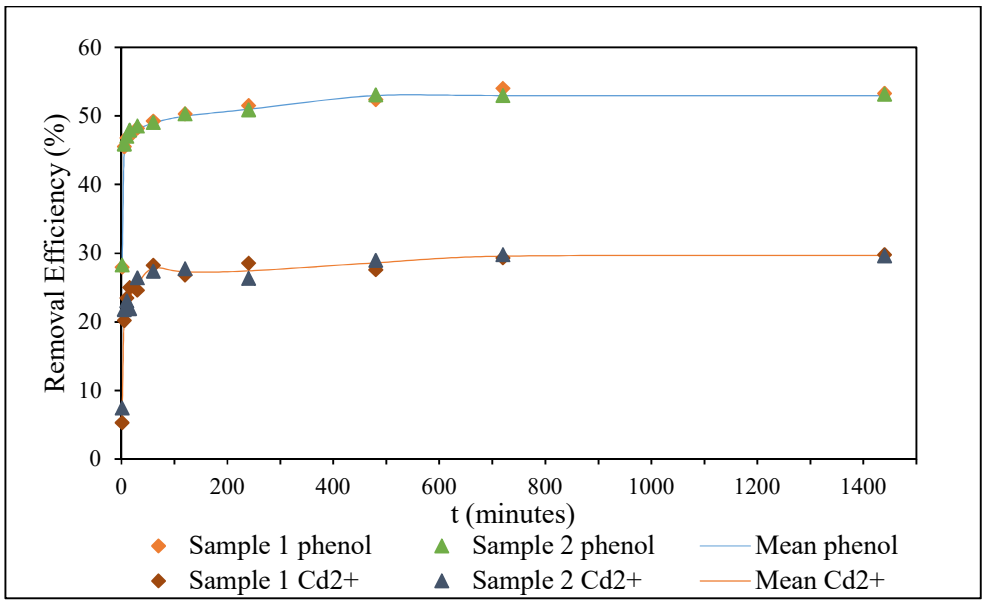

Figure 5.20: Effect of contact time on the multicomponent adsorption of Cd^{2+} and Phenol

5.3.4.3 Effect of adsorbent dosage

To investigate the effect of AC dosage on multicomponent adsorption of Cd^{2+} and phenol from the binary solution, equilibrium batch adsorption experiments were conducted by adding different amount of the AC (25, 50, 100, 200, and 300 mg) to 50 ml volume of 100 mg/l binary solution of Cd^{2+}-phenol, at pH of 5.5, and with a contact time of 480 minutes. Results in Figures 5.21 and 5.22 depict the removal efficiency and adsorption capacity, respectively for each component at various AC dosage. As expected, the removal efficiency of both Cd^{2+} and phenol from the binary solution increases with increasing AC dosage, while the adsorption capacities decrease as shown in Figure 5.22. When comparing the obtained results with those of their single solute system a decrease in removal efficiency and adsorption capacity was observed in the binary solute system. For instance, at 300 mg AC dosage in single solute system, the removal efficiency and adsorption capacity of Cd^{2+} and phenol were recorded as, Cd^{2+}: 40 % and 8.7 mg/g respectively, and phenol: 78 % and 12.45 mg/g respectively, which were greater than the value of Cd^{2+}: 30 % and 5.34 mg/g and phenol: 68 % and 12.17 mg/g recorded in the binary solute system. The observed decrease noticed for both Cd^{2+} and phenol in the binary solute system might have been due to the effect of competition for adsorption sites on the AC surface by each component in the binary solution.

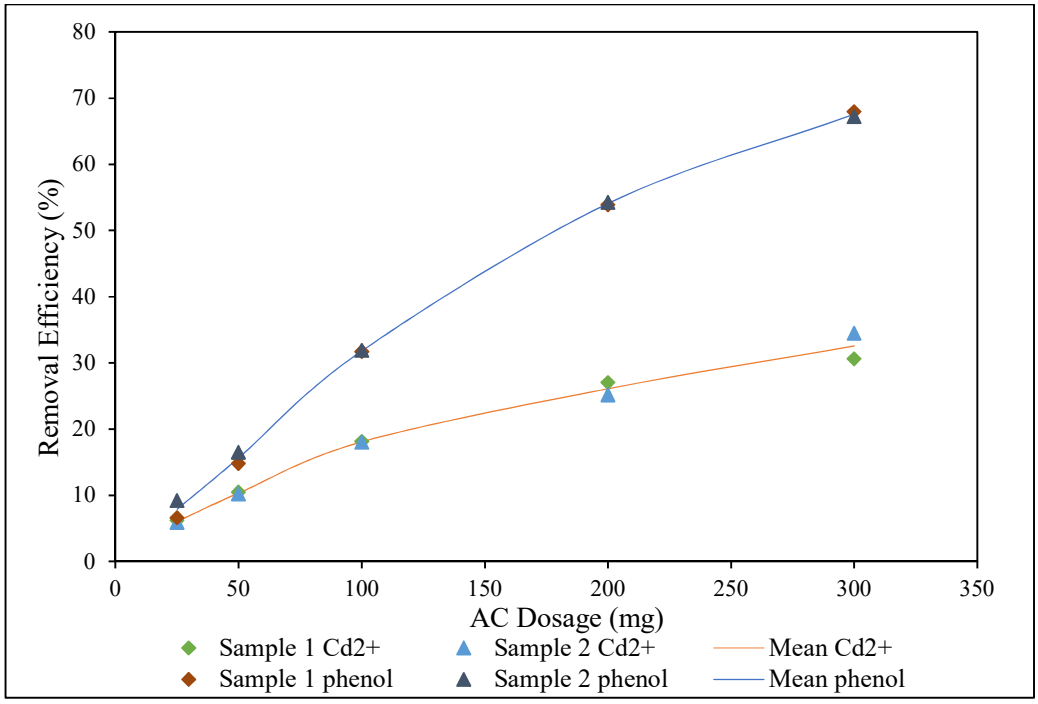

Figure 5.21: Effect of AC dosage on removal efficiency of Cd^{2+} and phenol from the binary solution

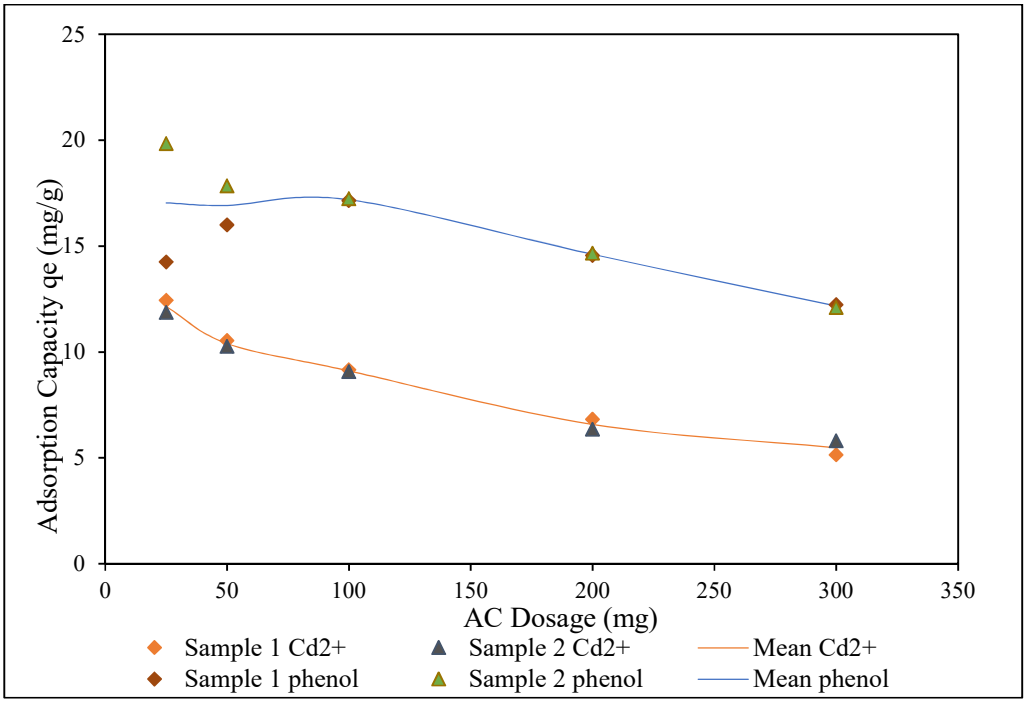

Figure 5.22: Effect of AC dosage on adsorption capacity of Cd^{2+} and phenol from the binary solution

5.3.4.4 Effect of initial concentration

The effect of initial concentration variation on multicomponent adsorption of Cd^{2+} and phenol from binary solution was also investigated. Equilibrium batch isotherm experiments were carried out with series of different concentrations of Cd^{2+} and phenol. Concentrations used for both components were from 25 to 300 mg/l, similar to those used in the single solute experiments (25, 50, 100, 200 and 300 mg), and were varied according to the experimental design in Table 4.5 in Chapter 4. AC dosage of 0.15 g, pH of 5.5, and a contact time of 480 minutes were used for all experiments. Results of the removal efficiency and adsorption capacity (q_e) of each component are depicted in Figures 5.23 and 5.24. It was observed that the increase in the initial concentration of Cd^{2+} and phenol in the binary solution resulted in increased removal efficiency and a decreased adsorption capacity for both.

Figure 5.24 a, shows the equilibrium adsorption capacities (q_e) of Cd^{2+} due to its concentration variation in the binary solution of Cd^{2+}-phenol, at a different initial concentration of phenol. It can be observed from the figure that phenol presence in the binary solution brought about a significant decrease in Cd^{2+} adsorption capacity by the AC. For the single solute adsorption isotherm of Cd^{2+} which has no phenol included, adsorption capacities were found to vary from 5 to19 mg/g as concentration increases from 25 to 300 mg/l. However, in the presence of 25 mg/l phenol, a decrease in Cd^{2+}adsorption capacities from 4.75 to 15 mg/g was observed for the same Cd^{2+} concentration variation. A similar decreasing trend was also noticeable at higher phenol concentrations in the binary solution. Figure 5.24 b present the effect of variable phenol concentration at a different initial concentration of Cd^{2+}, on adsorption capacities of phenol in the binary solution. It was

observed in this case that Cd^{2+} presence in the binary solution slightly enhance phenol removal, as its adsorption capacities were found to have increased with increasing Cd^{2+} concentration. At the fixed 25 mg/l Cd^{2+}concentration in the binary solution, phenol adsorption capacities were found to experience a slight increase from the range of 4.9 to 29 mg/g shown for its single solute isotherm to 6.13 to 30 mg/g in the figure. Although, this increase was not well pronounced at a higher Cd^{2+} concentration as evidenced from the overlapping plots, and could imply that effect is negligible at high concentrations.

The observed behavior exhibited by each component in their multicomponent adsorption from the binary solution can be explained via their various means of interaction with the AC. Heavy metals adsorption such as Cd^{2+} employed in this study on an AC normally results from the electrostatic force of interaction between the negatively charged functional groups on the AC surface with positively charged metal ions. The negatively charged functional groups on the AC surface must have accounted for Cd^{2+} removal in this study. Phenol adsorption mechanism as reported by several authors [10,14,75], is normally attributed to electron donor-acceptor reaction mechanism between the aromatic phenol ring and the carbonyl groups on the AC surface. The result of FTIR analysis conducted for the AC sample confirms the presence of several functional groups that include both the hydroxyl groups and carbonyl groups (C=O). As such, phenol removal by the AC might have been due to this mechanism.

The observed decrease in Cd^{2+}adsorption capacity in the presence of phenol can be attributed to the competition for adsorption sites by each component on the AC, and it could also be due to the steric hindrance that might have been created by adsorbed phenol on the AC surface [14]. The increase in adsorption capacity noticed for phenol in the

presence of Cd^{2+} can be associated with the stabilization effect that might have been created by the adsorbed Cd^{2+} ions on the AC surface which further allows the free interaction of the functional groups on the AC surface with the phenol ring molecules. It has been reported that at acidic pH values (5-6), acidic oxygen functional groups on the AC surface do suppress phenol removal due to the effect of the repulsive forces between these groups and phenol molecules [14]. The adsorbed Cd^{2+} ions might have counteracted this force, and in the process allowing the free interaction of phenol molecules with other functional groups, which might have accounted for the increased adsorption capacity noticed.

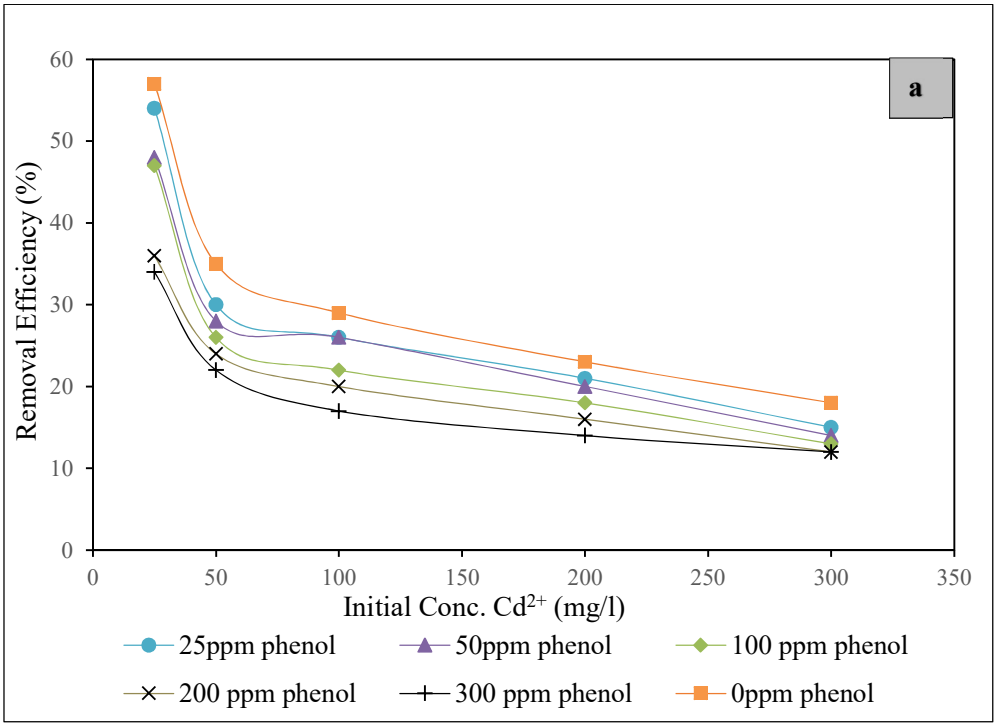

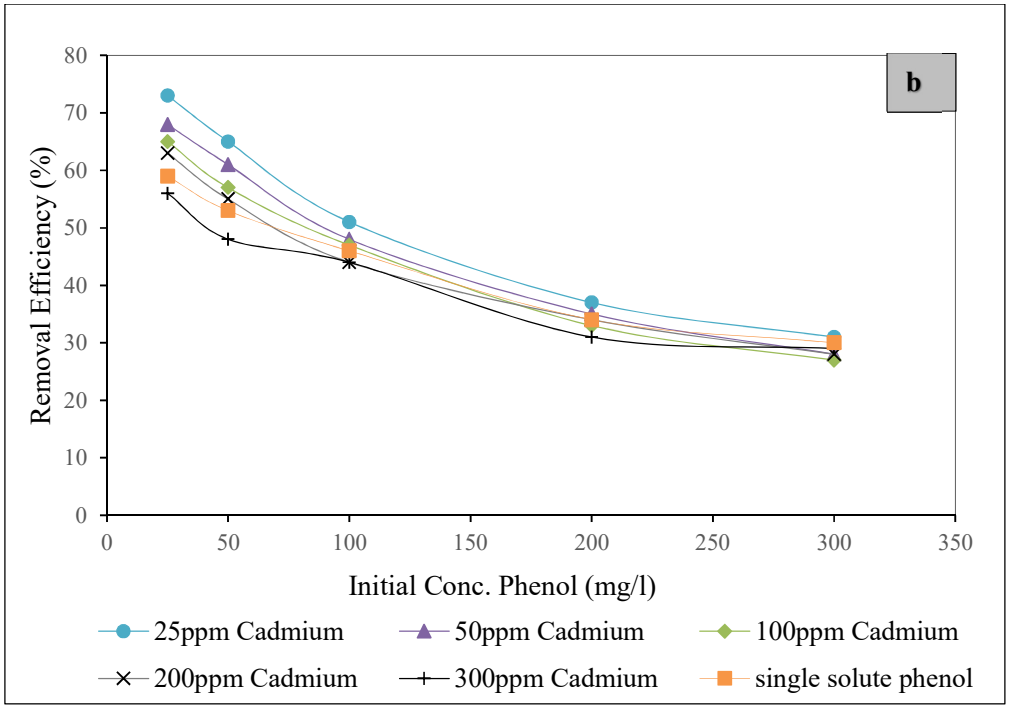

Figure 5.23: Effect of initial concentration on removal efficiencies of Cd^{2+} and phenol in binary solution: (a) cadmium and (b) phenol

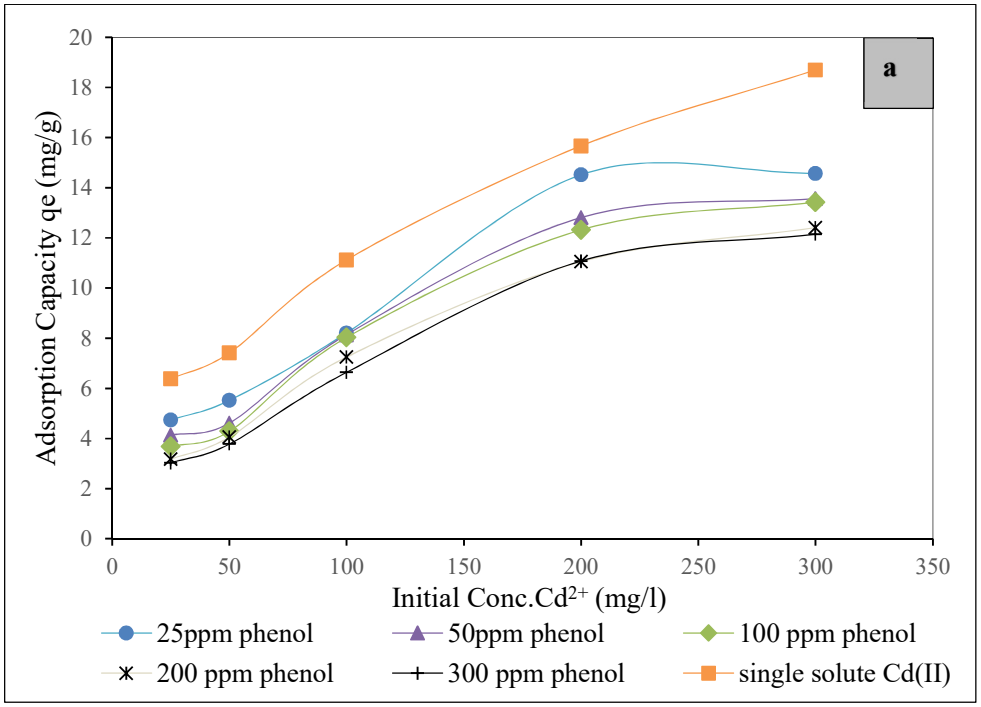

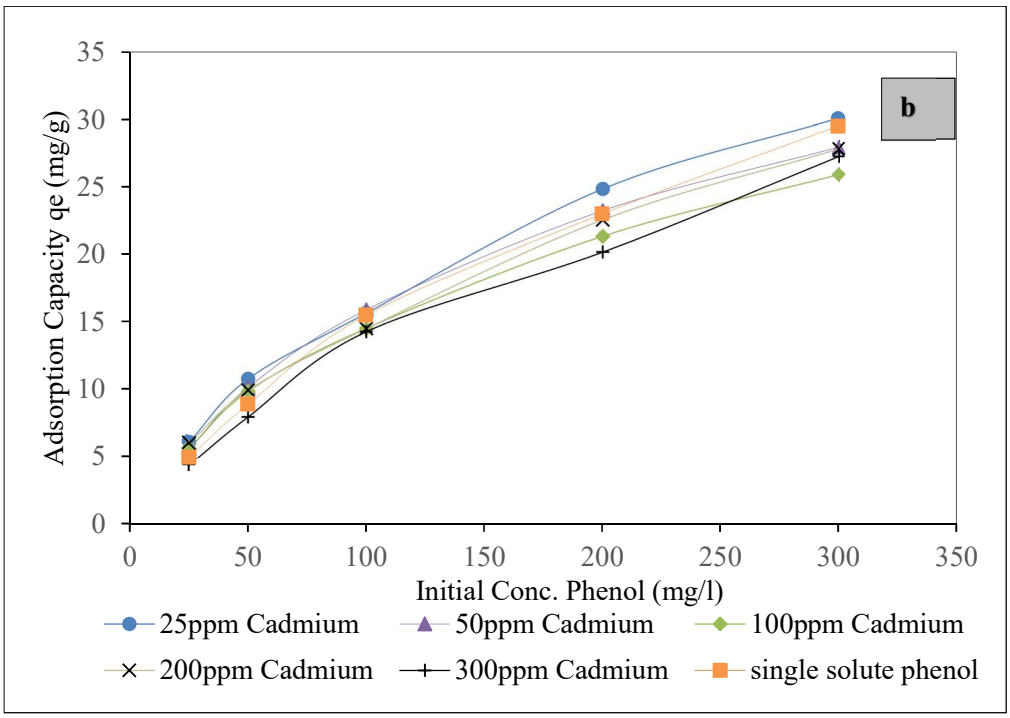

Figure 5.24: Effect of initial concentration on adsorption capacities of Cd^{2+} and phenol in binary solution: (a) cadmium and (b) phenol

5.3.5 Equilibrium Adsorption Isotherms for multicomponent adsorption of Cd^{2+} and Phenol onto the AC

The obtained equilibrium isotherm data of both Cd^{2+} and phenol adsorption in the binary solute system were modeled using Freundlich and Langmuir isotherm models. The models parameters in Table 5.16 were determined from the linear plots of the models term in Figures 5.25 and 5.26 for the respective models.

Analysis of the correlation coefficients (R^2) show that both the two isotherm models were able to adequately describe the experimental data, but the Freundlich isotherm offers the best fit to the data due to its high R^2 values for each component. Based on this, it was deduced that the binary solute adsorption of Cd^{2+} and phenol by the AC occur in multilayer, and adsorption sites with high affinity for each component were occupied first [69]. Also, the obtained n values (adsorption intensity) for all the samples in the Freundlich model were greater than 1, which implies that the adsorption process was highly favorable onto the heterogeneous surface of the AC. On comparing the two models parameters with what was realized in the single solute isotherm of each component, some few significant changes were observed. For instance, the maximum adsorption capacities (q_m) of Cd^{2+} in the binary solute system of the Langmuir model, were all found to be lower than 14.20 mg/g realized from the single solute Langmuir isotherm of Cd^{2+}. Also, phenol's maximum adsorption capacities from the binary solute system were slightly lower than the 33.11 mg/g computed from its single solute system. These observed changes can be attributed to the competitive phenomenon that might have existed between Cd^{2+} and phenol for adsorption sites on the AC surface. Another notable difference was Freundlich adsorption intensity constant (n), which were found lower for Cd^{2+} at all the initial concentrations of phenol, compared to

2.76 computed for its single solute system. This indicates that the AC adsorption intensity of Cd^{2+} in binary solution was suppressed by phenol. Similar observation was also reported by Arcibar-Orozco et al [14] in simultaneous adsorption of Cd^{2+}-phenol on activated carbon cloth. In the case of phenol, the Freundlich n constant computed from the binary solute isotherms were found to have increased when compared to the low 1.72 computed for the single solute isotherm, and this could further shed more light on the slight increase in phenol adsorption capacity noticed during the binary solute adsorption.

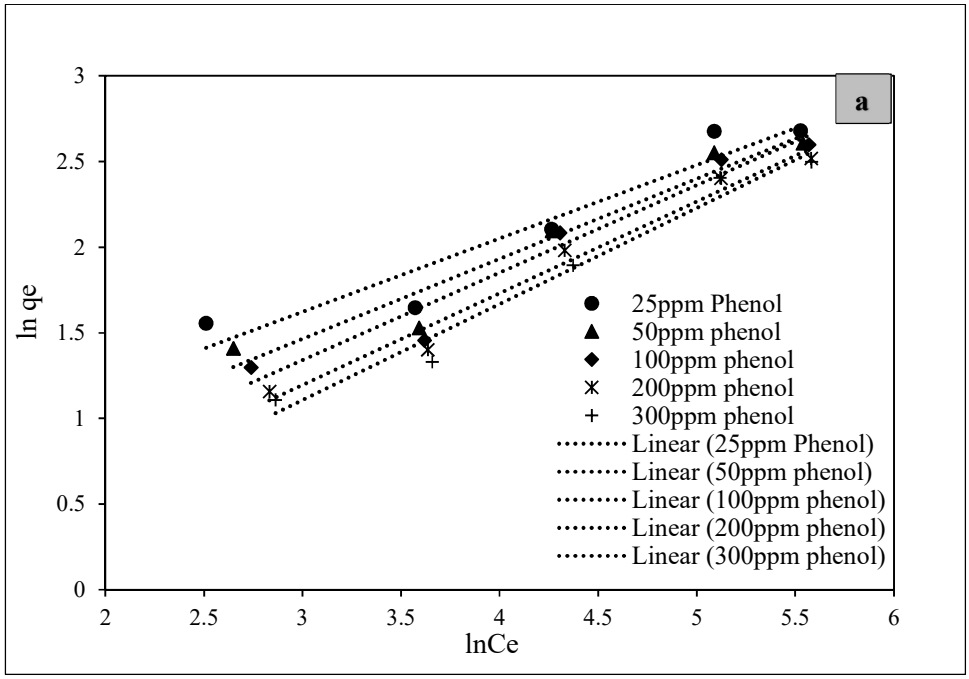

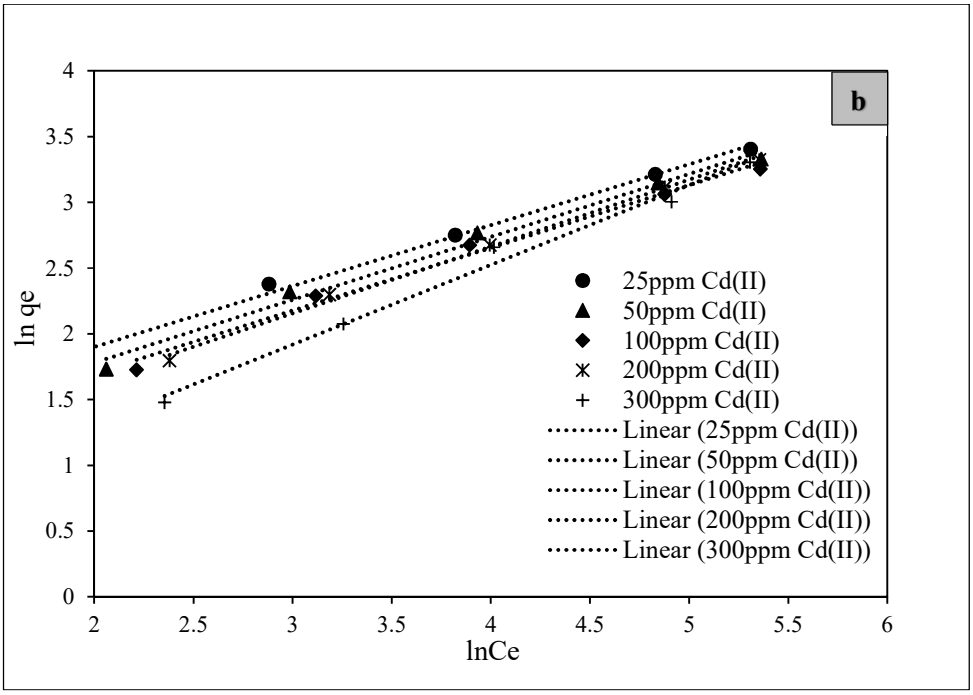

Figure 5.25: Freundlich isotherm plots for multicomponent adsorption of Cd^{2+} and phenol: (a) phenol and (b) cadmium

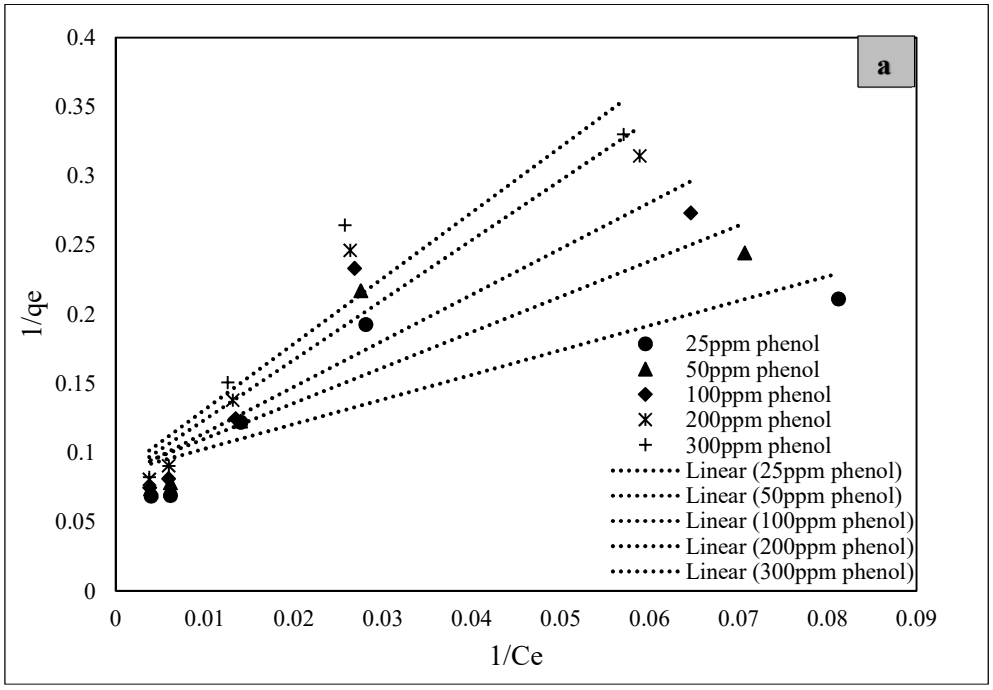

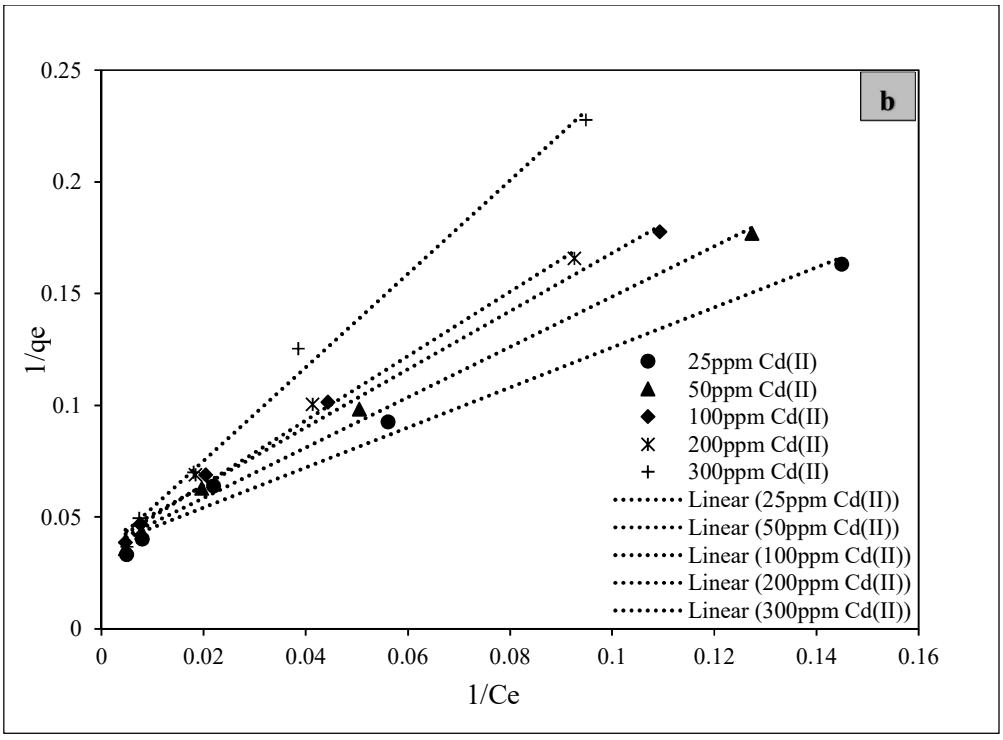

Figure 5.26: Langmuir isotherm plots for multicomponent adsorption of Cd^{2+} and phenol: (a) cadmium and (b) phenol

Table 5.16: Freundlich and Langmuir parameters for Cd^{2+} and phenol multicomponent adsorption onto the AC

Binary system		Freundlich Parameters			Langmuir Parameters		
	(mg/l)	n	k_F mg g-1$(Lmg^{-1})^{1/n}$	R^2	q_m (mg/g)	K_L (L/mg)	R^2
Cd^{2+} (with varying concentration of phenol)	25	2.33	1.46	0.9155	11.76	0.048	0.7175
	50	2.14	1.06	0.9419	11.86	0.033	0.7926
	100	1.97	0.827	0.9547	12.36	0.024	0.8414
	200	1.87	0.664	0.9760	12.44	0.019	0.9136
	300	1.78	0.563	0.9721	11.95	0.018	0.8975
Phenol (with varying concentration of Cd^{2+})	25	2.16	2.65	0.9945	27.55	0.040	0.9843
	50	2.09	2.28	0.9892	27.70	0.032	0.9931
	100	2.10	2.11	0.9890	26.18	0.029	0.9930
	200	1.97	1.88	0.9966	28.90	0.025	0.9883
	300	1.65	1.11	0.9890	30.03	0.016	0.9920

5.3.6 Adsorption Kinetics for multicomponent adsorption of $Cd^{2+}$and phenol onto the AC

The mechanism of adsorption of both components by the AC in their binary mixture was also investigated. The obtained experimental data was fitted to both the pseudo-first order and pseudo-second order kinetic models.

The computed model parameters for each model with respect to each component are listed in Table 5.17 as shown. Also, the model plots in Figures 5.26 and 5.27 depict the pseudo first order and second order models plots, respectively. The high R^2 values (Cd^{2+}: 0.9997 and phenol:0.9999) computed, and the theoretical q_e values that were in line with the experimental q_e values for the pseudo-second order model indicate that the obtained data of multicomponent adsorption of $Cd^{2+}$and phenol from binary solution can be well described by the model. The pseudo-first order model failed in describing the experiment data as it presented low R^2 values and q_e values that deviated greatly from the experimental q_e as presented in the Table. Therefore, based on this results it was concluded that multicomponent adsorption of Cd^{2+} and phenol by the AC followed the pseudo-second order model, with the main mechanism of adsorption being chemisorption that involves electron sharing or ion exchange between Cd^{2+}/phenol with AC surface functional groups [69]. It is also worth noting, that this same conclusion was reached in the single solute adsorption kinetic study of each component.

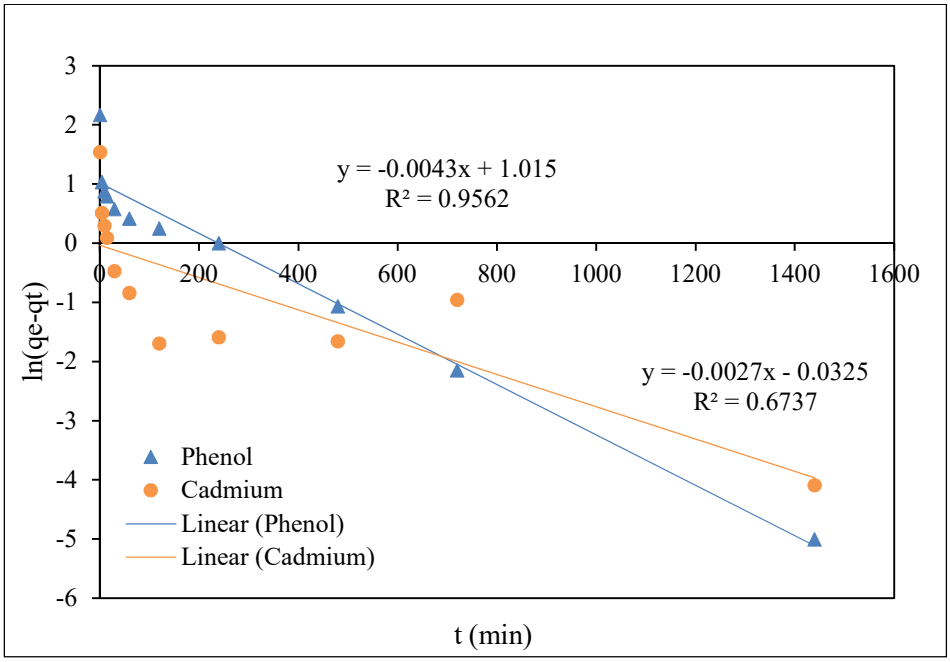

Figure 5.27: Pseudo-first order kinetic plot for multicomponent adsorption of Cd^{2+}-phenol onto the AC

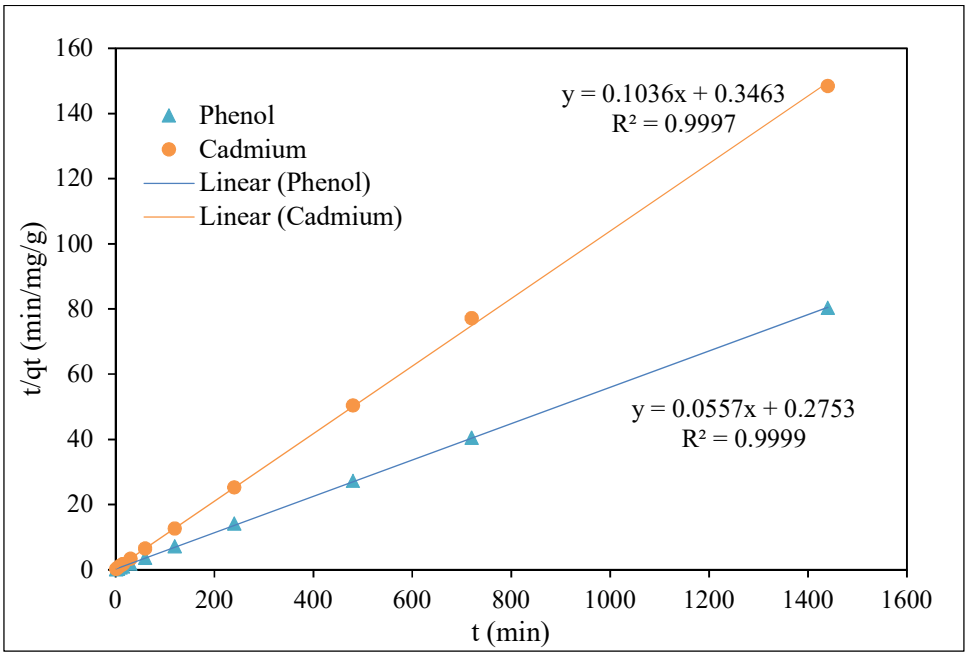

Figure 5.28: Pseudo-second order kinetic plot for multicomponent adsorption of Cd^{2+} -phenol onto the AC

Table 5.17: Linear pseudo-first and second order kinetic parameters for multicomponent adsorption of Cd^{2+}-phenol

Component	pseudo-first order model				pseudo-second order model			
	k_1 (min^{-1})	q_e (mg/g)	R^2	Exp. q_e (mg/g)	k_2 (L/gmin)	q_e (mg/g)	R^2	Exp. q_e (mg/g)
Cd(II)	0.0027	1.033	0.6737	9.72	0.031	9.65	0.9997	9.74
Phenol	0.0043	2.76	0.9562	17.93	0.013	17.95	0.9999	17.93

CHAPTER 6

CONCLUSION AND RECOMMENDATION

6.1 CONCLUSIONS

Municipal sewage sludge collected from a wastewater treatment plant was employed as a precursor for the production of low-cost AC. Several AC samples were prepared from the sludge using the chemical activation method with three activating agents namely, $ZnCl_2$, H_3PO_4, and KOH. The production process was designed and optimized using RSM technique with Box-Behnken design. The various factors of interest that affect the production process, such as the chemical impregnation ratio, activating temperature and dwell time were all investigated on the two chosen sets of responses, which were methylene blue removal efficiency and the yield of the AC samples. Based on the outcome of the production process and statistical analyses of the response data, three AC samples were selected from all the prepared samples for characterization studies. The AC samples were obtained from $ZnCl_2$ and KOH activation processes. Characterization of the selected samples for their surface properties and structures were conducted using several techniques that include FTIR, SEM, XRD, elemental analysis, TGA, porosity and surface area analysis. The best AC realized from the $ZnCl_2$ activation process with a specific BET surface area of 319.5 m^2/g, was achieved at an activation temperature of 700 ^oC, impregnation ratio of 1:0.6 (sludge: reagents) and dwell time of 60 minutes. Equilibrium batch adsorption experiments conducted using the best AC to investigate both the single and binary solute adsorption of Cd^{2+} and phenol from synthetic wastewater, showed that the AC offered high affinity for phenol removal than Cd^{2+} based on the reported adsorption

capacities and removal efficiencies for each component in both the single and binary solute adsorption experiments. Adsorption isotherm study conducted revealed a decrease in Cd^{2+} removal from the binary solution in the presence of phenol, which was attributed primarily to the existence of competition for adsorption sites on the surface AC by the two components. Moreover, it was also observed that Cd^{2+} presence in the binary solution slightly enhanced phenol removal, and this behavior was ascribed to Cd^{2+} acting as a stabilizer to the repulsive surface force that suppresses phenol removal on the AC, and by so doing its further allowed the free interaction of the AC functional groups with phenol molecules. The obtained isotherm data were correlated using both Langmuir and Freundlich isotherm models, and the Freundlich model showed the best fit to data based on its high R^2 and n values for each of component. Also, the equilibrium adsorption data for both the single and binary solute systems were correlated using pseudo-first order and second order kinetic models. Pseudo-second order model fitted well to the experimental data in both systems, and the mechanism of adsorption was attributed to chemisorption involving electron sharing or ion exchange between Cd^{2+}/phenol with the AC surface functional groups.

6.2 RECOMMENDATIONS

Based on the outcomes realized in this research study, these sets of recommendations were suggested:

1) Incorporation of inert gas should be included in the carbonization process so as reduce the high rate of carbon burn off witnessed in this study, and by so doing it could help in improving the surface properties and yields of the ACs.
2) Also, other carbonization methods such as hydrothermal carbonization (HTC), microwave carbonization can also be explored for the AC preparation, and the results might be compared with what was attained in this present study.
3) Also, the use of other activating agents such as H_2SO_4, K_2CO_3, and HNO_3 can also be tried out, in other to obtained high-performance AC with improved surface properties and pore structures
4) As of the adsorption experiments, an investigation of the other adsorption parameters such as temperature and sample agitation rate should be conducted, as these parameters were fixed in this research.

REFERENCES

[1] A. M. Abioye, F. N. Ani, and F. Nasir, "Recent development in the production of activated carbon electrodes from agricultural waste biomass for supercapacitors: A review," *Renew. Sustain. Energy Rev.*, vol. 52, pp. 1282–1293, 2015.

[2] İ. Demiral, C. Aydın Şamdan, and H. Demiral, "Production and characterization of activated carbons from pumpkin seed shell by chemical activation with $ZnCl_2$," *Desalin. Water Treat.*, vol. 3994, no. June, pp. 1–9, 2015.

[3] R. Subramaniam and S. Kumar Ponnusamy, "Novel adsorbent from agricultural waste (cashew NUT shell) for methylene blue dye removal: Optimization by response surface methodology," *Water Resour. Ind.*, vol. 11, pp. 64–70, 2015.

[4] S. Uçar, M. Erdem, T. Tay, and S. Karagöz, "Preparation and characterization of activated carbon produced from pomegranate seeds by ZnCl2 activation," *Appl. Surf. Sci.*, vol. 255, no. 21, pp. 8890–8896, 2009.

[5] M. A. Yahya, Z. Al-Qodah, and C. W. Z. Ngah, "Agricultural bio-waste materials as potential sustainable precursors used for activated carbon production: A review," *Renewable and Sustainable Energy Reviews*, vol. 46. pp. 218–235, 2015.

[6] M. H. Al-malack and A. A. Basaleh, "Adsorption of heavy metals using activated carbon produced from municipal organic solid waste," *Desalin. Water Treat.*, vol. 3994, no. February, 2016.

[7] A. A. Ahmad and A. Idris, "Preparation and characterization of activated carbons derived from bio-solid: a review," *Desalin. Water Treat.*, vol. 52, no. 25–27, pp. 4848–4862, 2014.

[8] J. Alvarez, G. Lopez, M. Amutio, J. Bilbao, and M. Olazar, "Preparation of adsorbents from sewage sludge pyrolytic char by carbon dioxide activation," *Process Saf. Environ. Prot.*, vol. 3, pp. 76–86, 2016.

[9] P. Fang, C. Cen, D. Chen, and Z. Tang, "Carbonaceous adsorbents prepared from sewage sludge and its application for Hg0 adsorption in simulated flue gas," *Chinese J. Chem. Eng.*, vol. 18, no. 2, pp. 231–238, 2010.

[10] A. Gupta and A. Garg, "Primary sewage sludge-derived activated carbon: characterisation and application in wastewater treatment," *Clean Technol. Environ. Policy*, vol. 17, no. 6, pp. 1619–1631, 2015.

[11] Ihsanullah, Al-Khaldi FA, Abusharkh B, Khaled M, Atieh MA, Nasser MS, et al. Adsorptive removal of cadmium(II) ions from liquid phase using acid modified carbon-based adsorbents. J Mol Liq. 2015;204:255–63.

[12] E. Gutiérrez-Segura, M. Solache-Ríos, a. Colín-Cruz, and C. Fall, "Adsorption of cadmium by Na and Fe modified zeolitic tuffs and carbonaceous material from pyrolyzed sewage sludge," *J. Environ. Manage.*, vol. 97, pp. 6–13, 2012.

[13] Qu G, Liang D, Qu D, Huang Y, Liu T, Mao H, et al. "Simultaneous removal of cadmium ions and phenol from water solution by pulsed corona discharge plasma combined with activated carbon," Chem Eng J [Internet]. Elsevier B.V.; 2013;228:28–35

[14] J. A. Arcibar-Orozco, J. R. Rangel-Mendez, and P. E. Diaz-Flores, "Simultaneous Adsorption of Pb(Ii)-Cd(Ii), Pb(Ii)-Phenol, and Cd(Ii)-Phenol by Activated Carbon Cloth in Aqueous Solution," *Water, Air, Soil Pollut.*, vol. 226, no. 1, pp. 1–10, 2014.

[15] K. Pirzadeh and A. A. Ghoreyshi, "Desalination and Water Treatment Phenol removal from aqueous phase by adsorption on activated carbon prepared from paper mill sludge," *Desalin. Water Treat.*, vol. 52, no. November, pp. 37–41, 2014.

[16] U. S. E. P. A. USEPA, "Priority Pollutant List," vol. 1986, pp. 1–2, 2014.

[17] M. Otero, F. Rozada, a. Morán, L. F. Calvo, and a. I. García, "Removal of heavy metals from aqueous solution by sewage sludge based sorbents: competitive effects," *Desalination*, vol. 238, no. 1–3, pp. 46–57, 2009.

[18] M. Kavand, M. Soleimani, T. Kaghazchi, and N. Asasian, "Competitive Separation of Lead, Cadmium and Nickel From Aqueous Solutions Using Activated Carbon: Response Surface Modeling, Equilibrium and Thermodynamic Studies," *Chem. Eng. Commun.*, no. August 2015, p. 150527094519003, 2014.

[19] C. Andriantsiferana, C. Julcour-Lebigue, C. Creanga-Manole, H. Delmas, A.-M. Wilhelm, and D. Ph, "Competitive Adsorption of p -Hydroxybenzoic Acid and Phenol on Activated Carbon : Experimental Study and Modeling," *J. Environ. Eng.*, vol. 139, no. March, pp. 402–409, 2013.

[20] E. I. Inam, U. J. Etim, E. G. Akpabio, and S. a. Umoren, "Simultaneous adsorption of lead (II) and 3,7-Bis(dimethylamino)-phenothiazin-5-ium chloride from aqueous solution by activated carbon prepared from plantain peels," *Desalin. Water Treat.*, no. April 2015, pp. 1–14, 2015.

[21] B. Kavitha and D. Sarala Thambavani, "Kinetics, equilibrium isotherm and neural network modeling studies for the sorption of hexavalent chromium from aqueous solution by quartz/feldspar/wollastonite," *RSC Adv.*, vol. 6, no. 7, pp. 5837–5847, 2016.

[22] Q. Wen *et al.*, "Study on activated carbon derived from sewage sludge for adsorption of gaseous formaldehyde," *Bioresour. Technol.*, vol. 102, no. 2, pp. 942–947, 2011.

[23] P. Hadi, M. Xu, C. Ning, C. Sze, K. Lin, and G. Mckay, "A critical review on preparation , characterization and utilization of sludge-derived activated carbons for wastewater treatment," *Chem. Eng. J.*, vol. 260, pp. 895–906, 2015.

[24] Suangusa Pullket, “Sewage sludge as source of activated carbon for the removal of endocrine disrupting chemicals in wastewater,”PhD Dissertaion, 2015, Imperial College London.

[25] K. M. Smith, G. D. Fowler, S. Pullket, and N. J. D. Graham, “Sewage sludge-based adsorbents: A review of their production, properties and use in water treatment applications,” *Water Res.*, vol. 43, no. 10, pp. 2569–2594, 2009.

[26] S. Rio, C. Faur-Brasquet, L. Le Coq, P. Courcoux, and P. Le Cloirec, “Experimental design methodology for the preparation of carbonaceous sorbents from sewage sludge by chemical activation - Application to air and water treatments,” *Chemosphere*, vol. 58, no. 4, pp. 423–437, 2005.

[27] “WASTEWATER SLUDGE TREATMENT AND DISPOSAL IN KSA”, source: http://www.sawea.org/pdf/waterarabia2013

[28] A. A. Zorpas, C. Coumi, M. Drtil, and I. Voukalli, “Municipal sewage sludge characteristics and waste water treatment plant effectiveness under warm climate conditions,” *Desalin. Water Treat.*, vol. 36, no. 1–3, pp. 319–333, 2011.

[29] Tchobanoglous, George, Franklin L. Burton, and H. David Stensel, " Wastewater engineering: treatment and reuse", Mc Graw Hill, 4th Ed. 2003.

[30] M. H. Al-malack, N. S. Abuzaid, A. a Bukhari, and M. H. Essa, “Characterization , Utilization , and Disposal of Municipal Sludge : the State of-the-Art,” *Arab. J. Sci. Eng.*, vol. 27, no. 1, pp. 3–27, 2002.

[31] D. Fytili and A. Zabaniotou, “Utilization of sewage sludge in EU application of old and new methods-A review,” *Renewable and Sustainable Energy Reviews*, vol. 12, no. 1. pp. 116–140, 2008.

[32] Q. Lu, Z. L. He, and P. J. Stoffella, “Land application of biosolids in the USA: A review,” *Applied and Environmental Soil Science*, vol. 2012. 2012.

[33] B. M. Cieślik, J. Namieśnik, and P. Konieczka, “Review of sewage sludge management: standards, regulations and analytical methods,” *J. Clean. Prod.*, vol. 90, pp. 1–15, 2015.

[34] Ferhan Çeçen and Özgür Aktaş, “Fundamentals of Adsorption onto Activated Carbon in Water and Wastewater Treatment,” pp. 13–41, 2011.

[35] E. Altintig, G. Arabaci, and H. Altundag, “Preparation and characterization of the antibacterial efficiency of silver loaded activated carbon from corncobs,” *Surf. Coatings Technol.*, vol. 304, pp. 63–67, 2016.

[36] G. Xu, X. Yang, and L. Spinosa, “Development of sludge-based adsorbents: Preparation, characterization, utilization and its feasibility assessment,” *J. Environ. Manage.*, vol. 151, pp. 221–232, 2015.

[37] A. Ros, M. a. Lillo-Ródenas, E. Fuente, M. a. Montes-Morán, M. J. Martín, and a. Linares-Solano, "High surface area materials prepared from sewage sludge-based precursors," *Chemosphere*, vol. 65, no. 1, pp. 132–140, 2006.

[38] Removals, "The Production of Activated Carbons from Sewage Sludge," 2007.

[39] O. I. Y. Light, "United States Patent [191," vol. 6, pp. 3–6, 1989.

[40] X. Wang, N. Zhu, and B. Yin, "Preparation of sludge-based activated carbon and its application in dye wastewater treatment," *J. Hazard. Mater.*, vol. 153, no. 1–2, pp. 22–27, 2008.

[41] J. Bohdziewicz, G. Kamińska, and M. Tytła, "the Removal of Phenols From Wastewater Through Sorption on Activated Carbon," pp. 89–94, 2012.

[42] S. Bousba and A. Hassen, "Removal of Phenol from Water by Adsorption onto Sewage Sludge Based Adsorbent," vol. 40, pp. 235–240, 2014.

[43] E. F. Mohamed, C. Andriantsiferana, a. M. Wilhelm, and H. Delmas, "Competitive adsorption of phenolic compounds from aqueous solution using sludge-based activated carbon," *Environ. Technol.*, vol. 32, no. 12, pp. 1325–1336, 2011.

[44] S. Tangjuank, N. Insuk, J. Tontrakoon, and V. Udeye, "Adsorption of Lead (II) and Cadmium (II) ions from aqueous solutions by adsorption on activated carbon prepared from cashew nut shells," vol. 3, no. Ii, pp. 110–116, 2009.

[45] Y. Ma, N. Gao, W. Chu, and C. Li, "Removal of phenol by powdered activated carbon adsorption," *Front. Environ. Sci. Eng.*, vol. 7, no. 2, pp. 158–165, 2013.

[46] B. H. Hameed and A. A. Rahman, "Removal of phenol from aqueous solutions by adsorption onto activated carbon prepared from biomass material," *J. Hazard. Mater.*, vol. 160, no. 2–3, pp. 576–581, 2008.

[47] W. Zhu, W. Yao, Y. Zhan, and Y. Gu, "Phenol removal from aqueous solution by adsorption onto solidified landfilled sewage sludge and its modified sludges," *J. Mater. Cycles Waste Manag.*, vol. 17, no. 4, pp. 798–807, 2015.

[48] Y. Bian, Z. Bian, J. Zhang et al, "Adsorption of cadmium ions from aqueous solutions by activated carbon with oxygen-containing functional groups," *Chinese J. Chem. Eng.*, vol. 23, no. 10, pp. 1705–1711, 2015.

[49] A. H. Ali, "Comparative study on removal of cadmium(II) from simulated wastewater by adsorption onto GAC, DB, and PR," *Desalin. Water Treat.*, vol. 51, no. 28–30, pp. 5547–5558, 2013.

[50] Y. Zhai, X. Wei, G. Zeng, D. Zhang, and K. Chu, "Study of adsorbent derived from sewage sludge for the removal of Cd2+, Ni2+ in aqueous solutions," *Sep. Purif. Technol.*, vol. 38, no. 2, pp. 191–196, 2004.

[51] S. Bekkouche, S. Baup, M. Bouhelassa, S. Molina-Boisseau, and C. Petrier, “Competitive adsorption of phenol and heavy metal ions onto titanium dioxide (Dugussa P25),” *Desalin. Water Treat.*, vol. 37, no. 1–3, pp. 364–372, 2012.

[52] P. E. Diaz-Flores, F. L??pez-Ur??as, M. Terrones, and J. R. Rangel-Mendez, “Simultaneous adsorption of Cd2+ and phenol on modified N-doped carbon nanotubes: Experimental and DFT studies,” *J. Colloid Interface Sci.*, vol. 334, no. 2, pp. 124–131, 2009.

[53] M. A. Bezerra, R. E. Santelli, E. P. Oliveira, L. S. Villar, and L. A. Escaleira, “Response surface methodology (RSM) as a tool for optimization in analytical chemistry,” *Talanta*, vol. 76, no. 5. pp. 965–977, 2008.

[54] K. Of and S. Arabia, “National Science , Technology and Innovation Plan National Science , Technology and Innovation Plan” pp. 1–56.

[55] E. Kacan, “Optimum BET surface areas for activated carbon produced from textile sewage sludges and its application as dye removal,” *J. Environ. Manage.*, vol. 166, pp. 116–123, 2016.

[56] D. Sheha, H. Khalaf, and N. Daghestani, “Experimental Design Methodology for the Preparation of Activated Carbon from Sewage Sludge by Chemical Activation Process,” *Arab. J. Sci. Eng.*, vol. 38, no. 11, pp. 2941–2951, 2013.

[57] Y. D. Chen, W. Q. Chen, B. Huang, and M. J. Huang, “Process optimization of K2C2O4-activated carbon from kenaf core using Box-Behnken design,” *Chem. Eng. Res. Des.*, vol. 91, no. 9, pp. 1783–1789, 2013.

[58] M H. Al-Malack, Nabil S. Abuzaid, and Alaadin A. Bukhari,"Physico-chemical Characteristics of Municipal Sludge Produced at Three Major Cities of the Eastern Province of Saudi Arabia” *J. King Saud Univ.*, vol. Volume 20, pp. 15–27, 2008.

[59] Carlos J. Durán-Valle, “Techniques Employed in the Physicochemical Characterization of Activated Carbons,” *Lignocellul. Precursors used Synth. Act. Carbon*, pp. 37–55, 2012.

[60] P. S., K. M. Smith, G. D. Fowler, and N. J. D. Graham, “Influence of source and treatment method on the properties of activated carbons produced from sewage sludge,” *J. Residuals Sci. Technol.*, vol. 6, no. 1, pp. 43–50, 2009.

[61] T. S. Hui, M. Abbas, and A. Zaini, “Potassium hydroxide activation of activated carbon : a commentary,” vol. 16, no. 4, pp. 275–280, 2015.

[62] Y. Li, Y. Li, L. Li, X. Shi, and Z. Wang, “Preparation and analysis of activated carbon from sewage sludge and corn stalk,” *Adv. Powder Technol.*, vol. 27, pp. 684–691, 2015.

[63] M. A. Lillo-Ródenas, A. Ros, E. Fuente, M. a. Montes-Morán, M. J. Martin, and A. Linares-Solano, “Further insights into the activation process of sewage sludge-based precursors by alkaline hydroxides,” *Chem. Eng. J.*, vol. 142, no. 2, pp. 168–

174, 2008.

[64] F. Zhang, H. Itoh, and J. O. Nriagu, “Activated carbons derived from organic sewage sludge for the removal of mercury from aqueous solution.”

[65] H. Djati Utomo, X. C. Ong, S. M. S. Lim, G. C. B. Ong, and P. Li, “Thermally processed sewage sludge for methylene blue uptake,” *Int. Biodeterior. Biodegrad.*, vol. 85, pp. 460–465, 2013.

[66] C. Li and S. Kumar, “Preparation of activated carbon from un-hydrolyzed biomass residue,” *Biomass Convers. Biorefinery*, 2016.

[67] G. S. dos Reis, M. A. Adebayo, E. C. Lima, C. H. Sampaio, and L. D. T. Prola, “Activated Carbon from Sewage Sludge for Preconcentration of Copper,” *Anal. Lett.*, vol. 49, no. 4, pp. 541–555, 2016.

[68] X. Li, W. Li, G. Wang, P. Wang, and X. Gong, “Preparation, characterization, and application of sludge with additive scrap iron-based activated carbons,” *Desalin. Water Treat.*, vol. 54, no. 4–5, pp. 1194–1203, 2015.

[69] C. Liu, P. Wu, Y. Zhu, and L. Tran, “Simultaneous adsorption of Cd2+ and BPA on amphoteric surfactant activated montmorillonite,” *Chemosphere*, vol. 144, pp. 1026–1032, 2016.

[70] F. Rozada, M. Otero, a. Morán, and a. I. García, “Adsorption of heavy metals onto sewage sludge-derived materials,” *Bioresour. Technol.*, vol. 99, no. 14, pp. 6332–6338, 2008.

[71] A. Gupta and C. Balomajumder, “Simultaneous Adsorption of Cr (VI) and Phenol from Binary Mixture Using Iron Incorporated Rice Husk : Insight to Multicomponent Equilibrium Isotherm,” vol. 2016, no. Vi, 2016.

[72] U. Beker, B. Ganbold, H. Dertli, and D. D. Gülbayir, “Adsorption of phenol by activated carbon: Influence of activation methods and solution pH,” *Energy Convers. Manag.*, vol. 51, no. 2, pp. 235–240, 2010.

APPENDIX

Appendix A

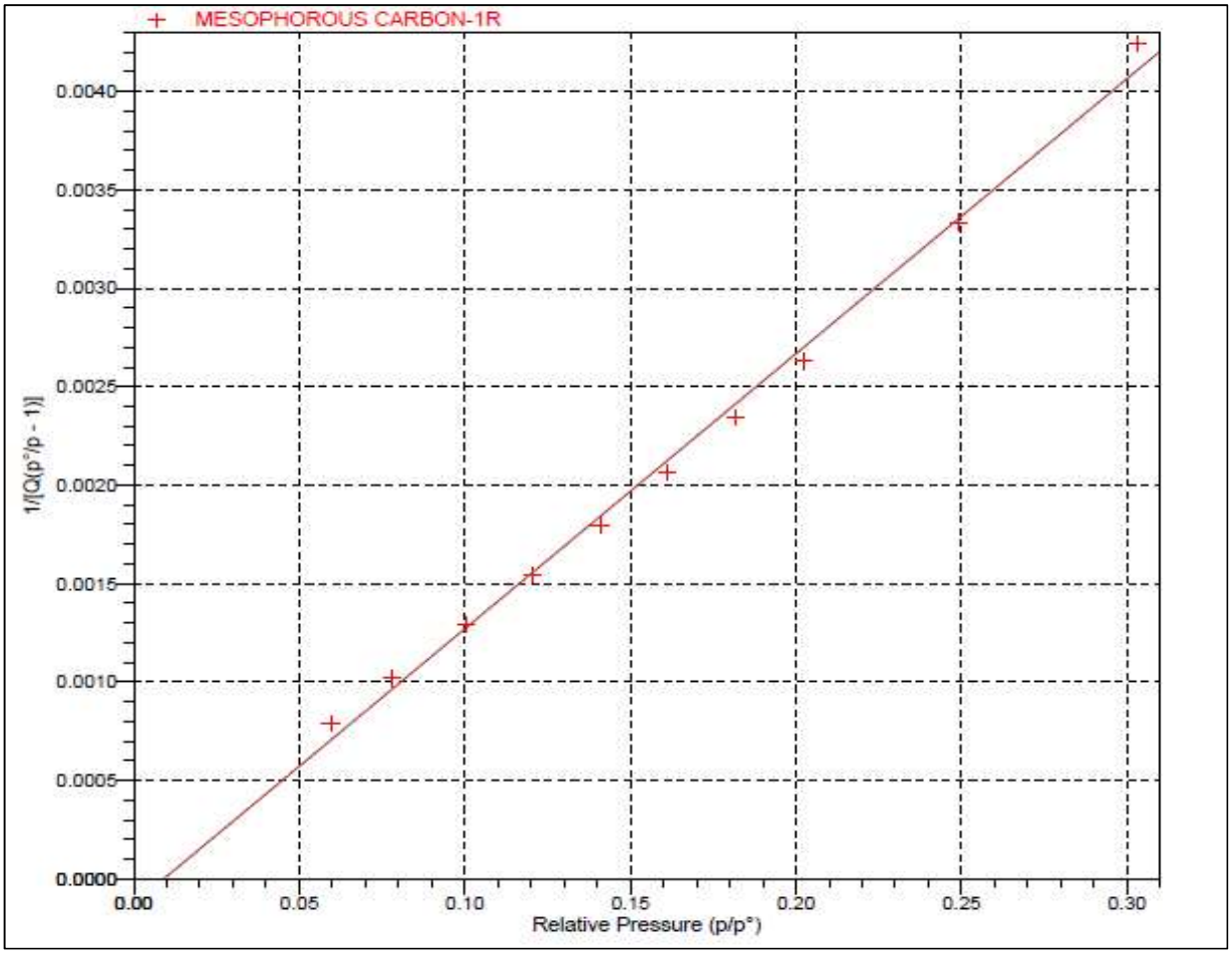

BET SURFACE AREA PLOT FOR AC1-$ZnCl_2$

Appendix B

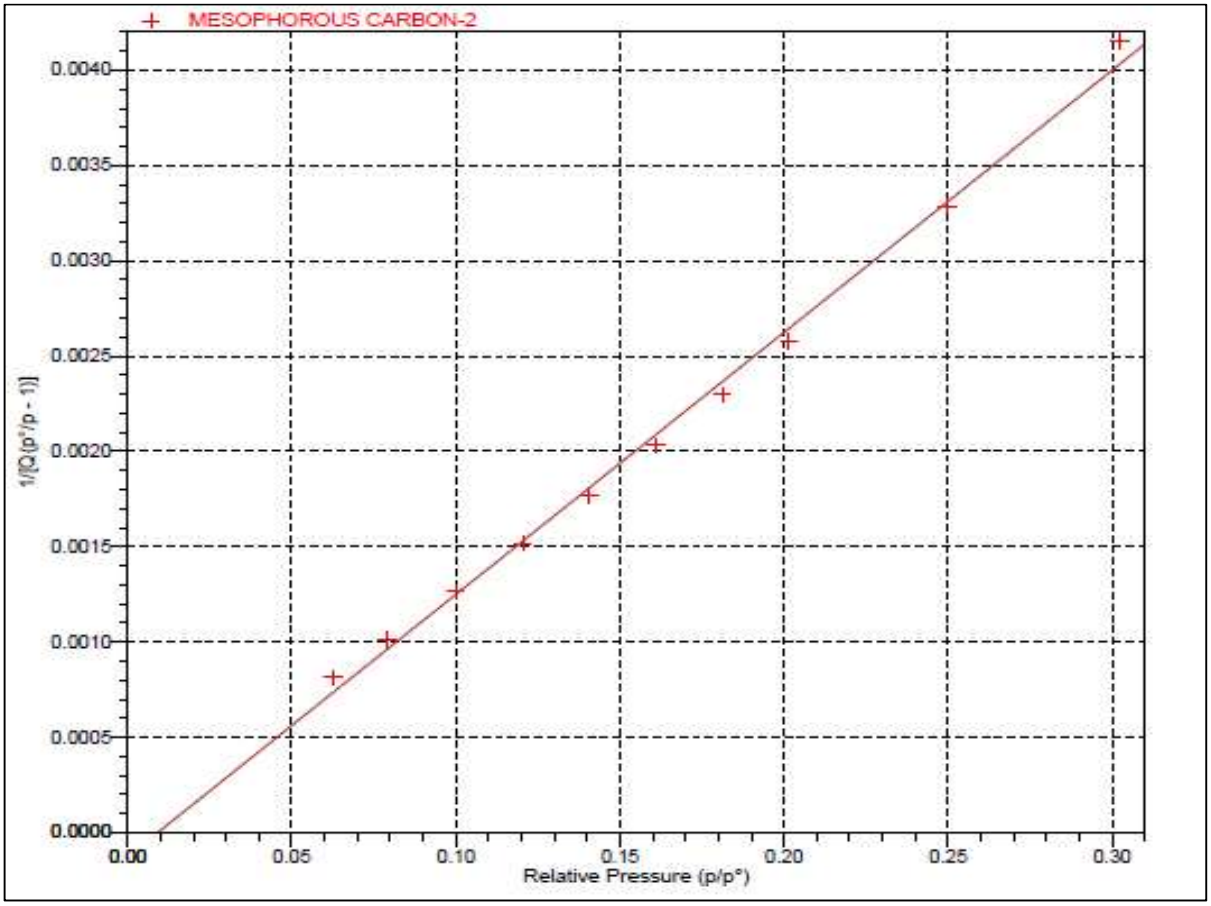

BET SURFACE AREA PLOT FOR AC2-$ZnCl_2$

Appendix C

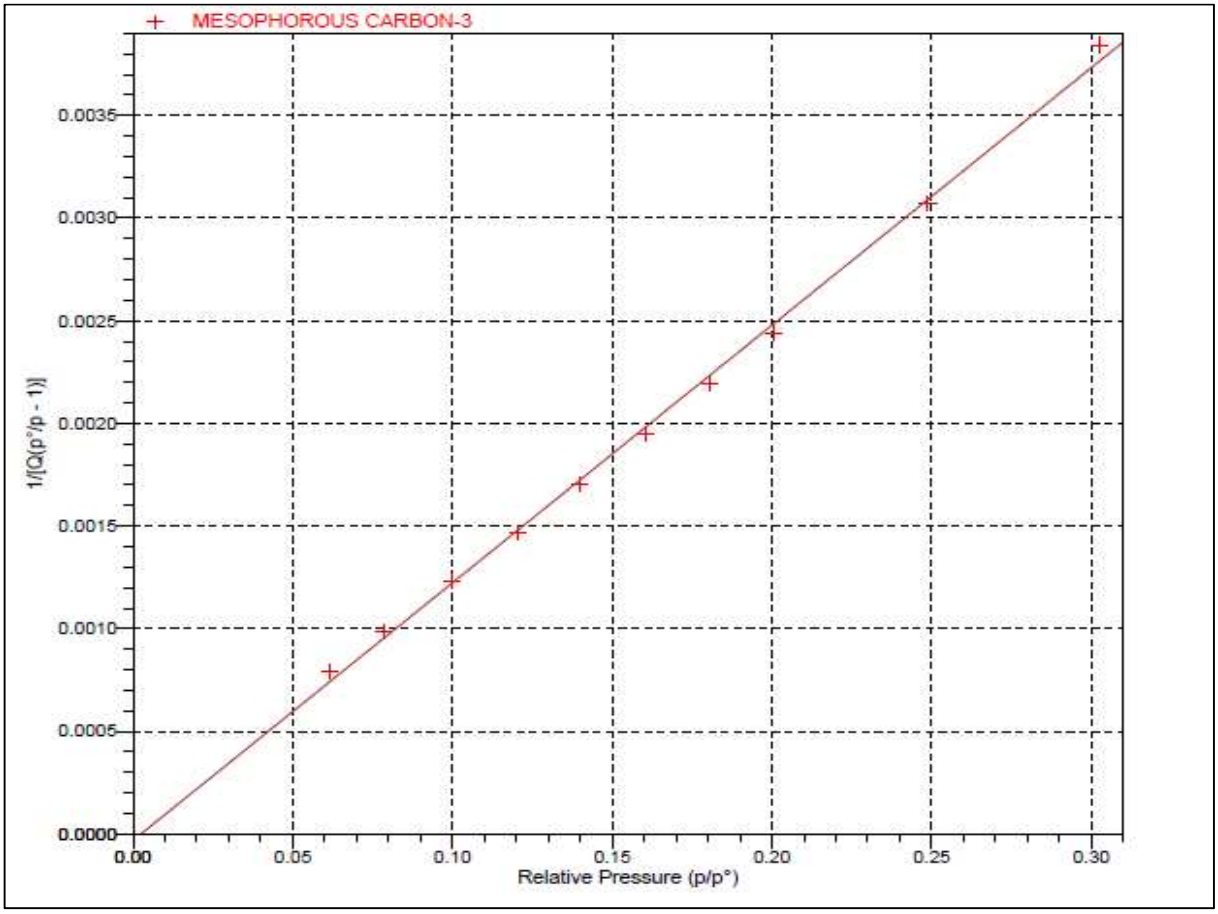

BET SURFACE AREA PLOT FOR AC3-KOH

Appendix D

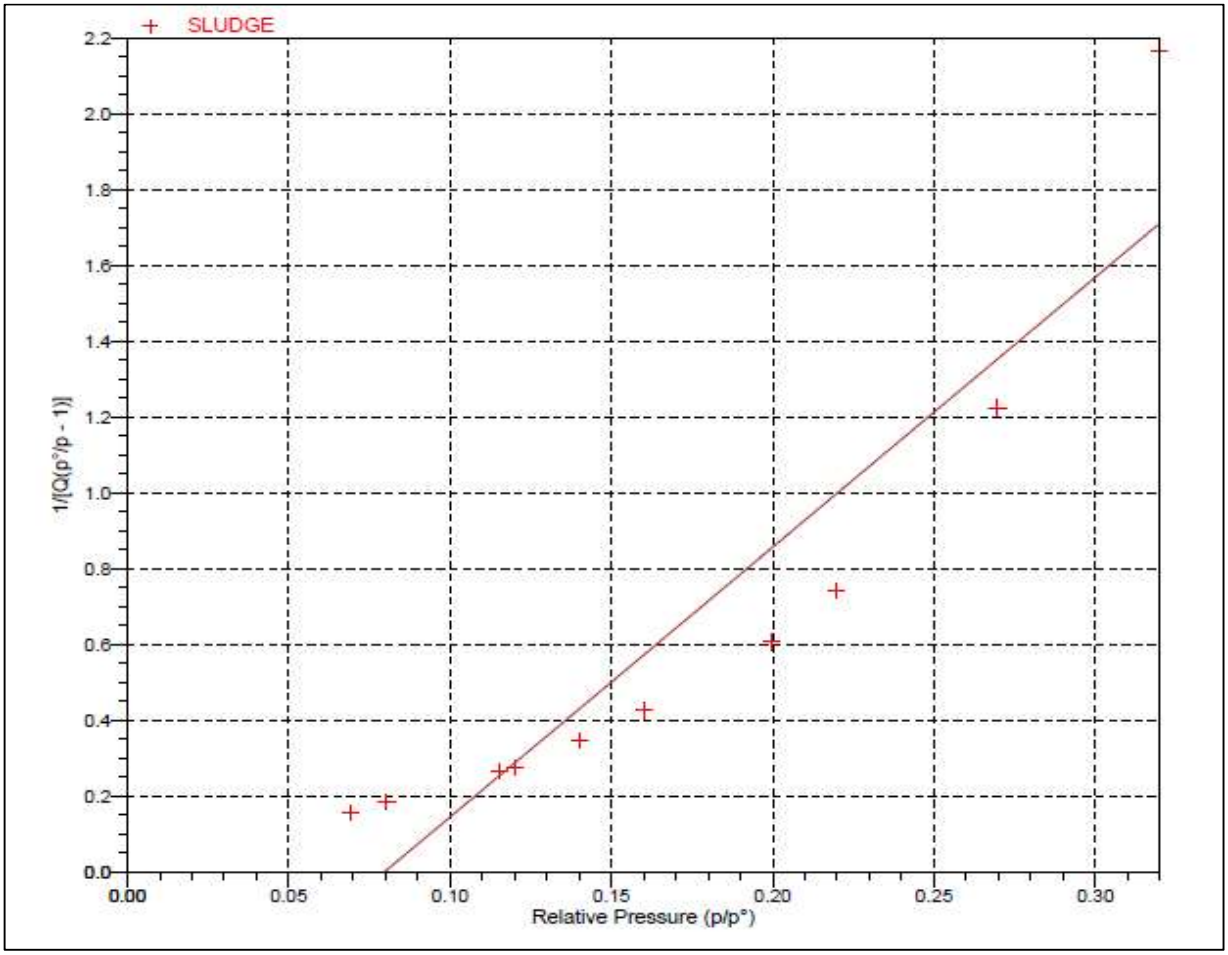

BET SURFACE AREA PLOT FOR SEWAGE SLUDGE

Vitae

Name :Mohammed Dauda

Nationality :Nigerian

Date of Birth :9/13/1988

Email :mohammeddauda18@gmail.com

Address :No 3 Aiyetoro gbede lane fate/tanke Ilorin, Kwara State

Academic Background:

- MSc. Civil & Environmental Engineering, December, 2016.

  King Fahd University of Petroleum and Minerals, Dhahran, Saudi Arabia.

  MSc. Thesis Title: Adsorption of Cadmium and Phenol on sludge based Activated Carbon

- B.Eng. Water Resources and Environmental Engineering. October, 2011.

  Ahmadu Bello University, Zaria. Nigeria.

  Project Title: Laboratory Investigation of Flow over some Hydraulic Structures.

Research Publication:

Competitive Adsorption of Cadmium and Phenol on Activated Carbon from Municipal Sludge (Under Review)